Discovery and Characterization of Inflammation-Induced Electrophilic Fatty Acid Derivatives

by

Alison Leigh Groeger

Bachelor of Science, Rhodes College, 2004

Submitted to the Graduate Faculty of

The School of Medicine in partial fulfillment

of the requirements for the degree of

Doctor of Philosophy

University of Pittsburgh

2009

UNIVERSITY OF PITTSBURGH

School of Medicine

This thesis dissertation was presented

by

Alison Leigh Groeger

It was defended on

August 6th, 2009

and approved by

Committee Chair: Thomas P. Conrads, Ph.D., Associate Professor, Department of Pharmacology and Chemical Biology

William C. de Groat, Ph.D., Professor, Department of Pharmacology and Chemical Biology

Donald B. DeFranco, Ph.D., Professor, Department of Pharmacology and Chemical Biology

Bret H. Goodpaster, Ph.D., Assistant Professor, Department of Medicine

Dissertation Advisor: Bruce A. Freeman, Ph.D., Professor, Department of Pharmacology and Chemical Biology

Discovery and Characterization of Inflammation-Induced Electrophilic Fatty Acid Derivatives

Alison L. Groeger, Ph.D.

University of Pittsburgh, 2009

Electrophilic lipids are emerging as critical mediators of anti-inflammatory signaling pathways, although many biologically relevant electrophiles may still remain unknown. Nitro derivatives (NO_2-FA) and α,β-unsaturated carbonyl derivatives of unsaturated fatty acids are naturally occurring electrophilic products of redox reactions, and can modulate a variety of cellular signaling processes including the transcriptional activity of the peroxisome proliferator-activated receptor-γ (PPARγ). PPARγ binds diverse ligands to regulate the expression of genes involved in metabolism and inflammation. Activators of PPARγ include anti-hyperglycemic drugs such as thiazolidinediones (TZDs) and intermediates of lipid metabolism and oxidation that bind PPARγ with very low affinity. Recently TZDs have raised concern after being linked with increased risk of peripheral edema, weight gain, and adverse cardiovascular events. In contrast, NO_2-FA act as partial agonists of PPARγ at nM concentrations and covalently bind PPARγ via Michael addition. NO_2-FA show selective PPARγ modulator characteristics by inducing coregulator protein interactions distinctively different from those induced by the TZD Rosiglitazone.

In further exploring the electrophilic lipidome, a new subclass of electrophilic lipid has been revealed. Using a recently developed β-mercaptoethanol (BME) alkylation reaction, followed by HPLC-MS/MS-based screening, we report six novel electrophilic fatty acid derivatives (EFADs) specifically formed during macrophage activation (RAW264.7 and THP-1

cell lines and primary macrophages treated with IFNγ and LPS). The major EFADs are α,β-unsaturated oxo-derivatives of ω-3 fatty acids as confirmed by cell culture and *in vitro* studies and by MS/MS structural analysis. The isomers of two major EFADs were identified as 13- and 17-keto derivatives of docosapentaenoic acid (DPA) and docosahexaenoic acid (DHA). Purified cyclooxygenase-2 (COX-2) product profiles and treatment of activated macrophages with COX-2 inhibitors confirmed EFAD synthesis to be catalyzed by inducible COX-2, followed by hydroxy-dehydrogenase activity. EFAD production was increased 2.5 fold in activated macrophages treated with acetylsalicylic acid (ASA; aspirin). Internal standard-based quantification showed that EFADs are highly abundant electrophiles in activated macrophages, reaching intracellular concentrations as high as 350 nM. Importantly, EFADs form reversibly reactive covalent adducts with both proteins and small molecule thiols in activated macrophages, supporting a potential for post-translational protein modification-mediated cell signaling. Furthermore, synthetic isomers of EFAD-1 and -2 (17-oxo-DHA and 17-oxo-DPA, respectively) act as partial agonists of peroxisome proliferator activated receptorγ (PPARγ), activate Nrf2 (nuclear factor-erythroid 2-related factor 2)-dependent gene expression, and inhibit pro-inflammatory cytokine production and iNOS expression in IFNγ and LPS-activated RAW264.7 cells and in primary macrophages. In conclusion, it has been demonstrated that upon activation macrophages generate omega-3 derived electrophilic signaling molecules at biologically relevant concentrations that act as autocrine mediators.

TABLE OF CONTENTS

LIST OF TABLES

LIST OF FIGURES

PREFACE

O snail
Climb Mount Fuji,
But slowly, slowly!

-Issa

ACKNOWLEDGEMENTS

To those who have cultivated my academic development, I would like to extend sincere thanks. I am very grateful to my mentor, Dr. Bruce Freeman, for imparting several unique learning experiences above and beyond standard graduate training. I value the members of my thesis committee for their insightful scientific questions and for pushing me to do my best while keeping my professional interests in mind. I would also like to acknowledge the exceptional labmates, friends, and teachers with whom I have worked during my time in the Freeman Lab: Francisco Schopfer, Eric Kelley, Tina Hallis, Carlos Batthyany, Marsha Cole, Steven Woodcock, Paul Baker, Phil Chumley, Scott Sweeney, Franca Gollin-Bisello, Nicholas Khoo, Gustavo Bonacci, Julia Chen, Tanja Rudolph, Volker Rudolph, Emilia Kansanen, Jeffery Koenitzer, Chiara Cipollina, and Nicholas Hundley. Additionally, I would like to thank the administrative staff of the Pharmacology department and the Interdisciplinary Biomedical Graduate Program, especially Georgeanna Robinson, Barb Martin, Patricia Smith, Cindy Duffy, and Veronica Cardamone. Their assistance made my journey through graduate school so much easier.

I would also like to acknowledge those who have influenced my life outside of my graduate studies. Sensei Bill Miller, Sensei Steve and Sensei Lisa Nakamura, and Sensei Rey George have taught me invaluable lessons about life, respect, self-confidence and martial arts. I am grateful to Dr. Mary Miller for her guidance and mentoring as well as initiating me into the world of scientific research and communication. I would also like to extend a special thanks to Dr. Linda Noble for introducing me to biomedical research, and to the teachers at the Schools of the Sacred Heart in San Francisco for honing my writing and persuasive argument skills and for nurturing my love of biology and nature. I would like to acknowledge my friends and classmates who have inspired and cheered me. Most importantly, I would like to thank my parents, my brother, Micio, and Taz for their constant support and unconditional love.

LIST OF ABBREVIATIONS

4-ONE 4-oxo-2-nonenal

5-oxoETE-d7.....5-oxo-6E,8Z,11Z,14Z-eicosatetraenoic-6,8,9,11,12,14,15-d7 acid

9-oxoODE .....9-oxo-10E,12Z-octadecadienoic acid (a.k.a. 9-KODE)

9-oxoOTrE .....9-oxo-10E,12Z,15Z-octadecatrienoic acid

12-oxoETE.....12-oxo-5Z,8Z,10E,14Z-eicosatetraenoic acid

15d-PGJ_2 .....15-deoxy-prostaglandin-J_2

15-oxoEDE .....15-oxo-11Z,13E-eicosadienoic acid

17-oxoDHA.....17-oxo-docosahexaenoic acid

17-oxoDPA .....17-oxo-docosapentaenoic acid

A_4/J_4-NPs .....Cyclopentenone neuroprostanes

AA.....Arachidonic acid

ALA .....α-linolenic acid

ASA.....acetylsalicylic acid (aspirin)

cGMP .....Cyclic guanosine monophosphate

COX .....Cyclooxygenase

CYP.....Cytochrome p450

DHA.....Docosahexaenoic acid

DPA.....Docosapentaenoic acid

DTA .....Docosatetraenoic acid

EFAD .....Electrophilic fatty acid derivative

eNOS.....Endothelial NOS

EPA .....Eicosapentaenoic acid

EpRE/ARE.....Electrophile response element/antioxidant response element

Erk-1/2 .....extracellular-signal regulated kinase-1/2

ESI LC/MS^n .....Electrospray ionization tandem mass spectrometry

ETYA.....Eicosatetrayonic acid

GAPDH.....Glyceraldehyde-3-phosphate dehydrogenase

GCL.....Glutamate-cysteine ligase

γ-GCS.....γ-glutamylcysteine synthetase

GPCR .....G-protein coupled receptor

GPx .....Glutathione peroxidase

GSH.....Glutathione

GST .....Glutathione S-transferase

HETE .....Hydroxy-eicosatetraenoic acid

HNE 4-hydroxy-2-nonenal

HO-1 .....Heme-oxygenase-1

HSF1 .....Heat shock factor 1

Hsp .....Heat shock protein

HPLC .....High performance liquid chromatography

IFN-γ .....Interferon-γ

IL-1β Interleukin-1β;

iNOS .....Inducible NOS

Kdo_2 .....Kdo_2-lipid A

Keap1 .....*kelch-like ECH-associated protein 1*

LDL .....Low-density lipoprotein

LNO_2 .....9-, 10-, 12-, and 13-nitro derivatives of linoleic acid

$LO^{\bullet}$ .....Lipid alkoxyl radical

$LOO^{\bullet}$ .....Lipid peroxyl radical

LOX .....Lipoxygenase

LPS.....Lipopolysaccharide

MAFP.....Methyl arachidonyl fluorophosphonate

MDA .....Malondialdehyde

$^{\bullet}NO$.....Nitric oxide

$^{\bullet}NO_2$ .....Nitrogen dioxide

N_2O_3 .....Dinitrogen trioxide

NOS.....Nitric oxide synthase

NQO-1.....NAD(P)H-quinone oxidoreductase 1

Nrf2.....nuclear factor-erythroid 2-related factor 2

NSAIDs.....Nonsteroidal anti-inflammatory drugs

OA-NO_2 .....9- and 10-nitro derivatives of oleic acid

p38 MAPK.....p38 mitogen-activated protein kinase

PG .....Prostaglandins

PGHS .....Prostaglandin H synthase isozymes

PGHS-1 .....Prostaglandin H synthase-1

PGHS-2 .....Prostaglandin H synthase-2

POX.....Peroxidase

PP2A .....protein serine/threonine phosphatase 2A

PPARγ.....Peroxisome proliferator-activated receptor γ

PUFA .....Polyunsaturated fatty acids

RES .....Reactive electrophilic species

ROS.....Reactive oxygen species

RvD1 .....Resolvin D1

RvE1 .....Resolvin E1

TLC .....Thin layer chromatography

TNF-α.....Tumor necrosis factor-α

TRPA1 .....Transient receptor potential A1 receptor

TRPV1 .....Transient receptor potential vanilloid-1 receptor

Trx1.....Thioredoxin-1

TrxR .....Thioredoxin reductase

TX .....Thromboxanes

TZD.....Thiazolidinedione

1.0 INTRODUCTION

During pathological inflammation the oxidative environment and the enzymatic production of lipophilic signaling mediators (*e.g.* prostanoids and nitric oxide; $^{\bullet}NO$) both contribute to the generation of reactive electrophilic species (RES). Furthermore, RES are emerging as key mediators of inflammatory processes and new RES are still being discovered. Oxygenase enzymes (*e.g.* cyclooxygenases, COXs; and lipoxygenases, LOXs) contribute to the first step in generating prostanoids, lipoxins, and families of RES, including α,β-unsaturated keto derivatives of fatty acids. RES, such as nitroalkene derivatives of fatty acids (NO_2-FA), are also formed independently of known enzymatic pathways or may be products of, pH-dependent NO_2^--mediated nitration. Regardless of their path of origin, many RES generated during inflammation are generally considered soft electrophiles[1] that can react reversibly with nucleophilic biomolecules by Michael addition. This reversible reactivity gives RES potential signaling capabilities that may inform the cell of its redox status or external environment.

Moderate exposure to oxidative and RES-instigated stress stimulates a cell to orchestrate the expression of cell survival proteins and thus better prepare for future insult. Conversely, acute and extreme oxidative and RES-induced stress trigger cell damage and often ends in senescence, apoptosis or necrosis. Cellular protective mechanisms for oxidative and RES-induced stress include the activation of transcription factors, the repair of DNA damage, and increased levels of protective proteins such as antioxidant enzymes, glutathione (GSH), and heat

shock proteins. Genes encoding many of these defenses contain an electrophile response element/antioxidant response element (EpRE/ARE). The transcription factor Nrf2 regulates the expression of EpRE/ARE-dependent genes and Nrf2 activity is determined by the state of its redox-sensitive inhibitor, Keap1 (*kelch-like ECH-associated protein 1*). Similarly, the nuclear receptor involved in the regulation of cell metabolism and prolferation/differentiation, PPARγ, is also sensitive to the cell's redox status and RES levels.

Herein, the roles of fatty acid-derived RES (*i.e.* NO_2-FA and α,β-unsaturated carbonyl compounds) in inflammation are explored. Thus, the beginning of this work will address general inflammation as it is mediated by a mononuclear phagocytic cells (*e.g.* monocytes and macrophages), the formation and actions of RES and specifically NO_2-FA, and the formation and signaling properties of oxidized fatty acids. The following chapters will focus on the PPARγ agonist activities of NO_2-FA and on the discovery and characterization of new RES formed during inflammation.

1.1 INFLAMMATION AND THE ROLE OF MONONUCLEAR PHAGOCYTES

Inflammation and the supporting role played by mononuclear phagocytes are intimately involved in the pathogenesis of important clinical disorders including asthma, atherosclerosis, diabetes, rheumatoid arthritis, inflammatory bowel disease, and multiple sclerosis. Under controlled conditions, acute inflammation is protective and beneficial by ridding the host of pathogens or toxins and by beginning the repair process by removing/destroying necrotic cells and tissues. Alternatively, poorly regulated chronic periods of inflammation, such as the disorders enumerated above, interfere with homeostasis and lead to tissue damage. Inflammation is

characterized by vascular changes including increased vessel permeability and modulation of blood flow, and by cellular events such as leukocyte adhesion, extravasation and phagocytosis. The cells and tissues involved in this process also produce chemical mediators including eicosanoids, resolvins, maresins, platelet activating factor (PAF), vasoactive amines, plasma proteases, complement, cytokines, $^{\bullet}NO$, and reactive oxygen species (ROS). During inflammation, ROS and reactive oxides of nitrogen are enzymatically produced at elevated levels and this can lead to nitration and oxidation of biomolecules such as lipids.

1.1.1 Role of Macrophages in Inflammation

Macrophages are responsible for phagocytizing foreign bodies and debris in inflamed tissue and for producing or responding to many of the chemical mediators involved in inflammation. Mononuclear phagocytes participate in inflammatory processes by assuming a specific polarization or functional program during their differentiation. The two major types of differentiation are classical activation (also known as M1 macrophage polarization) and alternative activation (the M2 series of macrophage polarization). Classical macrophage activation reflects a state of type I inflammation, characterized by Th1 responses, cell-mediated immunity, delayed-type hypersensitivity, killing of intracellular pathogens, tissue destruction, and tumor resistance. Furthermore, M1 polarized macrophages are effective sources of ROS, $^{\bullet}NO$ and secondary oxides of nitrogen[2]. Macrophages are derived from the myeloid progenitor lineage and enter the circulation as monocytes. When circulating monocytes encounter a chemotactic signal, they enter the tissue by extravasation and further differentiate into macrophages specialized to respond specifically to the tissue and the inflammatory microenvironment. Classical activation of monocytes/macrophages is often induced by

interferon-γ (IFNγ) alone or in combination with cytokines (*e.g.* TNFα) or foreign stimuli such as lipopolysaccharides (LPS). M1 polarized macrophages generally express high levels of the proinflammatory cytokines including interleukin-12 (IL-12), IL-23, TNFα, IL-1β, and IL-6. In contrast, cytokines which suppress macrophage function such as IL-10 are expressed at low levels[2,3].

1.1.2 Second Messengers in Macrophages

The chemical mediators that classically activate macrophages also induce the expression of cyclooxygenase-2 (COX-2), inducible nitric oxide synthase (iNOS), and NADPH oxidase (NOX) through multiple secondary messengers. STAT1 (signal transducer and activator of transcription-1) and NF-κB (nuclear factor κ-light-chain-enhancer of B cells) are two of the major regulators of the classical inflammatory response in macrophages. The binding of IFNγ to its receptor (IFNγR) activates JAK1 (Janus Kinase 1) and JAK2 to phosphorylate and activate STAT1. STAT1 in turn mediates the transcription of proinflammatory genes[4,5].

The binding of LPS to LPS-binding protein and CD-14 (cluster of differentiation 14) activates TLR4 (toll-like receptor-4) thus stimulating the activation of phosphatidylinositol 3-kinase (PI3K) and phosphoinositide-dependent kinase (PDK). Activation of the PI3K pathway triggers the phosphorylation of NOX subunits (p47phox and p67phox), initiating the assembly of NOX, and the subsequent production of superoxide[4]. The activation of PI3K and PDK leads to the transcription of NFκB-dependent genes, such as iNOS and COX-2 (For more information on COX-2 see section 1.5).

1.2 BIOLOGIC ELECTROPHILES AS SIGNALING MEDIATORS

The broad definition of an electrophile is a molecule having one or more electron-poor atoms, which can accept electrons from electron-rich donor molecules (nucleophiles). Thus cations (*e.g.* Hg^{2+}, Cd^{2+}, Zn^{2+}), polarized neutral molecules, polarizable neutral molecules (*e.g.* Cl_2 and Br_2), oxidizing agents, and some Lewis acids would all be included in this definition. Biologically relevant electrophiles will be referred to as RES. RES are generated during tightly controlled metabolic processes or during dysregulated pathological processes as by-products of oxidation. Following generation, RES may contribute to pathogenesis by altering cellular functions directly via the modulation of signaling pathways or indirectly by covalently modifying cellular macromolecules and by depleting the cell of reductants[6]. Thus, when produced in excess, RES are associated with the development and progression of a number of diseases including cancer[7-9], atherosclerosis[10], neurodegeneration[1], Alzheimer's disease[11], and chronic inflammation[12]. Alternatively at lower regulated levels, RES can induce protective effects against further insult by activating the expression of genes involved in xenobiotic detoxification and the antioxidant response (see section 1.2.7 for more details).

1.2.1 Electrophilic Fatty Acids Defined

In biology, RES are not only by-products of cellular-stresses, but are also crucial signaling mediators in organisms spanning the Eukaryote domain. In biologically relevant molecules, carbon atoms are often rendered electrophilic by conjugation to electron-withdrawing functional groups. Often, specific functional groups determine the reactivity of the electrophilic moiety[13]. Two prominent examples of these electron withdrawing groups are α,β-unsaturated carbonyls

and nitroalkenes, in which the β-carbon (if it is bound to at least one hydrogen atom) is electrophilic and hence susceptible to nucleophilic attack (**Fig. 1**). While RES can be derived from many sources, this work has focused on fatty acid-derived electrophilic products of oxidation, nitrosation and/or nitration reactions.

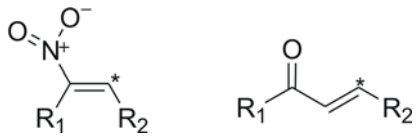

Figure 1. The β-carbons of nitroalkenes and α,β-unsaturated carbonyls are electrophilic.

The chemical structures of a nitroalkene (left) and an α,β-unsaturated carbonyl (right) are represented above, in which "*" indicates an electrophilic β-carbon.

At many levels, RES modulate cell survival mechanisms by chemically reacting with nucleophilic nucleic acids (see section 1.2.5 for more details), amino acid residues (cysteine, lysine, and histidine) on proteins and other small molecules[14-16]. For example, RES not only directly modulate protein function by reacting with sulfhydryl (-SH) groups on cysteine residues[17,18], but can also lower pools of small molecule sulfhydryls or cellular reductants such as GSH[19,20], thus indirectly interfering with basic homeostatic functions. Both RES and reactive oxygen species (ROS) alter the cellular redox state and share several other comparable features; both can be produced by either non-enzymatic or enzymatic processes (depending on the species in question). In both cases ROS and RES production and levels are metabolically controlled in healthy cells; low levels of these species induce the expression of cell survival genes, and in some cases prime the cell to survive periods of stress[17,21]. In contrast, under pathological conditions, RES and ROS are often produced in excess and accelerate cell damage by chemically modifying nucleophilic atoms in cellular molecules through uncatalyzed reactions[13,22].

1.2.2 Mechanisms of Electrophile Reaction with Biomolecules: Michael Addition and Schiff Base Formation

Michael reaction acceptors are molecules containing charged or polarized functional groups conjugated with alkenes or alkynes. The functional groups most commonly associated with Michael reaction acceptors in order of electron-withdrawing strength are as follows, starting with the most reactive: nitro groups (NO_2), α,β-unsaturated carbonyl groups (*i.e.* aldehydes and ketones), and esters[23]. The reactivity of a Michael acceptor with nucleophiles is positively correlated with the strength of the electron-withdrawing group(s) involved (see **Table 1** and **Fig. 2** for details). In terms of signaling, an interesting property of Michael acceptors is that the majority can react reversibly with sulfhydryl groups (thiol; R-SH)[23].

Table 1. Second-order rate constants for oxidants and RES reaction with the thiol of GSH.

Reactions were performed at 37°C and pH7.4[24]

Oxidant/electrophilic lipid	Second-order rate constant $M^{-1}s^{-1}$
$ONOO^-$	1350
H_2O_2	2.6 ± 0.9
4-Hydroxynonenal	1.3
4-Oxononenal	145
8-*iso* Prostaglandin A_2	0.7 ± 0.2
15-deoxy-$\Delta^{12,14}$-Prostaglandin J_2	0.7 ± 0.3
OA-NO_2	183 ± 6
LNO_2	355 ± 5

Data are expressed as mean ± S.D.

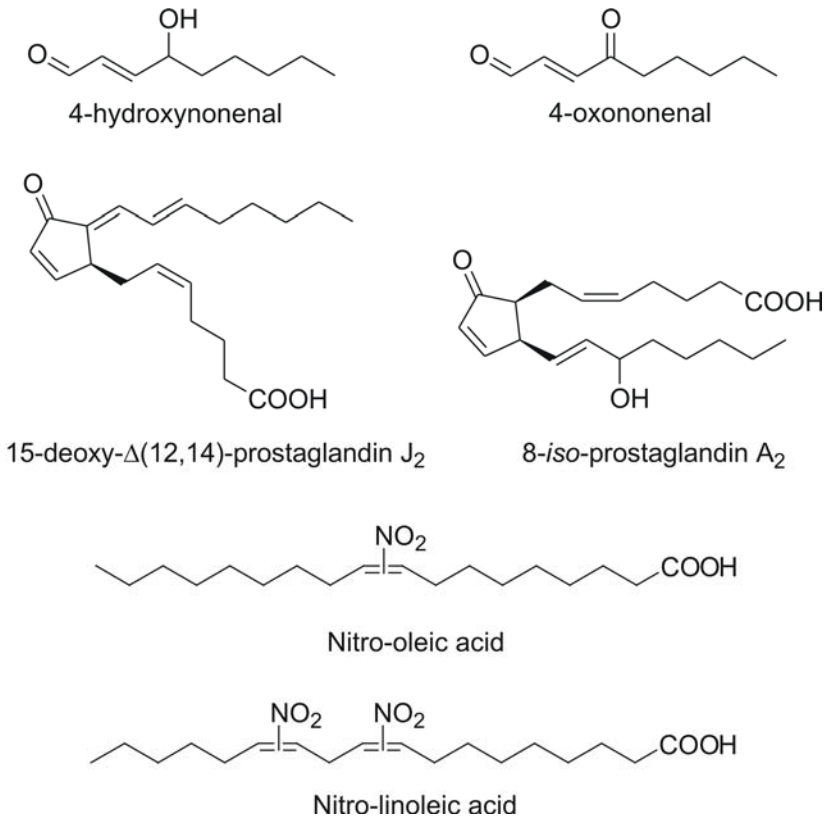

Figure 2. Chemical structures of electrophilic lipid derivatives that react with the thiol of glutathione.

One well-characterized type of Michael addition in biology is exemplified by the reaction of RES with thiols. This reaction is favored by deprotonation of the thiol to the more nucleophilic thiolate ($R\text{-}S^-$) species. Deprotonation of the thiol is dependent on its pK_a, *i.e.* the lower a pK_a the greater the proportion of thiolate species. Thus, the pK_a and the consequent abundance of the thiolate ion will determine a sulfhydryl's rate of reaction with electrophiles. In the case of both free cysteines and those incorporated into proteins, the pK_a is generally around 8.5[25] indicating a low proportion of tholates and subsequently mild reactivity at physiologic pH. However, the pK_a of cysteine thiols can be significantly lowered by proximity to basic amino acid residues such as lysine or arginine[26]. Protein structure can also affect the rate of a Michael

addition reaction in terms of sterically hindering the RES from association or dissociation with nucleophiles.

RES also modify proteins by reacting via Michael addition with the imidizole nitrogen of histidine residues and the ε-amino nitrogen of lysine residues. Furthermore, carbonyl-containing RES can react with lysine residues or free N-terminal amino groups to form Schiff base products. In some cases, bifunctional electrophiles (*e.g.* 4-oxo-2-nonenal; 4-ONE) form Michael adducts with one amino acid residue and induce protein cross-linking by forming a Schiff base with the amines of lysine residues[27,28]. By nature the Michael addition reaction is reversible, whereas Schiff base products are more stable and much less prone to reversible reactivity.

1.2.3 Sources and Metabolism of Reactive Electrophilic Species

RES can be generated by non-enzymatic free radical-mediated reactions or by enzyme-catalyzed reactions. Non-enzymatic generation of RES occurs under oxidizing conditions in which ROS or lipid alkoxyl/peroxyl radicals initiate and propagate the oxidation of PUFA. Termination of these reactions yields hydroxy and hydroperoxy lipid derivatives as well as fragments of peroxidized lipids, which can include short chain conjugated carbonyl products. In contrast, enzyme-catalyzed RES are products of more controlled conditions and can be generated both during periods of stress or normal metabolism. Under these circumstances, the production of many RES begins with oxygenases. Additionally, in mammalian systems, RES are consumed in the diet or are products of xenobiotic metabolism (see section 1.2.3.2).

1.2.3.1 Non-Enzymatic Generation of Reactive Electrophilic Species

Many RES produced by enzymatic oxidation of fatty acids are also generated independently of enzymatic catalysis. Malondialdehyde (MDA) is one of the major non-enzymatic products of lipid oxidation reactions in both mammalian and plant systems. Due to tautomerization, MDA exists primarily in the enol form as an α,β-unsaturated aldehyde. In healthy plant leaves MDA is produced continuously (mostly from trienoic fatty acids), and though its levels are relatively high they are maintained despite rapid turn-over or sequestration by the cell (**Fig. 3**)[13,29]. In humans MDA is the product of lipid peroxidation and is generated under pathological oxidative conditions, such as in macrophage-derived foam cells of atherosclerotic lesions[30]. Other products of lipid peroxidation, 4-ONE and 4-hydroxy-2-nonenal (HNE), are electrophilic alkenals closely related to MDA[13] and formed under similar oxidizing conditions[31]. Acrolein (2-propenal) another small molecule electrophile that has multiple origins, can be generated from a variety of organic molecules (*e.g.* carbohydrates, lipids, amino acids, and biodiesel) during oxidation or combustion[32]. Thus acrolein is present in cooked foods, air pollution, and especially cigarette smoke[32]. However not all electrophilic products of lipid oxidation are acyl chain fragments; an intact parent lipid may be oxidized to an electrophile itself. For example, cyclopentenone neuroprostanes are α,β-unsaturated keto products of DHA oxidation. These products are formed *in vivo* by non-enzymatic lipid peroxidation in which an endoperoxide intermediate of DHA is reduced, rearranged, and dehydrated to yield a cyclopentane ring containing an α,β-unsaturated carbonyl[33].

1.2.3.2 Enzymatic Generation of Reactive Electrophilic Species by Oxygenases or from Xenobiotics and Dietary Sources

Fatty acids (*e.g.* arachidonic acid; AA) and other lipophilic molecules are converted to hydroxyl species by oxygenases (*e.g.* COX and LOX enzymes) and can be further metabolized to RES by dehydrogenases[34,35]. Two of the well-characterized electrophilic fatty acid derivatives formed by these pathways are the α,β unsaturated keto electrophiles 15d-PGJ_2 and oxoETEs (see section 1.4.2 for more details). Drugs or other xenobiotics and their metabolites can also be converted to RES. For example, raloxifene, a selective estrogen receptor modulator, is metabolically converted to electrophilic quinoids, which can form adducts with nucleic acids, GSH, and proteins such as cytochrome p450 3A4 (CYP3A4)[36,37]. Additionally non-steroidal anti-inflammatory drugs (NSAIDs) are metabolized, mainly by CYP3A4, to electrophilic quinoid intermediates, which covalently react with GSH and liver microsomal proteins[38].

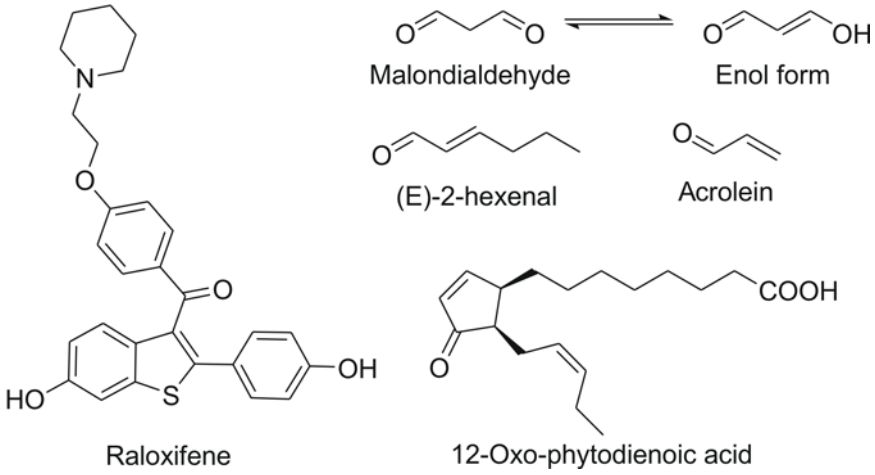

Figure 3. Chemical structures of reactive electrophilic products of oxidation and electrophiles from dietary sources.

RES can also be enzymatically formed in plants and subsequently consumed by animals. The increased production of RES in plants is concurrent with wounding, pathogenesis, and

environmental stress. While many RES are considered secondary metabolites, some act as volatile hormones that ultimately alter gene expression in response to various plant stresses[13,39]. In higher plants, two of the common RES, oxophytodienoic acid (the precursor to jasmonic acid) and (E)-2-hexenal, are produced by plant LOXs. Other phytochemicals with electrophilic or pro-electrophilic capacity include members of the capsaicinoid, isothiocyanates, and triterpenoid families, as well as other secondary metabolites.

Capsaicinoids are a family of secondary metabolites found in chili peppers that interact with mammalian capsaicin receptors (transient receptor potential vanilloid-1 receptor; TRPV1). The metabolism of capsaicinoids by CYP enzymes produces RES that can form covalent adducts with GSH[40]. Capsaicinoid activation of the TRPV1, a calcium channel expressed by sensory nerves, produces a burning sensation, hyperalgesia, erythemia, and irritation. Chronic exposure to capsaicinoids results in anti-inflammatory effects and long-term analgesia via desensitization of TRPV1[41].

Isothiocyanates are another family of phytochemical RES that are generally produced by *Brassica* vegetables (*e.g.* broccoli, cabbage, radish, etc.). Members of this RES family signal through the Keap1/Nrf2 pathway and through transient receptor potential-A1 (TRPA1) ion channels, which are involved in the perception of stimuli including cold temperatures and pungent compounds. Allylisothiocyanate acts as one of the major components responsible for the pungent flavor of mustard seeds and horseradish[42]. Broccoli also produces isothiocyanates such as sulforaphane[43]. Finally, wasabi, while not in the same genius, is a member of the same family as *Brassica* plants and has three isothiocyanates contributing to its flavor: 6-methylthiohexyl isothiocyanate, 7-methylthioheptyl isothiocyanate and 8-methylthiooctyl isothiocyanate[44]. While not an isothiocyanate, cinnamaldehyde, found in the bark of cinnamon trees, contains an α,β-

unsaturated aldehyde, giving it the ability to act as a Michael addition acceptor and a potent activator of TRPA1 as well[42].

A family of electrophilic triterpenoids containing a side chain with two α,β-unsaturated carbonyl groups, avicins, are produced by an Australian desert tree, *Acacia victoriae*. Avicins activate the antioxidant response pathway and have been observed to suppress carcinogenesis[45-47]. Synthetic electrophilic triterpenoid derivatives of oleanolic acid also display anti-inflammatory, antioxidant, and anti-proliferative effects[48-51].

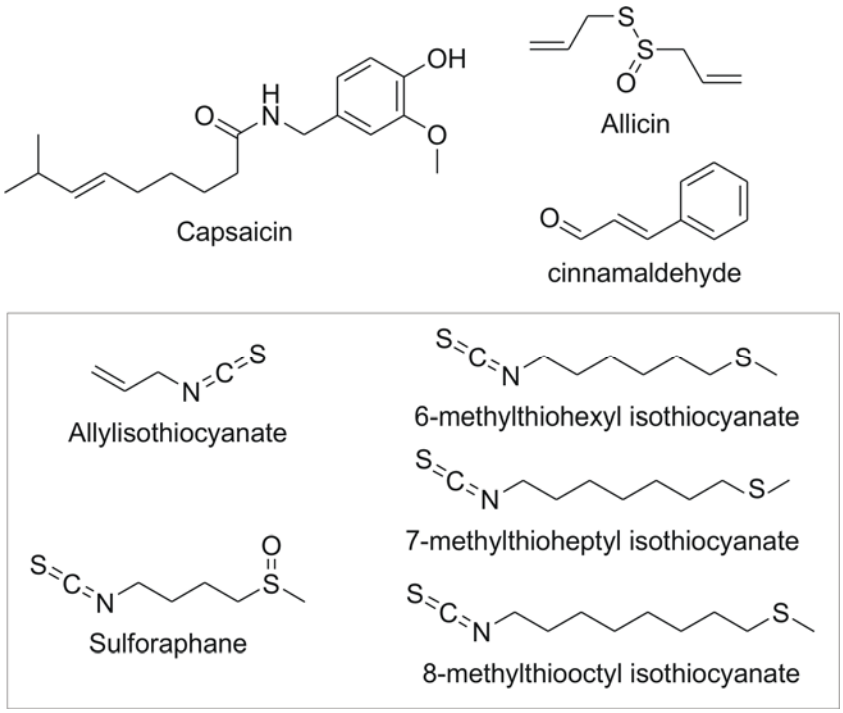

Figure 4. Chemical structures of electrophilic phytochemicals.

1.2.3.3 Electrophile Metabolism: Glutathione and Glutathione S-Transferases

GSH is a water-soluble tripeptide (glutamine-cysteine-glycine) that is an evolutionarily conserved molecule employed by plant, animal, fungal and some prokaryotic cells to combat endogenously or exogenously generated oxidative insult. GSH acts as a reducing agent, in conjunction with glutathione S-transferases (GSTs) and glutathione peroxidases (GPxs), to

detoxify a wide range of RES and peroxides. The thiol group on the cysteine residue in GSH has a pK_a of 9.2[52], limiting spontaneous reaction with RES or ROS at physiologic pHs. However, the high concentration of GSH in cells (~1-8 mM in mammalian tissue[53]) and GST catalyzed reactions significantly increase reaction rates. In order to ensure homeostasis cells must maintain an optimal ratio of GSH (reduced form) to GSSG (oxidized form); the GSH:GSSG ratio establishes the reducing potential of the cell. The reduction of GSSG is catalyzed by GSH reductase and requires NADPH. When GSH levels are low, the rate of GSH synthesis is increased. RES or ROS will induce the uptake of cysteine (the limiting reagent in making GSH) and increase the expression of γ-glutamylcysteine synthetase (γ-GCS), the enzyme before the final step of GSH synthesis.

The promoter regions of γ-*GCS* and *GST* genes contain EpREs that are regulated by the Keap1/Nrf2 pathway, among others. GSTs are part of the family of phase II detoxification enzymes and catalyze the adduction of GSH to endogenous and exogenous electrophilic compounds. Consequently, in the presence of GSTs the rate of reaction of a RES with the thiol of GSH is not as dependent on reactivities and concentrations as it would be with uncatalyzed reactions with other nucleophiles. Human GSTs have two super families: membrane-bound microsomal GSTs and cytosolic GSTs. Microsomal GSTs are involved in the metabolism of leukotrienes and prostaglandins. GPxs use GSH as electron donor to reduce peroxides and produce GSSG as an end product. GSH levels can also determine how a cell responds to signaling molecules; the GSH levels in antigen-presenting cells affects whether cells produce a Th1 or Th2 response [54].

1.2.4 Modification of Phospholipids and Nucleotides

RES react with nucleophilic biomolecules including phospholipids, nucleotides, and amino acid residues in proteins. For example, rabbit lenses exposed to oxidative stress *in vitro* display time-dependent cross-linking between MDA and the amino groups of phospholipids (*e.g.* phosphatidylserine and phosphatidylethanolamine)[55]. RES also react with DNA at low GSH:GSSG ratios, forming adducts with deoxyguanosine, deoxyadenosine, deoxycytidine[8]. Acrolein adducts deoxyguanosine by a Michael-type addition, thus yielding 1,N^2-propanodexoyguanosine *in vitro*[56]. Additionally, acrolein and crotonaldehyde form 1,N^2-propanodexoyguanosine diastereomers and effect base substitution, with G to T transversions being the most common. These adducts also cause, for example, a higher incidence of miscoding in human xeroderma pigmentosum A cells[57,58] and have also been observed in the DNA of liver tissues from healthy humans and rodents[59]. Moreover, during increased oxidative stress, due to the constitutive expression of COX-2, ONE adducts to DNA (heptanone-etheno-2′-deoxyguanosine) were detected in rat intestinal epithelial cells[60]. Finally, bis (2-chloroethyl) sulfide (also known as sulfur mustard or mustard gas), a lipophilic and particularly strong electrophile, forms covalent adducts with DNA (as well as RNA and protein residues) causing DNA damage and fragmentation. In mice and humans nucleic acid alkylation by bis (2-chloroethyl) sulfide contributes to severe toxicity and necrosis of multiple tissues including the liver[61].

1.2.5 Modification of Proteins and Protein Cross-Linking

RES post-translationally modify proteins by adducting to cysteine, histidine, and lysine residues, thus modulating protein function, subcellular location, and turnover. A classic example of all three of these actions is the modulation of the Keap1/Nrf2 pathway by RES (see section 1.2.6.3). RES protein modifications can also interfere with cytoskeletal structure; *in vitro* actin polymerization can be disrupted by 15d-PGJ_2 adduction to actin at Cys374[62].

RES-protein adducts modulate the activity and trafficking of other redox-sensitive proteins. OA-NO_2 forms reversible adducts with glyceraldehyde-3-phosphate dehydrogenase (GAPDH) at the catalytic Cys-149 (as well as other residues), thus inhibiting GAPDH activity and increasing its affinity for lipophilic environments, such as membranes[18]. Biotinylated-15d-PGJ_2 forms adducts with thioredoxin-1 (Trx1) at Cys35 and Cys69 *in vitro* as determined by mass spectrometry[63]. The enzyme responsible for maintaining a population of reduced Trx, Thioredoxin reductase (TrxR), is crucial for the proper structure and function of several redox-sensitive proteins, including p53. TrxR is especially susceptible to adduction by RES due to the low pK_a (5.2) of a selenocysteine in its C-terminal sequence[64]. This selenocysteine residue, while not present in the TrxR active site, is necessary for catalytic activity[65]. In RKO and HCT 116 cell lines, adduction of PGA_1 amidopentyl biotin (and other α,β-unsaturated carbonyl compounds such as HNE) to TrxR occurs concurrently with inhibition of p53 function[7].

RES that can undergo oxidation-reduction cycling (quinones) and bifunctional RES (*e.g.* HNE and ONE) readily generate intermolecular or intramolecular protein cross-links. Both the functional group and microenvironment determine the pK_a of nucleophilic amino acid residues, with lower pK_as will promote the possibility of adduct formation via nucleophilic attack. Structural motifs in proteins, such as cytochrome c, also determine the susceptibility and type of

adduct formation for amino acid residues[66]. For example, RES can cross-link solvent-exposed lysine residues in close proximity to each other, such as in the case of benzoquinone, which can adduct with proximal lysine residues (Lys25-Lys27 and Lys86-Lys87) on cytochrome c[66].

1.2.6 Electrophile Signaling

The properties of RES confer inherent signaling capabilities. However, each RES may result in distinct signaling depending on reactivity and structure; sets of genes that are activated by one type of RES may overlap with some of those activated by another. As Farmer notes[13], "transcriptome responses induced by treatment with one particular electrophile do not necessarily indicate that this RES is the *bona fide* regulator of the genes in question and indicates only that the genes are sensitive to RES." The vast majority of RES can modulate transcription through the Keap1/Nrf2 pathway, which regulates the electrophile response element/antioxidant response element (EpRE/ARE). Related to this issue, the EpRE-independent pathways of RES signaling will also be addressed.

1.2.6.1 Signaling Pathways Not Directly Related to the Electrophile Response Element

RES modulate several cell signaling pathways, including the heat shock response, apoptotic pathways, kinase/phosphatase activities, and nuclear transcription factors. Heat shock proteins (Hsps) are one of the cellular targets of RES. HNE, generated during oxidative stress, covalently modifies cysteine residues on Hsp72 (Cys267) and Hsp90 (Cys572) as confirmed by LC-MS/MS. In the case of Hsp72 (but not Hsp90), HNE adduction with Cys267 inhibited its ATPase activity[67,68]. HNE also disrupts the interaction between Hsp70-1 and heat shock factor 1 (HSF1) thus allowing HSF1 translocation to the nucleus and subsequent activation of transcription of

heat shock response genes[69]. RES can also induce the apoptotic pathway at higher concentrations. For example, HNE induces time- and concentration-dependent apoptosis via activation of the c-Jun N-terminal protein kinase (JNK) pathway. HNE activates JNK by first activating apoptosis signal-regulating kinase (ASK1), which phosphorylates stress-activated protein kinase (SEK1), an upstream kinase of JNK[70].

Kinase pathways such as the extracellular-signal regulated kinase-1/2 (Erk-1/2) pathway and the p38 mitogen-activated protein kinase (p38 MAPK) pathway are modulated by RES. HNE decreases Erk-1/2 phosphorylation and activity in primary rat hepatocytes by adducting to His178 on Erk-1/2[71]. Additionally, HNE potently induces COX-2 gene expression in RAW264.7 cells via activation of the p38 MAPK pathway and stabilization of COX-2 mRNA[10]. Finally, the protein serine/threonine phosphatase 2A (PP2A) shows decreased activity in HEK 293 cells upon alkylation of six cysteine residues by the biotin-labeled Michael addition acceptor, biotinamido-4-[4′-(maleimidomethyl) cyclohexanecarboxyamido]butane[72].

RES also modulate the activities of nuclear receptors and transcription factors such as PPARγ and NF-κB, both of which are involved in the regulation of inflammation. PPARγ is activated by 15d-PGJ_2, NO_2-FA, and other RES (see section 1.3.2 for more details). Many RES inhibit NF-κB signaling at one or more points in the pathway. For example, in RAW264.7 murine macrophages, A_4-NP, a cyclopentenone neuroprostane, significantly reduces LPS-induced iNOS expression and subsequent $^{\bullet}NO$ production (as measured by nitrite levels in the media) via inhibition of NF-κB signaling[73]. The expression of COX-2 was also reduced though not to the same extent as iNOS, which was attributed to the regulation of COX-2 by several pathways in addition to NF-κB. In luciferase reporter assays A_4-NP was found to inhibit NF-κB-mediated transcription induced by LPS, as well as TNFα and IL-1β, all of which activate IKK

and NF-κB via different receptors and mechanisms[73]. Further probing into the NF-κB pathway identified adduction of A_4-NP to Cys179 of Iκ-kinase (IKK) as the likely cause of inhibition; adduction to IKK prevents the phosphorylation and degradation of IκBα, an inhibitor of the NF-κB p65 subunit that prevents translocation to the nucleus[73]. NO_2-FA also inhibit LPS-stimulated NF-κB-mediated transcription in RAW264.7 cells transiently transfected with a NF-κB-luciferase reporter construct. The use of biotinylated NO_2-FA, immunoprecipitation, and mass spectrometry-based strategies further identified p65 as the covalently modified protein and the most likely point of NO_2-FA inhibition of the NF-κB pathway[74]

1.2.6.2 Electrophile Response Element Mediated Signaling

The EpRE is a *cis*-acting element in the regulatory region of over 200 genes[16] that assist in the response to oxidative or xenobiotic stresses. Some of the xenobiotic/drug metabolizing proteins and antioxidant proteins under EpRE regulation are GSTs, NAD(P)H-quinone oxidoreductases 1 (NQO1), heme-oxygenase-1(HO-1), subunits of γ-GCS, glutamate-cysteine ligase (GCL), and thioredoxin[6,75].

The metabolism of xenobiotics has been described as a two-phase process. During phase I, compounds are modified with new functional groups by oxidation, reduction and/or hydrolysis reactions. During phase II, the products of phase I are conjugated to molecules such as GSH or glucuronic acid, producing metabolites that are more hydrophilic and more easily exported and excreted[76]. Inducers of the ARE/EpRE can be monofunctional or bifunctional. Bifunctional inducers up-regulate the activities of both phase I and phase II enzymes, while monofunctional inducers only up-regulate the activities of phase II enzymes. There are up to ten major chemical classes of monofunctional inducers and among these are Michael reaction acceptors (including

RES and divalent metal cations such as Hg^{2+}, Cd^{2+}, and Zn^{2+}), hydroperoxides, phenolic antioxidants (BHA, BHT), 1,2-dithiole-3-thiones, and isothiocyanates. Monofunctional inducers typically activate phase II gene expression by reacting with sulfhydryl or disulfide groups, resulting in alkylation, oxidation, reduction, or thiol interchange. Thus Michael reaction acceptors (RES) are one subgroup of this inducer family[6,23].

1.2.6.3 The Role of Nuclear Factor-Erythroid 2-Related Factor 2 and Kelch-Like ECH Associated Protein 1 in Electrophile Response Signaling

One of the major transcriptional regulators of EpRE-dependent genes is the transcription factor Nrf2 (a.k.a. chicken erythroid-derived CNC-homology factor; ECH). Nrf2 is a member of a "Cap 'n' collar" (CNC) subfamily of basic-region leucine zipper proteins (bZIP) including NF-E2, Nrf1 and Nrf3. In order to bind to DNA, members of this subfamily, including Nrf2, heterodimerize with members of the Maf family (another family of bZIP transcription factors), as Maf recognition elements are often located near EpREs. Heterodimerization occurs via basic leucine repeat regions[6,23]. Nrf2 is turned over rapidly by the proteasome under basal conditions, but its half-life can be extended in the presence of RES. This is due to RES-induced disruption of binding between Nrf2 and its partner Keap1. Keap1 recruits Cul3 (an E3 ubiquitin ligase) to the Keap1/Nrf2 complex, allowing the ubiquitination of Nrf2. Keap1 directly binds Nrf2 at an ETGE tetrapeptide motif in the evolutionarily conserved N-terminal domain (the Neh2 domain) of Nrf2, thus targeting Nrf2 for proteasomal degradation[77]. By modifying Keap1, RES and ROS prevent the ubiquitination of Nrf2 and thus stabilize newly produced Nrf2, which can then activate EpRE-dependent genes[78].

Some of the major and most well studied sulfhydryl sensors in animal cells are located on Keap1. Keap1 is a dimeric metalloprotein with five major domains: 1) the N-terminal region, 2)

the BTB domain (a conserved protein-protein interaction domain), 3) the intervening region (IVR), 4) the double glycine repeat (Kelch domain) and 5) the C-terminal region. Keap1 binds the Neh2 domain of Nrf2 and actin through the Kelch domain[77]. Although the subcellular localization of Keap1 has not been definitively identified, based on immunocytochemical and immunoprecipitation studies Keap1 appears to localize near the nuclear periphery on the actin cytoskeleton and colocalizes with F-actin[6,79]. Murine Keap1 has twenty-five cysteines, nine of which are especially nucleophilic due to the presence of neighboring basic residues. These twenty-five cysteines are conserved in human Keap1. While twenty-three of these cysteine residues can react with RES, only six (Cys151, Cys257, Cys273, Cys288, Cys297 and Cys613) are most often reported to react with RES in cells[16,23]. Site-directed mutagenesis studies have demonstrated that Cys273 and Cys288 in the IVR of Keap1 (but not Cys257 or Cys613) are required for Keap1-mediated ubiquitination of Nrf2 and subsequent Nrf2 repression[6,23,80]. Additionally, Cys151 in the Keap1 BTB domain is required for inhibition of Keap1-dependent degradation of Nrf2 by sulforaphane and oxidative stress[80].

1.3 NITRATED FATTY ACIDS

The oxidative and free radical microenvironment of inflammation promotes oxidation, nitrosation, and nitration reactions by nitric oxide ($^{\bullet}NO$)-derived reactive species. While oxidized PUFA and most eicosanoids are pro-inflammatory mediators, nitro (NO_2) derivatives of unsaturated fatty acids (NO_2-FA) have emerged as endogenous anti-inflammatory messengers. For example, nitroalkene derivatives of oleic acid (OA-NO_2) and linoleic acid (LNO_2) induce a broad spectrum of biochemical, cellular and *in vivo* anti-inflammatory responses[74,81-86].

1.3.1 Biosynthesis and Detection of Nitrated Fatty Acids

In addition to concentrating O_2 and lipophilic nitrogen oxides (*i.e.* $^{\bullet}NO$ and N_2O_3), the hydrophobic environment of biological membranes facilitates and accelerates nitration, oxidation, and nitrosation reactions. This "molecular lens" influences the reaction rates and product profiles of $^{\bullet}NO$-derived species not only by promoting their accumulation, but also by providing an aprotic interior and unfavorable conditions for their hydrolysis[87]. Thus, it is not surprising that nitrated lipids have been identified *in vivo*. In the presence of $^{\bullet}NO$ and nitrite lipoxygenase-catalyzed oxidation of low-density lipoprotein (LDL) yields nitrogen-containing derivatives of oxidized lipids[88,89]. Free and esterified PUFA, such as arachidonate and linoleate, are especially predisposed to the formation of both reactive intermediates and bioactive products. $^{\bullet}NO$ can react with peroxidizing lipid mixtures to terminate radical chain propagation reactions and yield nitrogen-containing lipid species (see **Fig. 5**)[90]. Nitrated fatty acid derivatives of oleic ($OA\text{-}NO_2$), linoleic (LNO_2), linolenic, arachidonic ($AA\text{-}NO_2$) and eicosapentaenoic acids have been identified in mammals. Moreover, nitrated derivatives of unsaturated fatty acids are present in healthy human blood[83,91], and nitrohydroxy derivatives of arachidonate and linoleate have been detected in bovine cardiac tissue and in healthy human plasma and lipoproteins, respectively[83,92].

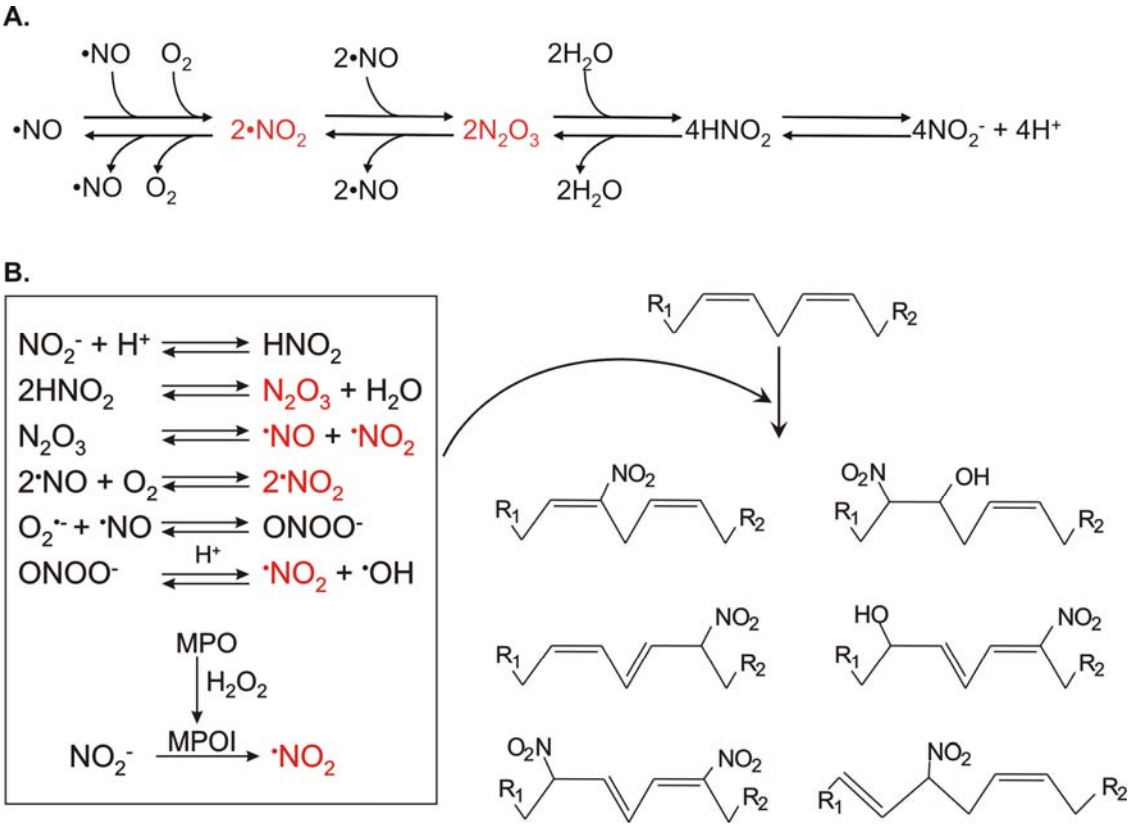

Figure 5. Multiple mechanisms can lead to the nitration of lipids.

(A) Reactive intermediates from autoxidation of •NO and acidification of nitrite. Under aerobic conditions •NO can react rapidly with O_2 to form •NO_2. When the O_2 concentration is significantly lower than atmospheric conditions, •NO_2 and •NO can be in equilibrium with N_2O_3. In aqueous milieu, N_2O_3 can be in equilibrium with HNO_2. Finally, HNO_2 is in equilibrium with is conjugate base NO_2^- (pKa=3.35). As all of these reactions are reversible, their order and equilibria depend on the source and site of production of NO_X, the concentrations of various intermediates, and their reaction with other biomolecules. (B) Biologically relevant reactions forming NO_X (in red) and potential NO_2-FA products resulting from reaction of polyunsaturated fatty acids with NO_X and reactive oxygen species.

1.3.2 Biological Activity of Nitrated Fatty Acids

Nitrated PUFA have unique chemical and signaling properties. LNO_2, chlolesteryl nitrolinoleate, and nitrohydroxylinoleate potentiate vasorelaxation in a concentration-dependent manner via

•NO release[92,93]. Nitrohydroxyarachidonate has also been identified as an endogenous mediator of vascular relaxation by releasing •NO and activating soluble guanylate cyclase[92]. The decay of LNO_2 also releases •NO, thus stimulating cGMP-dependent vessel relaxation[94]. In addition to serving as •NO donors, nitroalkene derivatives of PUFA can act as ligands for nuclear receptors responsible for regulating lipid metabolism and inflammation; LNO_2 is a potent ligand for PPARγ ($K_i \approx 133$ nM), and can activate the receptor within physiological concentration ranges[81,85]. The chemical properties of nitroalkenes greatly contribute to their ability to release •NO and act as unique ligands for nuclear receptors. •NO has been hypothesized to be released from nitroalkenes by a modified Nef reaction or by the isomerization of nitrite derivatives that undergo homolytic scission and/or transition metal-catalyzed reduction[93,95]. Additionally, LNO_2 has been shown to incorporate readily into the hydrophobic environment of biological membranes where it is stabilized by the aprotic environment[95]. NO_2-FA can also form adducts with H_2O via Michael addition to yield the corresponding nitrohydroxy-fatty acid[81,95]. This reaction explains the observation of coexisting nitroalkene and nitrohydroxy derivatives of fatty acids[81]. The same electrophilic carbon β to the nitro group in nitroalkenes (**Fig. 1**) that reacts with water also allows nitroalkenes to form adducts with nucleophilic amino acid residues in proteins (*i.e.,* cysteine and histidine) via the Michael addition reaction. Nitroalkene-protein adducts have been identified in healthy human red cells and nitroalkenes inhibit the enzymatic activity of glyceraldehyde-3-phosphate dehydrogenase (GAPDH) at physiologically relevant concentrations by covalent adduction to Cys-149[18]. In terms of other nitroalkene-protein adducts, NO_2-FA inhibit TNFα and LPS-induced macrophage activation by nitroalkylation of p65[74], inactivate xanthine oxidoreductase[96], and activate Keap1/Nrf2-dependent gene expression[97].

1.3.3 Modulation of Peroxisome Proliferator Activated Receptor-γ

In addition to serving as electrophilic signaling mediators, OA-NO_2 and LNO_2 bind to PPARγ, initially displaying a K_i (K_i LNO_2≈ 133 nM) similar to the agonist Rosiglitazone as determined by competition binding analysis of radiolabeled Rosiglitazone displacement from PPARγ[81,95]. PPARγ is a nuclear receptor expressed in a variety of cells/tissues including brown and white adipose tissue, vascular smooth muscle, and macrophages. It regulates lipid metabolism and storage, glucose uptake, and cell proliferation/differentiation[98-101]. As such, PPARγ plays an important role in both the development and treatment of Type II diabetes and hypertension[102,103]. Specifically, a mutation (P467L or V290M) in helix 12 of the ligand binding domain (LBD) of human PPARγ is associated with severe insulin resistance and results in the onset of juvenile Type II diabetes and hypertension[104]. As a ligand-dependent transcription factor, the ligand binding domain (LBD) of PPARγ accommodates a wide variety of ligands ranging from endogenous lipids to synthetic anti-diabetic drugs such as the thiazolidinediones (TZDs)[105]. Most proposed "natural" PPARγ ligands are intermediates of lipid metabolism and oxidation that bind with low-affinity at concentrations orders of magnitude greater than those found physiological conditions. This suggests that while naturally occurring compounds may activate PPARγ *in vitro*, they are probably not responsible for PPARγ activation *in vivo*. Among these natural ligands are saturated and unsaturated free fatty acids (palmitic acid; K_d= 156 μM and linoleic acid; K_d= 1 μM [106])[107,108], prostaglandins (15-deoxy-prostaglandin-J_2; 15-ΔPGJ_2; K_d≈ 300 nM[109,110]), leukotrienes and other oxidized lipid derivatives (9- and 13 hydroxy-octadecadienoic acid; K_d= 10-20 μM[111] and epoxyeicosatrienoic acids; K_d= 1.1-1.8 μM[112])[107,111], and lysophosphatidic acid[113]. Synthetic TZD ligands, such as Rosiglitazone (K_d= 40 nM-70 nM)[114,115], bind PPARγ avidly and have been shown to effectively increase insulin sensitivity via PPARγ signaling

pathways[116-118]. By activating PPARγ, TZDs restore insulin sensitivity to alleviate many of the symptoms associated with diabetes.

1.4 OMEGA-3 FATTY ACID AND EICOSANOID SIGNALING

Omega-3 PUFAs (ω-3-PUFAs) are a family of fatty acids in which the third carbon from the methyl end of the fatty acid is unsaturated. Because mammals lack the metabolic machinery to synthesize ω-3-PUFA, these fatty acids are considered vital dietary components and are also included in the category of essential fatty acids. Three of the most well characterized ω-3-PUFA are α-linolenic acid (ALA; 9,12,15-18:3), eicosapentaenoic acid (EPA; 5,8,11,14,17-20:5), and docosahexaenoic acid (DHA; 4,7,10,13,16,19-22:6). The salutary health effects of these ω-3-PUFA have been attributed to multiple mechanisms.

1.4.1 Benefits of Omega-3 Polyunsaturated Fatty Acids

The major ω-3-PUFA EPA and DHA have been associated with numerous beneficial health effects in humans. In particular, brain and retina tissues are enriched with DHA in healthy individuals and DHA is considered necessary for the normal development and function of these tissues[119,120]. The consumption of DHA in the diet has been implicated in reducing neurocognitive decline[121], improving insulin resistance in diabetics[122], decreasing incidence of cardiovascular risks such as myocardial infarction[123] (as determined by the GISSI trial), and reducing inflammation[124]. Moreover, ω-3-PUFA intake has been associated with decreased risk of aggressive prostate cancer via modulation of COX-2[125]. EPA and DHA are thought to have

anti-inflammatory effects by acting as competitive inhibitors of COX-generated arachidonic acid-derived pro-inflammatory prostanoids, and the subsequent production of ω-3 prostanoids with an ability to induce vasodilation and to inhibit platelet aggregation[126]. In terms of phagocytic immune cells, such as macrophages and neutrophils, the supplementation of DHA and EPA in the diet of healthy human volunteers was found to significantly increase phagocytic activity[127]. Additionally, the oxidized metabolites of ω-3-PUFA also exhibit beneficial biologic activities.

1.4.2 Oxidation of Fatty Acids

The oxidation of PUFA was reported as early as the 1900s while the knowledge of lipid oxidation dates back even further. The study of the free radical mediated oxidation of lipids is a well-established field (more than 60 years old), in which the autoxidation of DHA and the generation of 10 different positional isomers of hydroxy-DHA were described as early as the 1980s[128,129]. Several recently emerging classes of lipid mediators can be formed by enzymatic (*e.g.* oxygenases) or non-enzymatic oxidative processes and have demonstrated robust anti-inflammatory signaling activities. Among these are NO_2-FAs, resolvins, neuroprotectins, maresins, neuroprostanes and lipoxins (LXs, **Fig. 6**). For example, oxygenases, *i.e.* COX and LOXs, are one of the first catalytic mediators in the generation of resolvins; the COX oxidation products of DHA and EPA can be converted to the D (RvD) and E (RvE) series of resolvins respectively[130,131]. Signaling lipids, such as prostanoids (*i.e.,* PGs and thromboxanes, TXs), can mediate processes involved in the promotion or inhibition of inflammation[132,133], while in contrast, lipids such as NO_2-FAs, resolvins, neuroprotectins and neuroprostanes promote anti-inflammatory signaling effects. Both NO_2-FA[74] and neuroprostanes[73] suppress

lipopolysaccharide (LPS)-induced activation of the NF-κB pathway in macrophages via electrophilic activities. Additionally, RvE1 inhibits the production of proinflammatory cytokines in dendritic[134] cells via G-protein coupled receptor (GPCR) interactions[135].

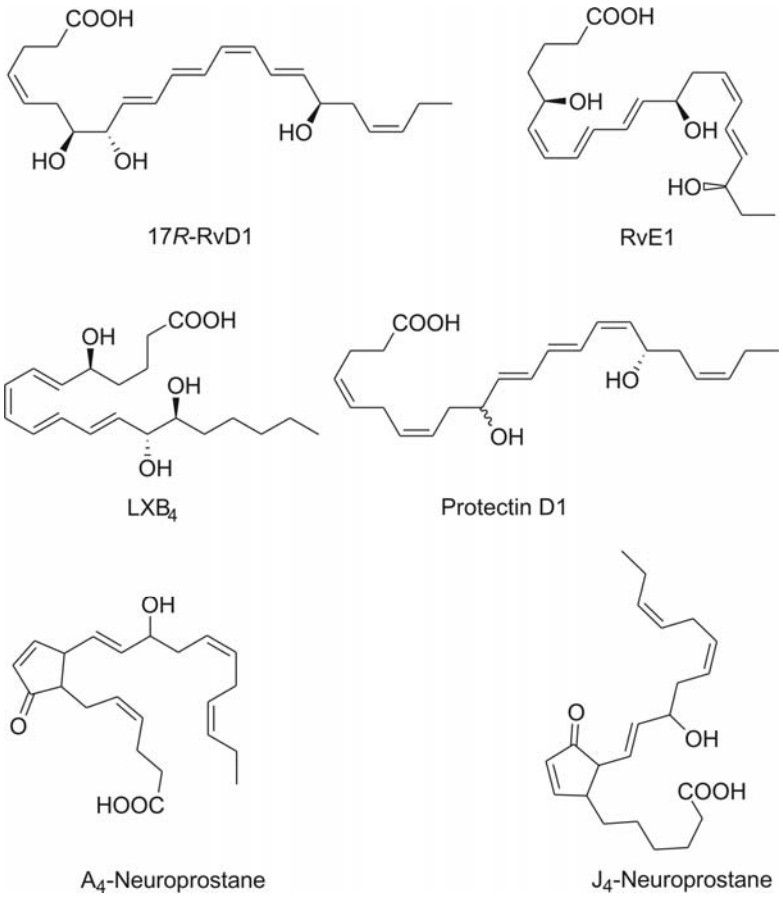

Figure 6. Chemical structures of oxidized lipids with anti-inflammatory signaling capabilities.

1.4.3 Biological Activity of Oxidized Fatty Acids

PGs, TXs, leukotrienes and hydroxy-eicosatetraenoic acids (HETEs) are subclasses of oxygenated PUFA collectively known as eicosanoids. Prostanoids are formed via the

cyclooxygenase pathway in which COXs catalyze the committed oxygenation step. In mammals, arachidonic acid (AA; 20:4, ω-6) is the major eicosanoid precursor and substrate for COX[132,133,136,137]. Four double bonds confer a proclivity to AA for reaction with O_2 and are critical elements of both enzymatic and non-enzymatic oxygenation reactions[138]. AA is converted by COX to PGH_2, which is the common substrate for a series of specific synthase enzymes that produce PGD_2, PGE_2, $PGF_{2\alpha}$, PGI_2 and TXA_2. Depending on the types of prostanoids and receptors present, these signaling lipids can mediate processes involved in the promotion or inhibition of inflammation including pain, fever, and regulation of vascular tone[133]. Classical PG signaling occurs via plasma membrane-derived GPCRs. Alternative PG signaling occurs via nuclear receptors (*e.g.,* 15d-PGJ_2)[12,14]. PGA_2 activates PPARγ, inhibits IκB kinase activity, and is generally thought to down-regulate angiogenesis[110,139,140]. Certain PG derivatives of the COX-2 pathway activate signaling cascades involved in inflammation, pain and fever. These derivatives have been identified in tissues damaged by chronic inflammation. For example, PGE_2 and PGI_2 have been detected in synovial fluid from knee joints of arthritic patients, rat models of carrageenan-induced paw edema and inflammatory lesions. Both have been implicated in mediating nociceptive responses to hyperalgesic agents and in potentiating erythema [132,133,136].

1.5 CYCLOOXYGENASE

COXs (also known as Prostaglandin H synthases (PGHS)) catalyze the two major reactions that convert AA to PGH_2. In the first reaction, the cyclooxygenase activity of COX catalyzes the bis-oxygenation and cyclization of AA to yield the endoperoxide-containing prostaglandin G_2

(PGG_2). In the second reaction, a separate peroxidase (POX) active site on the enzyme reduces the hydroperoxyl group of PGG_2 to a hydroxyl, thus forming PGH_2. Various bioactive prostaglandin derivatives are subsequently produced by isomerases and oxidoreductases using PGH_2 as a substrate [132,136,137,141]. The genes coding for COX are highly conserved, having been identified in both vertebrate and invertebrate species[132]. The two major isozymes of COX, COX-1 and COX-2, are active as homodimers and require a heme prosthetic group. Both isozymes consist of approximately 600 amino acids in all species, and within the same species COX-2 possesses 60% amino acid identity with COX-1. The sequences and structures suggest that both enzymes localize to the lumen of the nuclear envelope and endoplasmic reticulum, and this subcellular localization is thought to play a role in transporting COX products to their receptors. COX-1 and COX-2 have been shown to traffic within the nucleus following a variety of stimuli, and localization of COX isozymes in lumen of the ER is supported by numerous immunocytochemical studies[142-144]. COX-2 localizes primarily to the nucleus, but it also localizes to caveolin-1-containing vesicles in bovine arterial endothelial cells treated with phorbol ester or human fibroblasts treated with either phorbol ester or IL-1[145,146].

1.5.1 Cyclooxygenase Structure

The structures of COX-1 and COX-2 consist of four major domains: an amino-terminal signal peptide, a dimerization domain, a membrane binding domain, and a carboxy-terminal catalytic domain that comprises 80% of the protein (**Fig. 7**[147]). The amino-terminal hydrophobic signal peptide directs nascent COX polypeptides into the lumen of the ER where the signal sequence is cleaved. Once the nascent peptide is folded, COX enzymes dimerize via hydrophobic interactions, hydrogen bonding and salt bridges between the dimerization domains of each

monomer. The dimerization domain consists of approximately 50 amino acids adjacent to the amino terminus of the protein. Three disulfide bonds maintain the structure of the dimerization domain, while a fourth links the dimerization domain to the globular catalytic domain. A tandem series of four amphipathic helices immediately carboxy-terminal to the dimerization domain are responsible for the attachment of COX isozymes to the upper portion of the hydrophobic core of lipid bilayers[132,141,147].

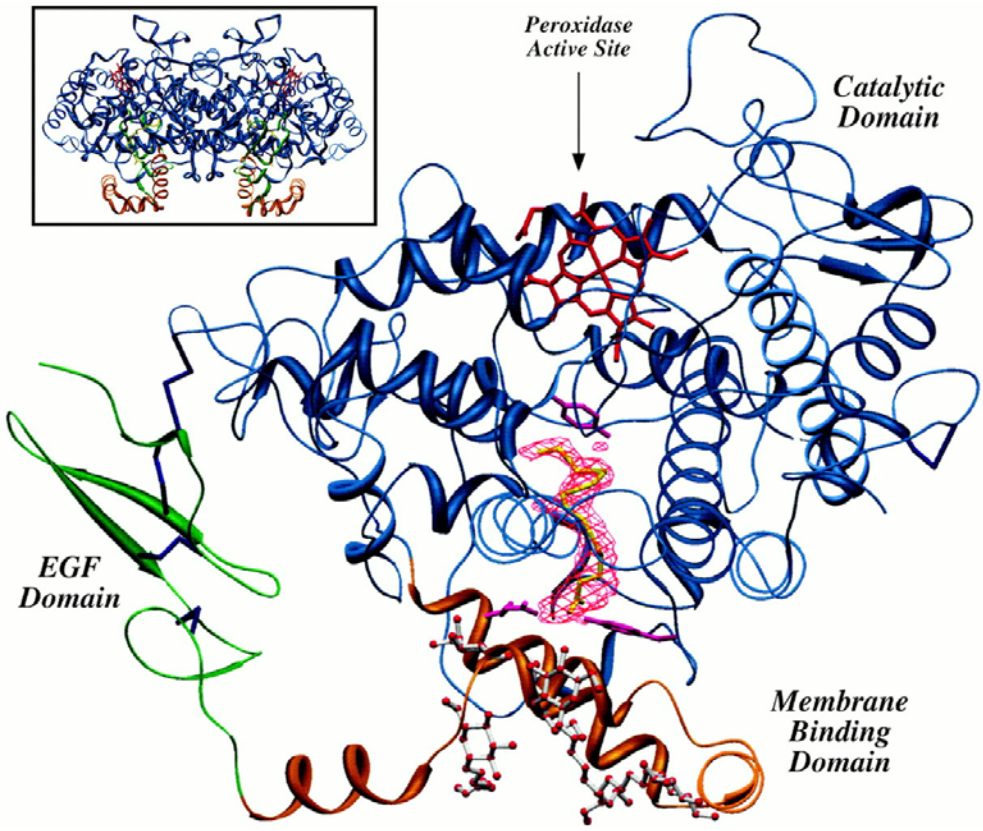

Figure 7. Ribbon diagram of arachidonic acid bound to ovine cyclooxygenase-1.

Figure also depicts the four major domains of COX-1 and a model of the COX-1 dimer[147]. From Malkowski, M.G., *et al*. The productive conformation of arachidonic acid bound to prostaglandin synthase. *Science* **289**, 1933-1937 (2000). Reprinted with permission from AAAS.

1.5.2 Cyclooxygenase Catalytic Domain

In addition to tethering COX to the membrane, the same four amphipathic helices of the membrane binding domain form the opening of a hydrophobic channel that constitutes the cyclooxygenase active site. One crucial structural difference between the COX-1 and the COX-2 cyclooxygenase channel is the substitution of isoleucine 523 in COX-1 for a valine in COX-2 (numbering uses ovine COX-1 as a reference). This substitution opens a hydrophobic out-pocketing in COX-2 that can be utilized by some COX-2-selective NSAIDs. The enlarged cyclooxygenase active site in COX-2 may explain why COX-2 recognizes more bulky substrates and has different reactivities with lipid substrates than COX-1. COX-2 efficiently oxidizes endocannabinoids (*e.g.,* anandamide (arachidonylethanolamide) and 2-arachidonylglycerol) as efficiently as the less bulky AA. Thus, COX-2 can produce endocannabinoid-derived endoperoxides, which can be utilized by downstream prostaglandin isomerases. COX-2 activity is further linked with endocannabinoid metabolism by the fact that the endocannabinoid analogue methanandamide up-regulates COX-2 expression [132,141]. The catalytic domain of COX also possesses POX activity. An iron-histidine bond involving His388 (ovine COX-1) coordinates the heme group of the POX cleft. The orientation of heme-binding exposes a large portion of one face of the heme to the open cleft allowing interaction with PGG_2 and other lipid peroxides[132,141].

1.5.3 Mechanism of Prostaglandin H_2 Synthesis by Cyclooxygenases

Over 50 hydrophobic interactions with 19 amino acid residues coordinate COX substrates (*i.e.,* AA) for hydrogen abstraction and facilitate conversion to PGG_2[148]. Arg120 assists in

coordinating the substrate by binding the arachidonyl carboxylate[147]. Endogenous radicals are believed to be required to activate COX holoenzymes by inducing the formation of a tyrosyl radical at Tyr385. Oxidation of Tyr385 by the heme radical is believed to be responsible for generating the Tyr385 radical[132,137,141]. Following initial COX activation the Tyr385 radical is regenerated with each catalytic event (**Fig. 8**[132], from Simmons, 2004).

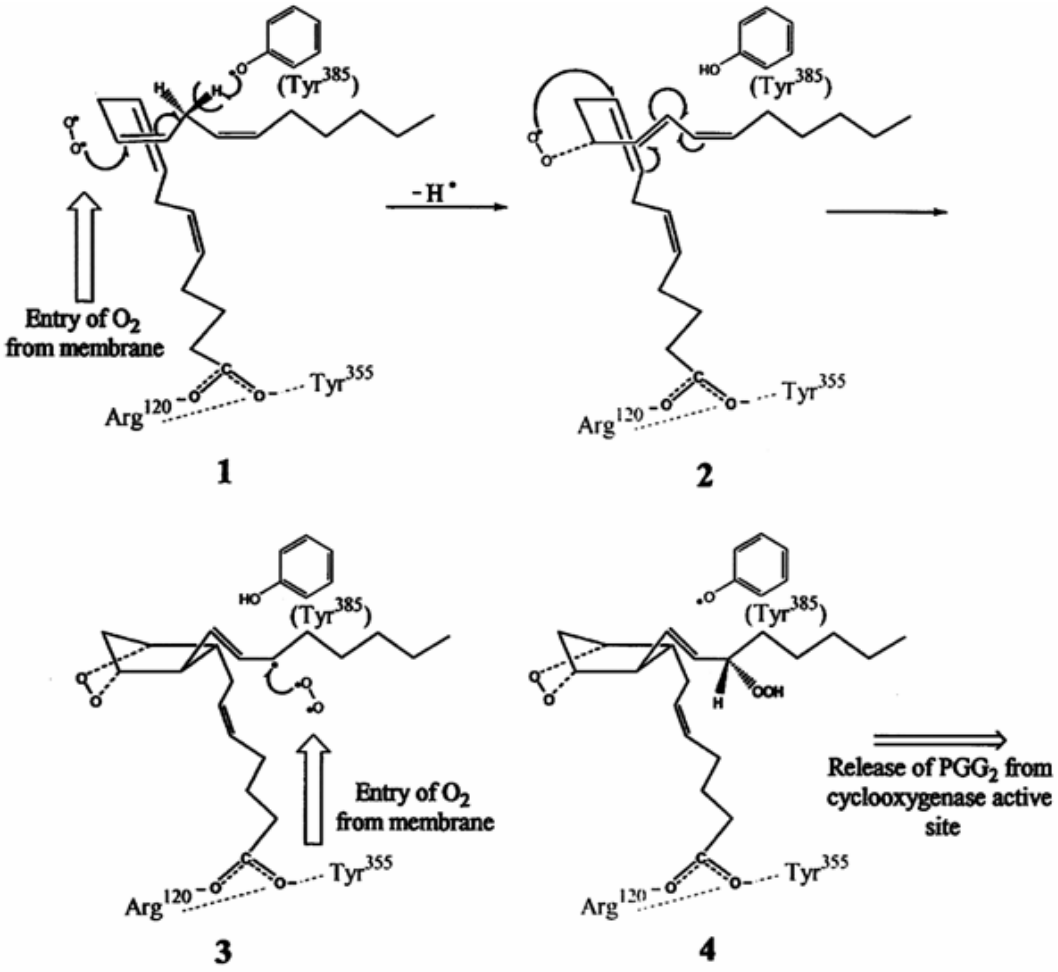

Figure 8. The molecular mechanism of prostaglandin G_2 formation from arachidonic acid in the cyclooxygenase active site is dependent on Tyrosine 385 radical formation and regeneration.

From Simmons D.L., *et al*. Cyclooxygenase Isozymes: The Biology of Prostaglandin Synthesis and Inhibition. *Pharmacol Rev* **56**, 387-437 (2004). Reprinted with permission from ASPET.

Once the Tyr385 tyrosyl radical has been formed, it abstracts the hydrogen from the pro-S-face of carbon 13 of AA producing an activated arachidonyl radical. Following hydrogen abstraction, the 11*R*-peroxyl radical is formed by the addition of O_2. The 11*R*-peroxyl radical then attacks carbon-9, which forms the endoperoxide and induces the isomerization of the radical to carbon-8. Concomitant formation of the endoperoxide bridge between carbon-11 and carbon-9 and rearrangement of the substrate induces ring closure between carbon-12 and carbon-8. This rearrangement produces a carbon-centered radical at carbon-15 allowing for the addition of a second molecule of O_2. Finally, the 15*S*-peroxyl radical is aligned below Tyr385 and abstracts a hydrogen radical to regenerate the Tyr385 radical. Thus, the cyclooxygenase active site requires the heme of the POX active site for initial activation and only after activation can the cyclooxygenase site function independently of the POX site. This model suggests that the POX site can act independently of the cyclooxygenase active site, an event which is observed when the cyclooxygenase site is inhibited by NSAIDs. Two molecules of O_2 are consumed during a controlled free radical chain reaction converting AA to PGG_2 by the cyclooxygenase site[149]. PGG_2 is then released from the cyclooxygenase site and travels to the POX site, which catalyzes a two-electron reduction of the 15*S*-hydroperoxyl group to an alcohol yielding PGH_2 [132,137,141].

1.5.4 Cyclooxygenase Inhibition

The COX cyclooxygenase channel accommodates a variety of compounds; some of which act as inhibitors (*e.g.* *N*-(Carboxyalkyl)maleimides), while others, such as arachidonylethanolamide, 2-arachidonylglycerol, and other arachidonate ester or amide derivatives, are oxidized as substrates by COX-2. When exposed to concentrations of AA that approach V_{max}, COX isozymes have relatively short half-lives (<1-2 minutes). One popular

explanation for this event is the attachment to and subsequent inactivation of COX by arachidonyl peroxides and other reactive species (*e.g.,* MDA) generated by COX activity. Furthermore, COX-2 possesses 13 cysteines that are accessible to post-translational modifications and one of these 13 (Cys526) is known to increase enzyme activity upon modification by $^{\bullet}NO$[150]. Interestingly, COX-2 activity is significantly decreased upon electrophilic maleimide modification of two COX-2 cysteine residues (Cys540 and Cys313) located on the catalytic domain outside of the active sites[151,152]. COX can also be inhibited by non-steroidal anti-inflammatory drugs (NSAIDs), which are a family of chemically distinct compounds representing one of the most important and most widely used groups of over-the-counter and prescribed pharmaceuticals[132,136]. The general therapeutic benefits of NSAIDs include inhibition of swelling and/or pain at the site of inflammation, though individual NSAIDs may each have their own favorable side effects; for example, ASA in addition to its actions as an NSAIDs, protects against stroke and thrombosis, Alzheimer's disease and some cancers independently of COX inhibition. ASA is the only NSAID in medical use that covalently modifies COX-1 and COX-2. NSAIDs other than ASA inhibit COX activity by competing with AA for binding the cyclooxygenase active site. Inhibition by some NSAIDs occurs almost instantaneously, while inhibition by other NSAIDs is time-dependent. Ibuprofen is one such NSAIDs that has a rapid on and off rate, readily binding to and dissociating from the cyclooxygenase active site. Time-dependent inhibition of COX by NSAIDs is characterized by the amount of time the compound remains in contact with the enzyme[153]; time-dependent NSAIDs (*e.g.,* indomethacin and the COX-2 selective inhibitors celecoxib and rofecoxib) require seconds to minutes to bind the cyclooxygenase active site, and once bound may require hours to dissociate [132,154].

1.6 SIGNIFICANCE

Inflammation is intimately involved in the pathogenesis of important clinical problems including atherosclerosis, diabetes, asthma, respiratory distress syndromes, carcinogenesis, and arthritis. NO_2-FA display anti-inflammatory signaling properties and can be formed under acidic and oxidative conditions from reactions of various oxides of nitrogen. While nitrated derivatives of fatty acids have already been identified in healthy human blood, it remains unclear as to which specific structural features or isomers of nitrated fatty acids produce a particular cell signaling response. For example, mixtures of synthetic nitroalkene fatty acid derivatives activate PPARγ, but the specific regioisomers and mechanisms responsible for this activation are unknown.

Furthermore, the field of RES formation and signaling is still developing. This work describes the discovery of mono-oxygenated ω-3-PUFA derivatives, termed electrophilic fatty acid derivatives (EFADs) that are produced by COX-2 during inflammatory conditions and are generated at increased rates with ASA-acetylation of COX-2. The most common way of treating inflammation is the use of NSAIDs. However, despite their wide use, some of the mechanisms by which NSAIDs work are not fully understood. NSAIDs have long been known to inhibit prostaglandin formation by COX-2 but recent literature suggests that ASA may also redirect COX-2 activity toward oxidation of long-chain fatty acids that help to reduce inflammation. Thus this class of newly discovered EFADs display a distinct capability to act as important endogenous mediators of the resolution of inflammation.

2.0 MATERIALS AND METHODS

2.1.1 Materials

Diclofenac, methyl arachidonyl fluorophosphonate, MK886, (±)-ibuprofen, indomethacin, NS-398, 15d-PGJ_2, 4-HNE, 9-oxo-10E,12Z-octadecadienoic acid (9-oxoODE, a.k.a. 9-KODE), 5-oxo-6E,8Z,11Z,14Z-eicosatetraenoic-6,8,9,11,12,14,15-d7 acid (5-oxoETE-d7), 12-oxo-5Z,8Z,10E,14Z-eicosatetraenoic acid (12-oxoETE), 15-oxo-11Z,13E-eicosadienoic acid (15-oxoEDE), 9-oxo-10E,12Z,15Z-octadecatrienoic acid (9-oxoOTrE), 17-oxo-docosapentaenoic acid (17-oxoDPA), and 17-oxo-docosahexaenoic acid (17-OxoDHA) were purchased from Cayman Chemicals (Ann Arbor, MI). Ovine placental COX-2 (Cayman 60120) was also from Cayman Chemicals. DPA and DHA were from NuCheck Prep (Elysian, MN). Kdo_2-lipid A was from Avanti Polar Lipids, Inc (Alabaster, AL) HPLC solvents were from Honeywell Burdick and Jackson (USA). Glutathione and glutathione S-transferase were purchased from Sigma-Aldrich.

2.1.2 Cell Culture

Murine monocyte/macrophage cells (RAW264.7) and human monocyte cells (THP-1) were obtained from ATCC (USA) and maintained at 37°C in 5% CO_2 in DMEM + 10% FBS (RAW264.7) and RPMI + 10% FBS (THP-1) according to ATCC guidelines. L-cells were

obtained from ATCC (CCL-1) and maintained at 37°C in 5% CO_2 in DMEM supplemented with 10% FBS, glutamine (2 mM), sodium pyruvate (1 mM), penicillin, streptomycin and non-essential amino acids.

2.1.3 Murine Studies

Bone marrow derived macrophages were isolated from C57BL/6 mice according to the protocol developed by Davies [155]. Briefly, femurs and tibiae were isolated from euthanized mice, severed at both ends by scissors, and their contents flushed with 10 ml of DMEM. Freshly isolated bone marrow cells were then differentiated to macrophages by MCSF produced by L-cells and maintained in DMEM supplemented with 30% L-cell supernatant, 20% FBS, L-glutamine (2 mM), sodium pyruvate (1 mM), penicillin, and streptomycin.

2.1.4 *In Vitro* Competitive Binding Analysis of Peroxisome Proliferator Activated Receptor γ-Ligand Interactions

Agonist binding to PPARγ was obtained by time-resolved-Förster resonance energy transfer (TR-FRET) analysis (LanthaScreen™ TR-FRET competitive binding assay, Invitrogen.; Madison, WI) according to the manufacturer's procedure. Recombinant human PPARγ ligand binding domain (PPARγ-LBD) expressed as a GST-tagged fusion protein and purified from baculovirus-infected insect cells was used at a purity of $\geq$ 85%. The GST-tagged PPARγ-LBD, terbium (Tb) labeled anti-GST antibody and Fluormone™ Pan-PPAR Green tracer were added to ligand in a black 384-well assay plate (Corning #3677) for final assay concentrations of 5 nM

PPARγ, 5 nM antibody and 5 nM tracer. After a 1 h incubation at RT, the Tb emission at 495 nm and the FRET signal at 520 nm were measured following excitation at 340 nm using a Tecan Ultra 384 microplate reader (Tecan Group Ltd., Maennedorf, Switzerland).

2.1.5 *In Vitro* Peroxisome Proliferator Activated Receptorγ-Coactivator Recruitment Studies

Coregulator peptide binding to PPARγ (in the prescence of OA, Rosiglitazone, or OA-NO_2 as ligands) was determined by time-resolved-Förster resonance energy transfer (TR-FRET) analysis (LanthaScreen™ TR-FRET PPARγ receptor coactivator assay, Invitrogen; Madison, WI) according to the manufacturer's procedure. In brief, the GST tagged PPARγ ligand binding domain (PPARγ-LBD), terbium (Tb) labeled anti-GST antibody and fluorescein labeled peptide were added to ligand in a black 384-well assay plate (Corning #3677) for final assay concentrations of 5 nM PPARγ, 5 nM antibody and 125 nM peptide. For fold-change experiments, CBP-1, PGC-1α, TRAP/DRIP-2, NCoR ID2 and SMRT ID2 peptides (Invitrogen) were used at final assay concentrations of 500 nM. After a 2 h incubation at RT, the Tb emission at 495 nm and the FRET signal at 520 nm were measured following excitation at 340 nm using a TECAN Ultra 384 microplate reader (Tecan Group Ltd., Maennedorf, Switzerland).

2.1.6 Activation of Cells

Monocytes were activated with pro-inflammatory compounds using the following methods unless otherwise indicated. RAW 264.7 cells were seeded, incubated overnight, and treated at approximately 80% confluence. Activation was initiated by exposure to IFNγ (200 U/ml) and the

synthetic endotoxin Kdo_2 (0.5 μg/ml) (see **Appendix B Fig. 46** for structure) as described previously[156-158]. This method of activation reproduced the rate of nitrate/nitrite accumulation in the media as reported previously[157] (**Appendix B Fig. 45**). Non-activated controls were treated with vehicle (DMSO) alone. During activation, cells were maintained in an activation medium (SMEM) of Minimum Essential Eagle Medium (Cellgro, 17-305) + 2% FBS supplemented with L-glutamine (584 mg/L), Na-pyruvate (110 mg/L) and Hepes (3.57 g/L, pH 7.4). For inhibition studies, potential inhibitors were added to the medium at the time of activation. Cells were harvested 20 h post activation (unless otherwise indicated) in 50 mM phosphate buffer (pH 7.4) and snap frozen in liquid N_2 or finely crushed dry ice. For inhibitor experiments, MTT assays were used to confirm that the concentrations used were not toxic to the cells (**Appendix B Fig.** 47). THP-1 cells were first differentiated with PMA (50 ng/ml) for 16 h, activated with IFNγ (200 U/ml) and Kdo_2 (0.5 μg/ml) in RPMI + 2% FBS and harvested 40 h after differentiation. DMSO was used as vehicle control for THP-1 cells. BMDMs were activated with PMA (50 ng/ml), IFNγ (200 U/ml) and (0.5 μg/ml) and were harvested 24 h post activation.

2.1.7 Alkylation Reaction of Electrophiles with β-mercaptoethanol

Upon thawing, lysates were exposed to BME (500 mM) (± internal standard, 5-oxoETE-d7 (1.25 ng/ml)) and incubated at 37°C for 1 h in 50 mM phosphate buffer (pH= 7.4) as previously described [159]. Protein was precipitated with acetonitrile (4 x reaction volume) and the supernatant containing BME-adducted electrophilic lipids was analyzed by reversed-phase high performance liquid chromatography electrospray ionization tandem mass spectrometry (RP-HPLC-ESI-MS/MS). *BME-alkylation reactions to determine free and adducted EFADs.* RAW264.7 cells were activated with Kdo_2 and IFNγ, harvested and the cell lysates split in two.

The first lysates fraction was reacted directly with BME (500 mM), followed by protein precipitation with acetonitrile to yield the total EFAD content in the cell lysates. In the second group of cell lysates, the protein was precipitated first with acetonitrile and the supernatant was reacted with BME to yield the subpopulation of EFADs that were free or adducted to small molecules.

2.1.8 High Performance Liquid Chromatography and Mass Spectrometry

The analysis and quantification of BME-adducted molecules were performed using a hybrid triple quadrupole-linear ion trap mass spectrometer (4000 Q trap, Applied Biosystems/MDS Sciex) in the neutral loss (NL) scan mode, multiple reaction monitoring (MRM) scan mode, and the enhanced product ion analysis (EPI) mode. BME adducts were detected by monitoring for molecules that undergo a $M^-/[M - BME]^-$ transition. The declustering potentials were -90 and -50 V for free fatty acids and BME-adducts, respectively. The collision energies were -30 and -17 V for free fatty acids and BME adducts, respectively. Zero grade air was used as source gas, and N_2 was used in the collision chamber. Data were acquired and analyzed using Analyst 1.4.2 software (Applied Biosystems, Framingham, MA).

2.1.8.1 High Performance Liquid Chromatography for Rapid Separation and Quantification

Samples were separated by reversed-phase HPLC using a 20 x 2 mm C18 Mercury MS column (3 μm, Phenomenex). BME adducts were separated and eluted from the column using a gradient solvent system consisting of mobile phase A (water containing 0.1% formic acid) and mobile phase B (acetonitrile containing 0.1% formic acid) at 750 μl/min under the following conditions:

hold at 35% B for 0.5 min, then 35-90 % B for 4 min, then 90-100 (0.1 min; hold for 1.4 min); and 100-35% B (0.1 min; hold for 1.9 min).

2.1.8.2 High Performance Liquid Chromatography for Resolution of Isomers

Samples were separated by reversed-phase HPLC using a 150 x 2.00 mm C18 Luna column (3 μm, Phenomenex). A flow rate of 250 μl/min was used under the following conditions: hold at 35% B for 3 min, then 35-90 % B for 23 min, then 90-100 (0.1 min; hold for 5.9 min); and 100-35% B (0.1 min; hold for 7.9 min).

2.1.9 Mass Spectrometry Standardization and Quantification of Electrophile-β-mercaptoethanol Adducts

EFADs were quantified using an external standard of synthetic 17-oxoDPA and 17-oxoDHA and by comparing peak area ratios between analytes and a 5-oxoETE-d7 internal standard.

2.1.10 Cyclooxygenase-2 Reactions

PUFA were exposed to purified COX-2 and products were detected by reverse-phase HPLC-MS/MS as previously described[131,160,161]. Briefly, ovine placental COX-2 was preincubated in Tris/heme/phenol (THP) buffer ± ASA to reconstitute the enzyme with heme and to give the ASA time to interact with the enzyme (THP buffer, consisting of Tris•Cl (100 mM, pH 8.1), hematin (1 μM), and phenol (1 μM) was freshly prepared before each reaction). The reaction was initiated by addition of the fatty acids. Each reaction was carried out at 37°C with

gentle shaking. The final concentrations of each reagent were as follows: COX-2 (20 U/ml), DPA (or DHA; 10 μM), and ± ASA (2 mM). Reactions were terminated by addition of ice-cold acetonitrile (9 x reaction volume) and COX-2 protein was removed by centrifugation. Samples of each reaction were taken at the indicated times and the formation of the hydroxy-precursors of EFAD-2 and EFAD-1 were monitored by RP-HPLC-MS/MS in selected reaction monitoring (MRM) mode following the loss of CO_2 (transitions for EFAD-2 and EFAD-1 hydroxy-precursors were *m/z* 345/301 and *m/z* 343/299 respectively).

2.1.11 Luche Reaction

The Luche reaction was used to reduce putative keto groups to their corresponding alcohol. Samples were added to 1 ml of 200 mM $CeCl_3$ and $NaBH_4$ was added in excess (~200 mM final). Samples were incubated for 1 h with shaking at RT. The reaction was terminated by the addition of a few drops of glacial acetic acid and the lipids were extracted by the method of Bligh and Dyer[162]. Samples were dried and reconstituted in methanol at 1 or 2x the original sample volume.

2.1.12 Peroxisome Proliferator Activated Receptor-γ Reporter Assay

The PPAR gamma-UAS-bla 293H cells (Invitrogen, Madison, WI) used in the PPARγ reporter cell-based assay contained a PPARγ ligand-binding domain/GAL4 DNA-binding domain chimera stably integrated into a parental cell line previously engineered with a beta lactamase reporter gene under control of a UAS response element. PPAR gamma-UAS-bla 293H cells were plated in black-walled clear bottom, Poly-D-Lysine coated 384-well plates at a density of 30,000

cells per well in assay medium (Phenol red-free DMEM with 0.1% charcoal-stripped FBS (Invitrogen)). Cells were then treated with serial dilutions of the indicated ligands and incubated 37°C (95% air 5% CO_2) for 16 h. Following the incubation, LiveBLAzer^{TM}-FRET B/G Loading solution (Invitrogen) was added to the cells and they were incubated at room temperature for 2 h. Fluorescence intensity at 460 nm and 530 nm emission following excitation at 406 nm was measured using a Molecular Devices SpectraMax M2^{e} plate reader (Molecular Devices, Sunnyvale, CA). After subtraction of fluorescence background from cell-free wells, the ratio of fluorescence intensity at 460 nm versus 530 nm (designated as 460 nm/530 nm) was calculated.

2.1.13 Mass spectrometry of 17-Oxodocosapentaenoic acid alkylation of Glyceraldehyde-3-Phosphate Dehydrogenase.

GAPDH (1.25 mg/ml) was reacted for 2 h at ambient temperature with 100 µM EFAD-2. Samples were then reduced using 10 mM TCEP and free cysteines alkylated with 20 mM iodoacetamide (IAM). The native and EFAD-2 modified proteins were digested with sequencing grade trypsin in 50 mM phosphate buffer pH 7.4, at 37 °C overnight using an enzyme:substrate ratio of 1:50 (w/w) and subjected to nanoLC/ESI MS/MS, using a Thermo-Fisher LTQ for analysis. A reversed-phase trap column (Waters Symmetry C18-20 mm-180 µm ID and 5 µm particle size) was loaded with 1 µl of digested sample at a 5 µl /min flow rate for 3 min in 1 % mobile phase B (acetonitrile + 0.1 % Formic acid). Peptides were resolved using a Waters BEH130 column (C18-100 mm-75 µm ID and 1.7 µm particle size) at 40 °C with a linear gradient of solvent B (1–40% in 59 min) at a flow rate of 0.5 µl/min followed by a linear gradient of mobile phase B (60–80% in 20 min). Electrospray voltage was 1.4 kV, and ion

transfer capillary temperature was 200 °C. Peptides were detected in the positive ion mode using a mass range of 100–2000. Instrument and source parameters were optimized by tuning for GS-EFAD-2 adducts. Mass tolerance was set to 1 Da and the sequence of rabbit GAPDH was obtained from the National Center for Biotechnology Information. Peptide identification was performed using Bioworks 3.0 with variable modifications set as methionine +/- oxidation (16 Da), cysteine +/- IAM or +/- EFAD-2.

2.1.14 Statistics

Data are expressed as mean ± SD and were evaluated by a one-way analysis of variance, post-hoc Tukey's test for multiple pairwise comparisons. Significance was determined as $p<0.01$ unless otherwise indicated.

3.0 NITRO-FATTY ACID MODULATION OF PEROXISOME PROLIFERATOR-ACTIVATED RECEPTOR GAMMA

3.1 INTRODUCTION

The rapidly expanding global burden of type II diabetes mellitus (DM) and the concomitant increased risk for cardiovascular disease (CVD)[163,164] has motivated better understanding of relevant cell signaling pathways and potential therapeutic strategies. One major characteristic of metabolic syndrome and DM is insulin resistance, leading to hyperglycemia and dyslipidemia. Following initial clinical use of TZDs as anti-hyperglycemic agents to treat DM in the late 1990s, the nuclear receptor PPARγ was discovered as their molecular target. This receptor is expressed primarily in adipose tissue, muscle and macrophages, where it regulates glucose uptake, lipid metabolism/storage and cell proliferation/differentiation[98,100,165]. Thus, PPARγ ligands and downstream signaling events play a pivotal role in both the development and treatment of DM[102,166]. This is underscored by the observation that mutations in the C-terminal helix 12 of the ligand binding domain (LBD) of PPARγ (e.g., P467L or V290M) are linked with severe insulin resistance and the onset of juvenile DM[104].

The oxidizing inflammatory milieu contributing to the pathogenesis of obesity, diabetes and CVD also promotes diverse biomolecule oxidation, nitrosation, and nitration reactions by O_2 and $^{\bullet}NO$-derived species. While oxidized fatty acids typically propagate pro-inflammatory

conditions, the recently detected NO_2-FA appear to act as anti-inflammatory mediators. Nitroalkene derivatives of oleic acid (OA-NO_2) and linoleic acid (LNO_2) have been detected in healthy human blood and murine cardiac tissue, and mediate anti-inflammatory signaling responses *in vitro* [169,170]. Furthermore, the levels of free/unesterified OA-NO_2 are around 0.6-3 nM in human plasma[167,168], and OA-NO_2 is produced at increased rates during inflammatory and metabolic stress. The signaling actions of NO_2-FA are primarily ascribed to the electrophilic olefinic carbon situated β to the electron-withdrawing NO_2 substituent, facilitating kinetically rapid and reversible Michael addition with nucleophilic amino acids (*i.e.* Cys and His)[24]. NO_2-FA adduction of proteins and glutathione (GSH) has been identified clinically, and NO_2-FA adduction of critical Cys residues *in vitro*, mediates the inhibition of macrophage activation via NFκB[74,171], inactivates xanthine oxidoreductase[96] and activates Phase 2 gene expression[97]. In addition to serving as electrophilic signaling mediators, OA-NO_2 and LNO_2 bind to PPARγ, displaying a K_d (K_d LNO_2≈ 133 nM) similar to that of Rosiglitazone (K_d= 40 nM-70 nM[116,172]) as determined by competition binding analysis of radiolabeled Rosiglitazone displacement from PPARγ [81,95]. While OA-NO_2 and LNO_2 transactivate PPARγ as potently as Rosiglitazone in luciferase-based assay systems, NO_2-FA-induced differentiation of pre-adipocytes to adipocytes and subsequent triglyceride accumulation was diminished when compared to Rosiglitazone [81,95]. These results suggest that NO_2-FA act as partial rather than full agonists of PPARγ and that a more complex ligand-receptor interaction than originally described is occurring[81,95].

The large, relatively non-selective ligand binding pocket of PPARγ binds eicosanoids and oxidized fatty acid derivatives at μM concentrations[173], conferring to this receptor an ability to sense and transduce signals generated by the oxidizing inflammatory milieu that can also form NO_2-FA. Most proposed "natural' PPARγ ligands are intermediates of lipid metabolism and

oxidation that bind with low-affinity at concentrations orders of magnitude greater than physiological conditions. Among these natural ligands are saturated and unsaturated free fatty acids, prostaglandins, leukotrienes and other oxidized lipid derivatives, and lysophosphatidic acid. Synthetic TZD ligands, such as Rosiglitazone, bind PPARγ avidly and have been shown to effectively increase insulin sensitivity via PPARγ signaling pathways[116]. By activating PPARγ, TZDs restore insulin sensitivity to alleviate many of the symptoms associated with diabetes. Unfortunately, full activation of PPARγ by TZDs also results in undesirable side effects such as weight gain, edema, and increased adverse cardiovascular events[174,175]. Consequently there has been significant motivation to identify PPARγ agonists with an activation profile that differs from that of TZDs.

The indication that NO_2-FA act as partial PPARγ agonists led to the investigation of the mechanisms linking PPARγ binding of NO_2-FA to physiological outcomes. Thus the impact of NO_2-FA association with PPARγ and the subsequent influences on coregulator interactions were characterized. It was observed that NO_2-FA covalently adducted to PPARγ, induced coregulator interactions distinct from those of Rosiglitazone.

3.2 RESULTS

3.2.1 The Reducing Environment Determines the EC_{50} of Nitrated Fatty Acid Binding to Peroxisome Proliferator Activated Receptor-γ

The binding affinity of NO_2-FA for PPARγ and their electrophilic reactivity suggested that NO_2-FA may covalently modify nucleophilic amino acid residues in the LBD. Thus, the

impact of PPARγ adduction by NO_2-FA was assessed utilizing TR-FRET to quantify competitive PPARγ-LBD ligand displacement. In this assay, a Pan-PPAR Green tracer is incubated with GST-tagged PPARγ-LBD, and labeled with anti-GST antibody covalently bound to terbium. When the tracer is bound to the PPARγ-LBD, energy is transferred from the terbium fluorophore to the tracer fluorophore following excitation at 340 nm, resulting in an observed TR-FRET signal at 520 nm (green channel). When the tracer is not bound or displaced by another ligand, the terbium emits a fluorescent signal at 495 nm (blue channel) following excitation at 340 nm. Initially, it was important to determine the optimal concentrations of dithiothreitol (DTT) for the assay, as the potential reaction of the NO_2-FA with DTT could significantly lower the actual concentration of NO_2-FA available to the LBD. Revealing insight came from the use of DTT in this analysis, as DTT is required to maintain Cys285 thiol reduction and receptor activity. PPARγ-LBD (0.5 nM) was incubated for 1 h with fluorescent ligand and the ligand of interest. Lowering DTT concentration decreased the fold change between maximum Rosiglitazone concentrations and no treatment (**Fig. 9**), and revealed that DTT also reacts with added NO_2-FA, resulting in a right-shift of the EC_{50} value with increasing DTT concentration (**Fig. 10**).

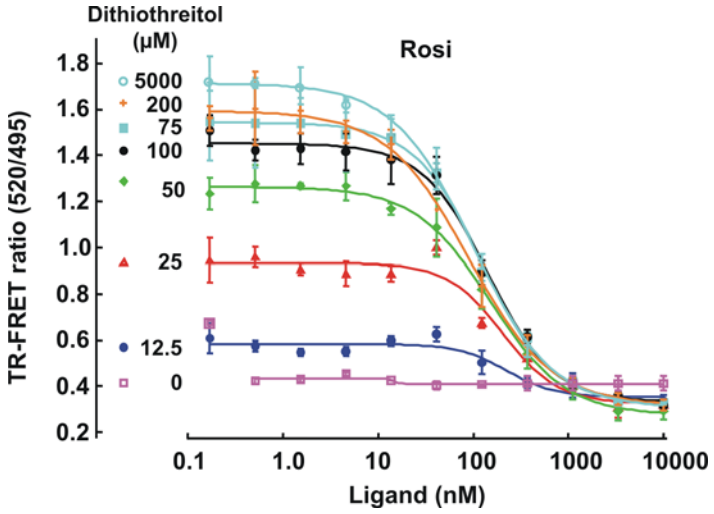

Figure 9. Peroxisome proliferator activated receptor-γ ligand activity of Rosiglitazone and the effect of dithiothreitol.

Ligand binding curves for Rosiglitazone (Rosi; 0.17-10,000 nM) at varying concentrations of DTT. Curve fitting equations and EC_{50}s were determined by XLfit4 and are displayed in inset.

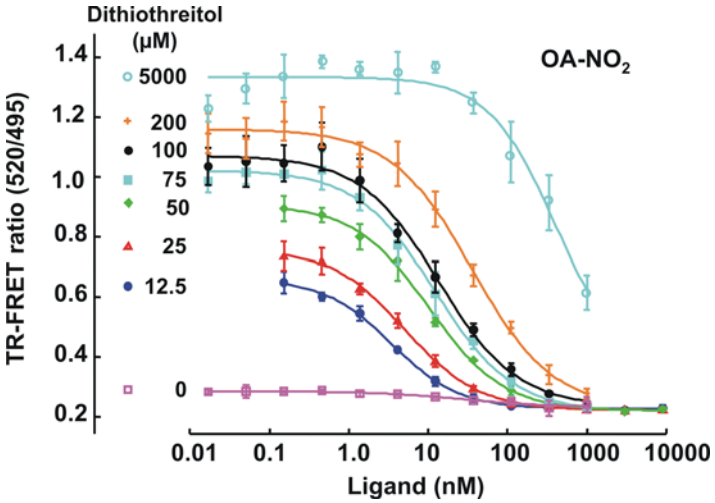

Figure 10. Peroxisome proliferator activated receptor-γ ligand activity of nitroalkene derivatives of oleic acid and the effect of dithiothreitol.

Ligand binding curves for $OA\text{-}NO_2$ (0.17-10,000 nM) at varying concentrations of DTT. Curve fitting equations and EC_{50}s were determined by XLfit4 and are displayed in inset.

Thus, measuring EC_{50} values for ligands at varying DTT concentrations allowed extrapolation of an EC_{50} value for OA-NO_2 of <1 nM in the absence of DTT (**Fig. 11**). These data suggest that the unlike Rosiglitazone, the EC_{50} value of OA-NO_2 is dependent on the redox environment and that under oxidizing conditions OA-NO_2 can be a more potent ligand.

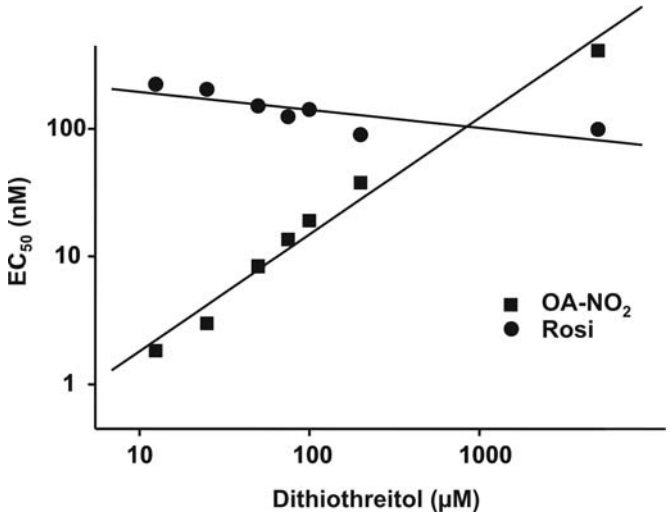

Figure 11. The concentration of dithiothreitol affects the EC_{50} for nitroalkene derivatives of oleic acid.

EC_{50} values were plotted against DTT concentration (12.5-5,000 μM) to determine the EC_{50} of OA-NO_2 in the absence of reducing agent. Linear fitting equations are as follows: OA-NO_2: Y= 0.91x - 0.65, r^2= 0.99 and Rosiglitazone: Y= -0.14x +2.43, r^2= -0.801.

For comparing various ligands, 125 μM DTT was uniformly used, with the expectation that actual EC_{50} values (in the absence of DTT) for electrophilic FA can be >10-fold less than observed (OA-NO_2 and LNO_2, 13 nM and 36 nM, Rosiglitazone, 31 nM respectively, **Fig. 12**).

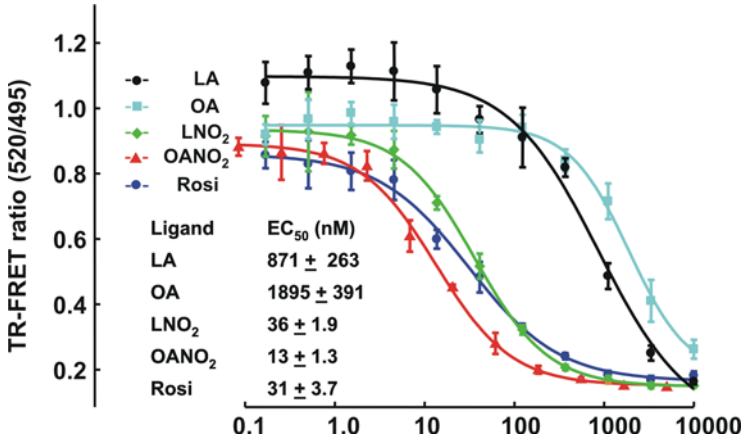

Figure 12. Nitroalkene derivatives of oleic acid have EC_{50} values that rival those of Rosiglitazone.

Ligand binding curves for linoleate (LA), oleate (OA), LNO_2, OA-NO_2 and Rosiglitazone (Rosi) with concentrations ranging from 0.17-10,000 nM and containing 125 μM DTT. Curve fitting equations and EC_{50}s were determined by XLfit4 and are displayed in inset.

The EC_{50} of native oleic acid and linoleic acid were 1900 nM and 870 nM, respectively. These data indicate the potent and unique nature of PPARγ binding by NO_2-FA. The ligand binding curves for additional nitrated fatty acid derivatives were also determined by this method (**Appendix A Fig. 43** and **44**). While TZDs bind and activate PPARγ through both hydrophobic and hydrogen bonding interactions[176], electrophilic NO_2-FA bind and activate PPARγ by not only hydrophobic and hydrogen bonding interactions, but also by covalent reaction with the nucleophilic LBD Cys285.

Adduction of OA-NO_2 with the LBD was also tested by monitoring competitive binding of ligands over time. In the absence of excess DTT, the covalent nature of NO_2-FA binding to the LBD should result in a left-shift of the EC_{50} over time as more and more of the receptor is adducted. In this experiment, GST-purified PPARγ-LBD (0.5 nM) was incubated with fluorescent ligand and the ligand of interest, and the terbium emission and FRET signals were measured at various times during incubation (3, 10, 20, and 60 min). The results of this

experiment show a lowering in EC_{50} values over time for OA-NO_2 indicating that the dissociation rate of OA-NO_2 from PPARγ is much lower than those of Rosiglitazone or nitrostearic acid (**Table 2** and **Fig. 13**). This significant time-dependent reduction in NO_2-FA EC_{50}s as compared to ligands that lack electrophilic reactivities (*i.e.* Rosiglitazone, oleic acid and nitro-stearic acid, a nitroalkane) affirmed the covalent interaction of OA-N_2 with PPARγ.

Table 2. Ligands that bind peroxisome proliferator activated receptor γ covalently display decreasing EC_{50} values over time.

Table indicates ligand binding curves for OA-NO_2, 9-OA-NO_2, 9-nitro-stearic acid, 12-nitro-stearic acid, Rosiglitazone, GW9662 (a ligand that binds PPARγ covalently), and oleic acid with concentrations ranging from 0.17-10,000 nM and containing 125 μM DTT. Curve fitting equations and EC_{50}s were determined by XLfit4.

	EC_{50} (nM)			
	3 min	**10 min**	**20 min**	**1 hr**
9- and 10-Nitro-oleic acid	239	88	58	35
9-Nitro-oleic acid	555	159	108	61
9-Nitro-stearic acid	6795	8552	8358	8961
12-Nitro-stearic acid	3023	2772	2290	1477
Rosiglitazone	17	24	28	44
GW9662	206	65	34	13
Oleic acid	7904	12066	13385	16118

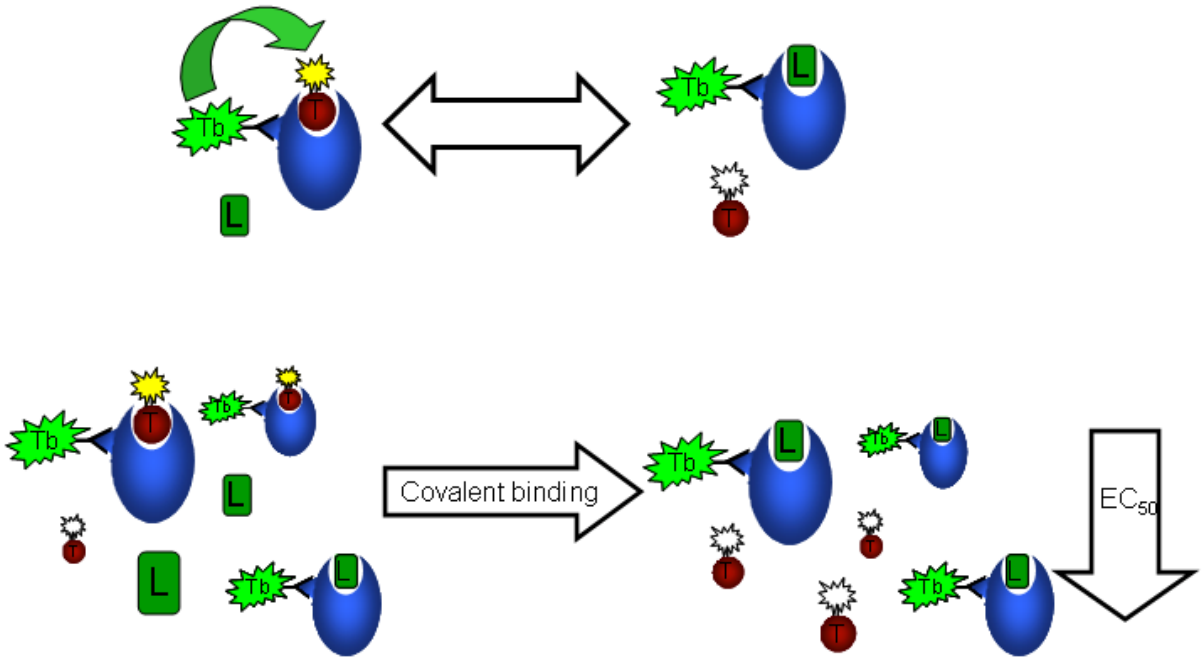

Figure 13. Scheme of covalent ligand binding in TR-FRET-based PPARγ competitive binding assay.

Binding of a fluorescent tracer ligand to the ligand binding domain labeled with a terbium-linked anti-GST antibody gives a TR-FRET signal. When the tracer is reversibly out-competed by the ligand of interest, a loss in TR-FRET signal is observed (top). On the other hand, if the ligand binds the receptor covalently, the tracer will have less of an opportunity to bind as time goes on and there will be a decrease in the EC_{50} value.

3.2.2 Binding of Nitroalkene Derivatives of Oleic Acid to PPARγ Results in a Unique Set of Interactions with Coregulators Compared to Rosiglitazone

The specific ligand and cell type combine to define the available coregulator pool that interacts with PPARγ. Hundreds of coregulator proteins have been identified that are either

protein-modifying enzymes or scaffolds for transcriptional machinery that promote (coactivators) or prevent (corepressors) transcription. Rosiglitazone recruits and displaces a specific pattern of coregulators upon PPARγ binding to effect the biologic response characteristic of full PPARγ agonists. In contrast, binding of partial agonists induces a modified coregulator-PPARγ interaction pattern that differentially transactivates target genes[177]. While specific downstream PPARγ signaling has been described for individual coregulatory proteins, a definitive linkage between the integrated actions of multiple coregulators and physiological outcome is missing.

Herein, TR-FRET-based analysis of >20 coregulator peptides indicates that PPARγ binding by NO_2-FA induces a significantly altered pattern of interactions compared to Rosiglitazone (not shown). This assay was chosen based on the ability to rapidly screen a wide variety of coregulator peptides and NO_2-FA derivatives, thus identifying promising coregulators and ligands for follow-up in cell culture and *in vivo* experiments. Additionally this assay detects potential transient coregulator peptide-LBD interactions that may not be as easy to detect in cells or *in vivo*. However, it is also important to consider that while the peptides used in this assay consist of primary sequences determined to be critical for interaction with the PPARγ-LBD, they lack the tertiary structure that may contribute to interaction with or function of the ligand-bound PPARγ and other transcription factors. These data are represented in **Fig. 14** by the coregulator peptide binding patterns for peptides derived from the following coregulators: CREB-binding protein, motif 1 (CBP-1), thyroid hormone receptor-actived protein 220, also known as VDR-interacting protein, motif 2 (TRAP220/DRIP-2) PPARγ coactivator 1α (PGC-1α) and nuclear corepressor proteins, interacting domain 2 (NCoR ID2) and the silencing mediator of retinoid and thyroid hormone receptors interacting domain 2 (SMRTI D2) (**Fig. 14**).

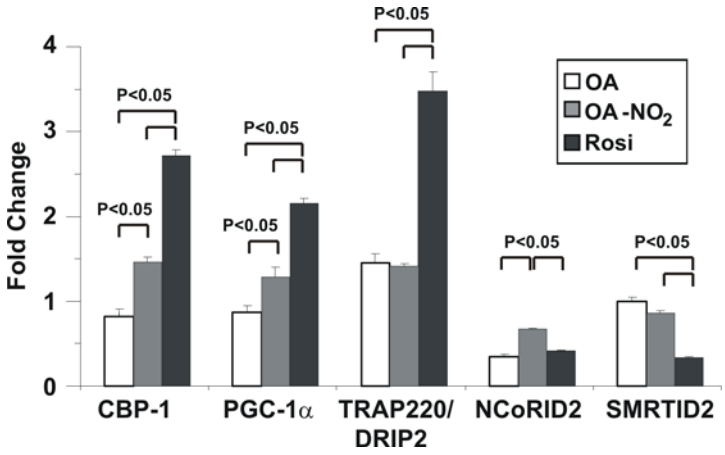

Figure 14. Nitroalkene derivatives of oleic acid are partial peroxisome proliferator activated receptor-γ agonists.

Fold change in TR-FRET ratios (ligand/no ligand) was determined for the ligands Rosiglitazone (5 μM), OA (20 μM), and OA-NO_2 (5 μM) and for indicated coregulator peptides (500 nM). Ligand concentrations were utilized that induced maximum receptor occupancy as reflected by fluorescent reporter-ligand displacement. Statistics were calculated by a one-way ANOVA (post-hoc Tukey).

In contrast to Rosiglitazone, which strongly recruits the coactivator peptides of CBP-1, TRAP220/DRIP-2 and PGC-1α and strongly displaces the corepressors NCoR ID2 and SMRT ID2, OA-NO_2 induces a weaker recruitment and displacement of coregulator peptides, supporting a partial PPARγ agonist activity (**Fig. 14** and **Table 3**).

Table 3. Comparison of Rosiglitazone and nitroalkene modulation of coregulator interaction with peroxisome proliferator activated receptor-γ.

Fold change in TR-FRET ratios (ligand/no ligand) was determined for the ligands Rosiglitazone (2 μM) and OA-NO_2 (2 μM) and for indicated coregulator peptides (62.5 nM).

	Fold Change			
Peptide ID	Rosiglitazone 2μM	SD	$OANO_2$ 2μM	SD
CBP-1	6.99	0.806	1.64	0.185
NCoRID2	0.53	0.062	0.68	0.029
PGC1a	2.55	0.201	1.25	0.165
PGC1b	1.69	0.143	0.99	0.041
TRAP220/DRIP2	7.46	0.563	1.73	0.069
SRC1-4	1.65	0.083	1.10	0.045
SMRTID2	0.60	0.033	0.90	0.040
TIF-1	1.24	0.166	0.96	0.114
DAX1-3	2.88	0.410	1.41	0.086
EA2	1.30	0.154	1.10	0.049
EAB1	1.26	0.068	1.01	0.044
PRIP/Rap250	2.15	0.219	1.18	0.087
LCoR	1.58	0.064	1.00	0.045
NCoRID1	0.92	0.067	0.99	0.075
NSD1	1.12	0.033	0.99	0.075
RIP-140 L6	2.45	0.064	1.12	0.110

This unique pattern of PPARγ-coregulator interaction with OA-NO_2 is also exemplified by the ligand concentration-dependent displacement of SMRTID2 and the lower extent of SMRTID2 displacement that is induced by OA-NO_2 compared with Rosiglitazone (**Fig. 15**).

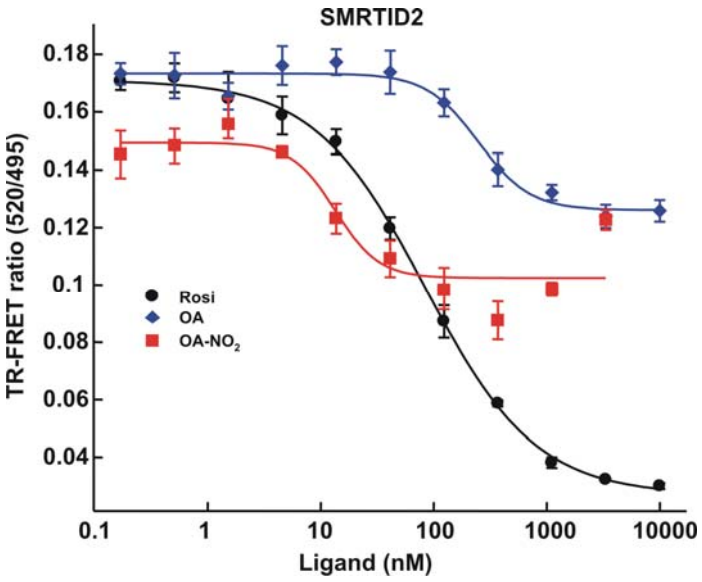

Figure 15. Ligand titration curves for PPARγ coactivator 1α and silencing mediator of retinoid and thyroid hormone receptors interacting domain 2 coregulator peptides indicate that nitroalkene derivatives of oleic acid are partial agonists of peroxisome proliferator activated receptor-γ.

TR-FRET ratios for the coregulator SMRT ID2 peptide and the ligands Rosiglitazone, OA, and OA- NO_2. Curve fitting equations were determined by XL-fit.

This modified interaction with coregulators is further confirmed by the partial agonism observed for NO_2-FA in a cell-based beta lactamase reporter assay (**Fig. 16**). In this assay 293H cells contained a PPARγ ligand-binding domain/GAL4 DNA-binding domain chimera and a beta lactamase reporter gene under control of a UAS response element. Cells were plated and treated with serial dilutions of the indicated ligands. Following a 16 h incubation, a fluorescent substrate containing two fluoroprobes (coumarin and fluorescein) linked by a beta lactam ring was added to the cells. Without beta lactamase activity the substrate will remain whole and the excitation of coumarin at 406 nm will result in the transfer fluorescence resonance energy to fluorescein, which will then fluoresce at 530 nm. In cells that express beta lactamase activity, the substrate is cleaved and coumarin fluoresces at 460 following excitation at 406 nm. The TR-FRET emission

ratio (460 nm/530 nm) is then used to determine the extent of beta lactamase expression (460 nm signal) with normalization (530 nM signal) for well-to-well variation of cell number and substrate loading.

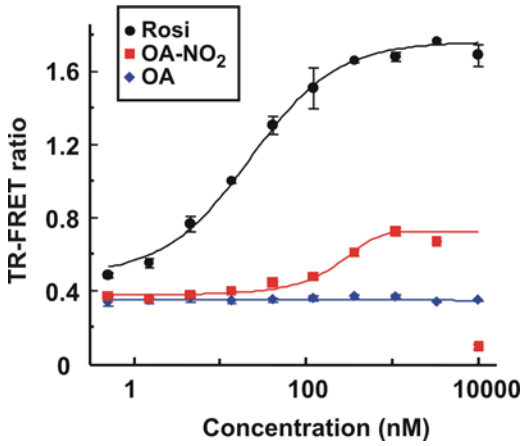

Figure 16. Beta-lactamase reporter assays indicate nitroalkene derivatives of oleic acid are partial agonists of peroxisome proliferator activated receptor-γ

Rosiglitazone, OA, and OA-NO_2 concentrations ranged from 0.5-10,000 nM. Curve fitting equations were determined by XLfit4.

Oleic acid was used as a negative control for receptor activation and Rosiglitazone was used as a positive control. The efficacy of NO_2-FA for receptor activation is considerably lower than for Rosiglitazone, with potency remaining in the high nM range. Thus, PPARγ agonism by electrophilic NO_2-FA manifests unique binding kinetics and induces conformational influences on PPARγ that results in self-specific patterns of coregulator recruitment. These properties suggest that NO_2-FA might induce physiologic responses that differ from Rosiglitazone[173,176-178].

3.3 CONCLUSIONS

PPARγ activation by full agonists such as Rosiglitazone induces the expression of proteins that regulate cell differentiation, lipid trafficking, glucose metabolism and inflammation, thus increasing insulin responsiveness and decreasing blood glucose. However, full PPARγ agonists also stimulate adipocyte differentiation *in vitro* and induce weight gain *in vivo*, leading to the search for selective modulators that activate a subset of PPARγ regulated genes with reduced side-effects[166,179]. Electrophilic NO_2-FA derivatives, products of the oxidizing and nitrating conditions promoted by inflammation, bind to and react avidly with the redox-sensitive LBD Cys285 of PPARγ. This NO_2-FA adduction may also serve to protect the oxidation-sensitive Cys285 of the LBD from inflammatory-derived reactive species. While OA-NO_2 and Rosiglitazone both bind PPARγ with high affinity, distinctively different patterns of coregulatory protein recruitment and release are induced. This crucial aspect of ligand-specific receptor conformation and subsequent patterns of transcriptional complex assembly, receptor-DNA binding and gene expression lends a second level of specificity to PPARγ signaling and defines how a particular ligand influences downstream events such as adipocyte differentiation, lipid metabolism, renal fluid regulation and cellular bioenergetics[180-183]. NO_2-FA induce multiple salutary anti-inflammatory actions and thus, in addition to serving as partial PPARγ agonists, can attenuate other adverse consequences of obesity and diabetes[164]. Overall, NO_2-FA are redox-derived signaling mediators that link inflammatory reactions with metabolic regulation.

4.0 COX-2-DEPENDENT GENERATION OF ELECTROPHILIC α,β-UNSATURATED DERIVATIVES OF OMEGA-3 FATTY ACIDS IN ACTIVATED MACROPHAGES

4.1 INTRODUCTION

The major ω-3-PUFA EPA and DHA have been associated with numerous beneficial health effects in humans. In particular, brain and retina tissues are enriched with DHA in healthy individuals and DHA is necessary for the normal development and function of these tissues[119,120]. The dietery consumption of DHA has been implicated in reducing neurocognitive decline[121], improving insulin resistance in diabetics[122], decreasing incidence of cardiovascular events such as myocardial infarction[123], and reducing inflammation[124]. EPA and DHA are thought to have anti-inflammatory effects by competitive inhibition of arachidonic acid-derived prostanoid synthesis, and subsequent production of ω-3 prostanoids with the ability to induce vasodilation, inhibit platelet aggregation[126] and promote a series of anti-inflammatory events whose mechanisms remain to be elucidated.

Several emerging classes of anti-inflammatory lipid mediators have been recently reported. Among these are nitroalkene derivatives of fatty acids NO_2-FAs, 15d-PGJ_2, and neuroprostanes which are formed during non-enzymatic oxidative events and suppress lipopolysaccharide (LPS)-induced activation of the NF-κB pathway in macrophages via

electrophilic activities[73,74]. A second group of such lipid derivatives include the enzymatically-derived resolvins, neuroprotectins, maresins, and lipoxins (LXs). The enzymes cyclooxygenase-2 (COX-2) and lipoxygenase (LO) are involved in these biosynthetic processes, and are currently emerging as key enzymes in not only the prompt activation of inflammatory events but also their finely orchestrated resolution[184]. Although structurally related to pro-inflammatory prostanoids, these hydroxylated lipid derivatives promote resolution of inflammation by suppressing NF-κB activation, modulating cytokine expression, activating GPCRs[135] and generally promoting cytoprotective responses[185].

The formation of multiple subclasses of lipid signaling mediators is dependent on leukotrine synthase, LOX, cytochrome p450 oxidases (*e.g.* the CYP2C subfamily[186-188], CYP2J2[189], CYP4F3B[190] and CYP4F8[191]) and in particular cyclooxygenase (COX) enzymes[192,193]. Prostanoids are formed via cyclooxygenase catalysis wherein AA is the major eicosanoid precursor. AA (and other PUFA) can be converted by COXs to PGH_2, which is the common substrate for a series of specific synthase enzymes that produce a variety of prostanoids[132,133,136,137]. Depending on the types of prostanoids and receptors present, these signaling lipids can mediate processes involved in the promotion or inhibition of inflammation through GPCR signaling or alternative pathways[133]. Alternative paths of PG-dependent signaling events occur via alterations in nuclear receptor and transcription factor actions (*e.g.* 15d-PGJ_2 and PGA_2 activate PPARγ and inhibit the NFκB pathway)[110,139,140]. In addition, oxygenases, *i.e.* COX and LOs, initiate the multi-step generation of resolvins, a process that is enhanced by ASA-acetylated COX-2[130,131].

Some of the lipid mediators mentioned above (*e.g.* 15d-PGJ_2, neuroprostanes, and NO_2-FA) are RES. RES are molecules characterized by having an electron-withdrawing functional

group that renders the β-carbon electron-poor and reactive towards electron-rich donor molecules (nucleophiles). The strength of the electron-withdrawing group will determine the reactivity of the electrophile[13]. Two prominent examples of these electron withdrawing groups are α,β-unsaturated carbonyls and nitroalkenes, in which the β-carbon (if it is bound to at least one hydrogen atom) is the site of nucleophilic attack. The resonance structures of electrophiles such as the aforementioned allow them to react reversibly with many nucleophiles via Michael addition (or in the case of nitroalkenes a modified Michael addition reaction).

At many levels, reversibly-reacting RES can modulate cell survival mechanisms by reacting with nucleophilic nucleic acids, amino acid residues (cysteine, lysine, and histidine) of proteins and other small molecules. For example, RES not only modulate protein function by reacting with nucleophilic residues, but can also decrease reserves of cellular reductants such as GSH. By covalently modifying proteins, RES can initiate cell signaling events and modulate enzymatic activity and subcellular localization. RES production and levels are tightly controlled in healthy cells with low levels of these species inducing the expression of cell survival genes, in some cases preparing the cells to survive periods of stress. In contrast, under pathological conditions, RES are often produced in excess and accelerate cell damage[13]. Recently, RES have been tested as potential agents in the prevention or treatment of various diseases such as neurodegeneration, cancer, and other pathologies presenting a significant inflammatory component. Electrophilic cyclopentenone PG derivatives (*e.g.* neurite outgrowth-promoting prostaglandin metabolites) display protective effects during cerebral ischemia/reperfusion, which have been attributed to their accumulation in neurons and subsequent activation of the Keap1/Nrf2 pathway[194]. Other RES (e.g. avicins[46], bis(2-hydroxybenzylidene)acetone[195], and isothiocyanates[196]) are potential chemopreventative agents, due to their ability to induce

apoptosis of precancerous cells and tumor cells. Additionally, 15d-PGJ_2 demonstrates a protective role in animal models of acute lung injury[197].

The present study reports the discovery of six electrophilic fatty acid derivatives called EFADs which are produced by activated macrophages via a COX-2-dependent mechanism. These six EFADs are present at 65 nM to 350 nM concentrations in RAW264.7 and THP-1 cell lines and in primary murine macrophages following activation by LPS and IFNγ. EFADs 1-3 have been characterized as α,β-unsaturated oxo-derivatives of the ω-3 fatty acids DHA, docosapentaenoic acid (DPA), and docosatetraenoic acid (DTA) respectively. Specific 13-keto and 17-keto positional isomers have been identified for EFADs 1 and 2, and were also synthesized *in vitro*. Notably, EFADs formed adducts with proteins and GSH in activated RAW264.7 cells. The 17-oxo synthetic homologues of EFAD-1 and EFAD-2 (17-oxoDHA and 17-oxoDPA) activated PPARγ and the Keap-1/Nrf2 pathway and inhibited iNOS and cytokine expression in activated macrophages. Thus these species may contribute to the beneficial effects of ω-3 fatty acids and ASA on human health.

4.2 RESULTS

4.2.1 Electrophilic Fatty Acid Derivatives are Produced by Activated Macrophages.

The previously reported robust, unbiased method for the detection of reversibly-reacting RES *in vivo* employs a BME-driven alkylation reaction with RES (**Fig. 17**) coupled with reverse phase-high pressure liquid chromatography tandem mass spectrometry (RP-HPLC-MS/MS)[159].

Figure 17. Reactive electrophilic species that react reversibly with biomolecules (*e.g.* cysteine residues on proteins) can be transferred to β-mercaptoethanol.

By applying this method to the detection of reversibly-reacting RES formed during inflammatory events, it was hypothesized that previously undescribed or poorly characterized species that could be overlooked in traditional LC-MS-based methods of detection would be more readily identified by this new approach. The alkylation reaction with BME standardizes the MS/MS conditions for various adducted RES, conferring similar ionization and fragmentation properties to a range of RES, each with their own particular MS/MS characteristics. Accordingly, reversibly-reacting RES that might normally be free or adducted to protein or GSH, species that fragment poorly during MS/MS, species that might be in concentrations at or below the limits of detection, and species whose formation is not predictable based on current knowledge could be identified by this method. The formation of RES was initially screened by following the neutral loss of BME (78 amu) by RP-HPLC-MS/MS (data not shown). This resulted in the detection of six major RES species formed during activation of RAW 264.7 cells by PMA, LPS, and IFNγ (**Fig. 18**).

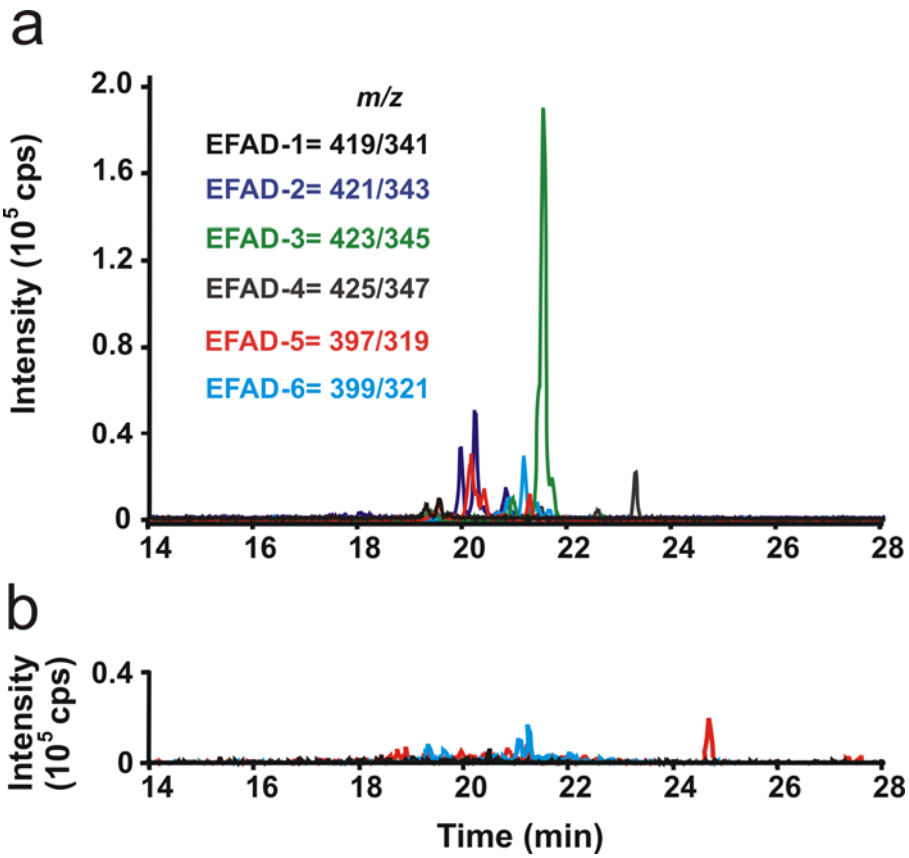

Figure 18. Electrophilic fatty acid derivatives are produced during RAW264.7 cell activation.

RAW 264.7 cells were activated with PMA (3.24 μM), LPS (0.5 μg/ml), and IFNγ (200 U/ml) and harvested 20 h post activation. (a) MRM scans following the neutral loss of 78 were used to detect electrophilic fatty acid BME adducts isolated from activated and non-activated RAW 264.7 cell lysates.

Subsequently, MS/MS experiments were performed to confirm the neutral loss of BME from each of the six EFADS. The MS/MS spectrum for BME-adducted EFAD-2 (*m/z* 421 [M-H]) displayed characteristic fragment ions at *m/z* 403 ([M-H]-H_2O), 377 ([M-H]-CO_2), 343 ([M-H]-BME), 325 ([M-H]-BME-H_2O), and 299 ([M-H]-BME- CO_2) (**Fig. 19**). The MS/Ms spectra for all other EFADs showed the same characteristic losses and similar intensity ratios (data not shown).

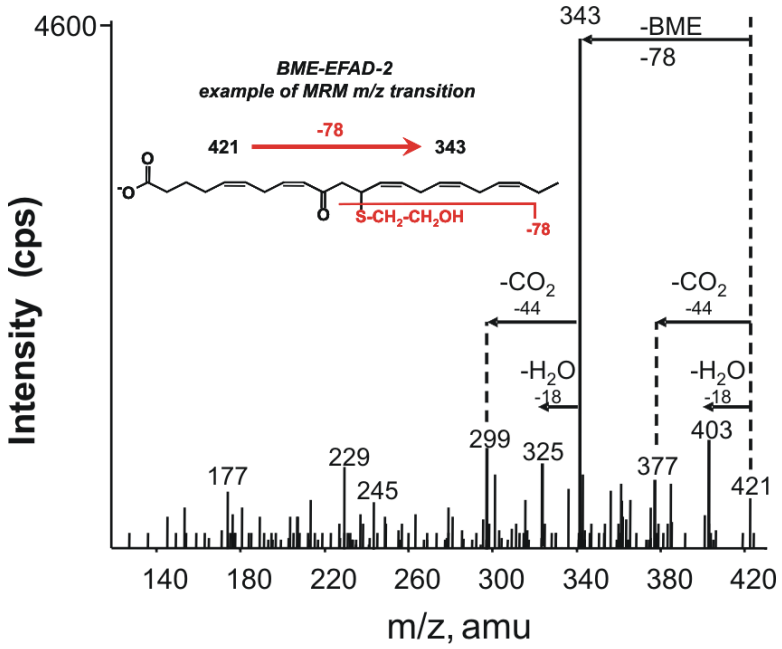

Figure 19. Electrophilic fatty acid derivative-2 adducts to β-mercaptoethanol and displays the neutral loss of β-mercaptoethanol, water, and carbon dioxide upon MS/MS fragmentation.

A characteristic BME-electrophile adduct fragmentation pattern showing the major neutral loss of 78 amu (corresponding to the loss of BME) is represented by the enhanced product ion analysis of EFAD-2.

The same electrophilic species were detected in PMA, Kdo_2 and IFNγ-activated THP-1 cells, a human monocyte/macrophage cell line and were confirmed by MRM transition co-elution with the species identified in RAW264.7 cells (**Fig. 20 and Appendix B Fig. 52**). Although their relative abundance differed between the two cell lines, MS/MS spectra showed the same characteristic losses and similar intensity ratios (data not shown).

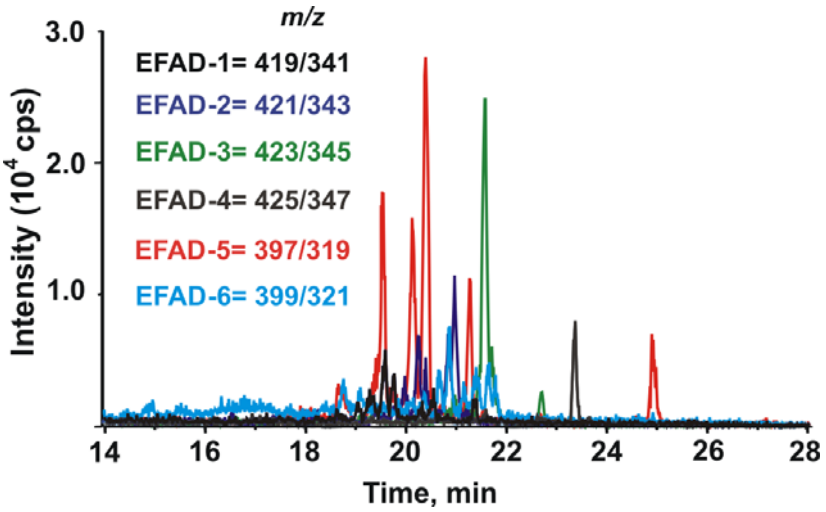

Figure 20. THP-1 cells activated with PMA, Kdo_2 and IFNγ produce electrophilic fatty acid derivatives.

THP-1 cells were differentiated with PMA (86 nM) for 16 h, activated with Kdo_2 Lipid A (0.5 μg/ml) and IFNγ (200 U/ml), and EFAD-2 levels were detected 8 h post activation.

Although the discovery of six EFADs is being reported, the rest of this work will focus mainly on EFAD-2 (as well as EFAD-1) due to its high abundance in activated cells and the biological relevance and beneficial health effects of its precursors.

In order to build on experiments in which accurate detection of EFAD levels was required for comparison purposes, it was important to identify which mass spectrometric method would be best for quantification of these electrophilic species. The robustness of the BME method for the detection and quantification of electrophilic lipids was further tested by comparing the mass spectrometric responses of different electrophilic fatty acids containing α,β-unsaturated moieties using the BME method, selected ion monitoring (SIM) and multiple ion monitoring (MRM) mode following the loss of CO_2 (**Fig. 21**). The standard deviation for the overall responses obtained for the different fatty acid at each concentration tested ranged from 40% to 50% for BME, 60-83% for MRM and 15-35% for SIM analysis.

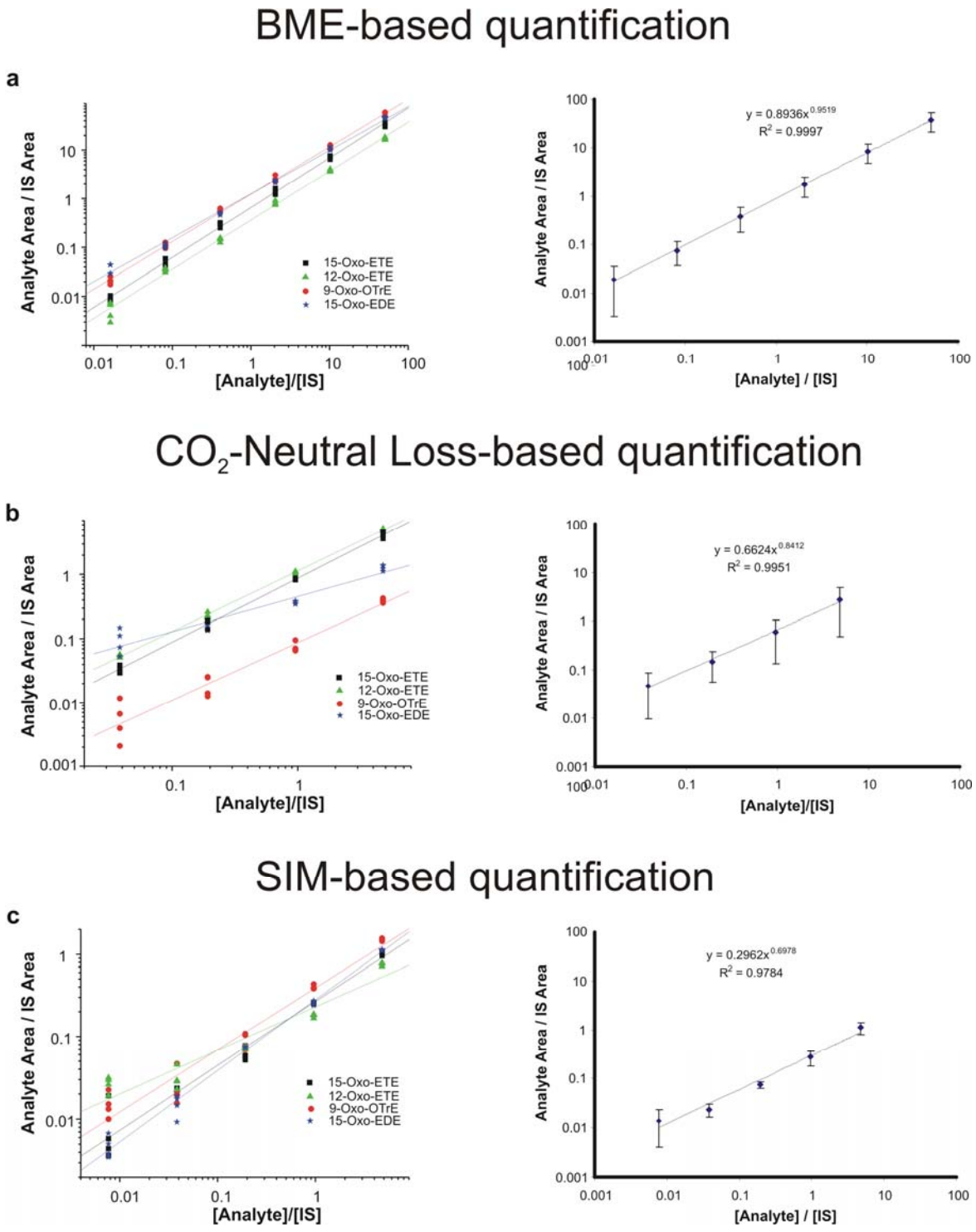

Figure 21. BME adducts with α,β-unsaturated keto-derivatives yield the most reliable concentration curves for quantification by MS/MS.

The compounds 9-oxoODE, 12-oxoETE, 15-oxoEDE and 9-oxoOTrE were reacted with BME for 2 h and concentration curve was prepared by serial dilution (5-oxoETE-d7 was used as an internal standard). Each

compound was quantified by MRM following the neutral loss of BME and their peak areas were plotted against their concentrations with normalization to the internal standard (a). Serial dilutions of the free compounds were performed to make concentration curves and each compound was quantified by MRM following the loss of $-CO_2$ (b) or by a scan for the parent ion (c).

The BME method was clearly superior in terms of signal intensity, background levels and linearity. For prediction purposes and for the initial quantification of unknown species in biological samples, the BME method was chosen as the one giving overall exceptional performances especially when applied to biological samples in which SIM and MRM analyses rendered very poor results because of high background levels. (**Fig. 21**). Thus, the use of the BME method and standard curves of 17-oxoDHA, allowed the estimation of intracellular EFAD concentrations ranging form 65 to 350 nM (**Table 4**).

Table 4. Summary of data on electrophilic fatty acid derivatives 1-6.

Name	EFAD-1	EFAD-2	EFAD-3	EFAD-4	EFAD-5	EFAD-6
Cellular concentration nM	65 ± 5	238 ± 16	348 ± 26	106 ± 6	326 ± 15	169 ± 18
Mass *(m/z)*	341.2	343.2	345.2	347.2	319.2	321.2
FA precursors supporting formation	22:6 ω-3	18:3n-6, 20:5 ω-3	20:4, 18:3n-6, 20:5, 18:3n-3 ω-3 and ω-6	18:3n-6, 20:4 ω-6	18:3n-6 ω-6	FBS, 18:1 ω-9
Series						
Keto group present/position	13- or 17-positon	13- or 17-position	Yes	?	Yes	?
Formula	$C_{22}H_{29}O_3$	$C_{22}H_{31}O_3$	$C_{22}H_{33}O_3$	?	$C_{20}H_{31}O_3$	$C_{20}H_{33}O_3$
Identity	Keto-DHA	Keto-DPA	Keto-DTA	ω-6 derivative	Keto-20:3	Keto-20:2
Activated (Area/[protein])±SD	$8.2e^4$ ±0.55e^4	$3.3e^5$ ±0.38e^5	$2.9e^5$ ±0.32e^5	$7.5e^4$ ±0.53e^4	$1.7e^5$ ±0.11e^5	$2.8e^5$ ±0.24e^5
+ETYA (↓COX)	→	→	→	→	→	→
+Aspirin (↓COX)	←	←	←	→	←	→
+Ibuprofen (↓COX)	NE	→	→	→	→	→
+Indomethacin (↓COX)	→	→	→	→	→	→
+Diclofenac (↓COX)	→	→	→	→	→	→
+NS-398 (↓COX)	→	→	→	→	→	→
+Genistein	→	→	→	→	→	→
+MAFP (↓PLA_2)	→	→	→	→	→	→
+MK886 (↓5-LOX)	NE	NE	NE	NE	NE	NE
+OKA	NE	NE	NE	NE	NE	NE

NE = little/no effect

4.2.2 Electrophilic Fatty Acid Derivative Production is Time Dependent Following Macrophage Activation with Lipopolysaccharide and Interferon-γ.

The formation of EFADs under different inflammatory conditions was confirmed by treating the cells with a variety of stimuli. Thus, macrophages were activated with various combinations of LPS, IFNγ, PMA, fMLP, and Kdo_2-lipid A (Kdo_2) (**Fig. 22** and **Appendix B Fig. 53**).

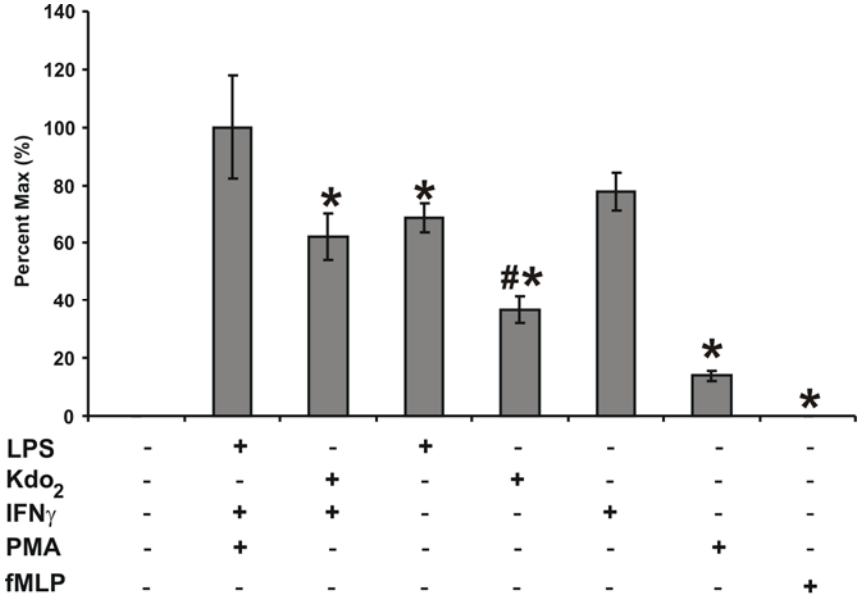

Figure 22. Lipopolysaccharide and Interferon-γ initiate Electrophilic Fatty Acid Derivative-2 formation in RAW264.7 cells.

RAW264.7 cells were activated with the indicated compounds and EFAD-2 levels were quantified 20 h post activation. Compound concentrations are as follows: LPS (0.5 μg/ml), Kdo_2 Lipid A (0.5 μg/ml), IFNγ (200 U/ml), PMA (3.24 μM), and fMLP (1 μM). Data are expressed as mean ± S.D. (n=4), where * = significantly different ($p<0.01$) from "PMA + IFNγ + LPS," and # = a significant difference ($p<0.01$) between LPS and "Kdo_2 + IFNγ" (one-way ANOVA, post-hoc Tukey's test).

Kdo_2, a synthetic endotoxin[198], was used to avoid the contribution of potential LPS preparation contaminants to EFAD formation. Since the combination of Kdo_2 and IFNγ behaved nearly identically to LPS, it was used for all of the following experiments. This further confirmed that no components or contaminants in the LPS itself were acting as precursors of EFADs. Additionally, a time course analysis showed that EFAD formation was time dependent, starting 4-6 h post RAW264.7 cell activation and reaching a peak at approximately 10 h. EFAD levels remained stable for up to 24 h (**Fig. 23** and **Appendix B Fig. 54**).

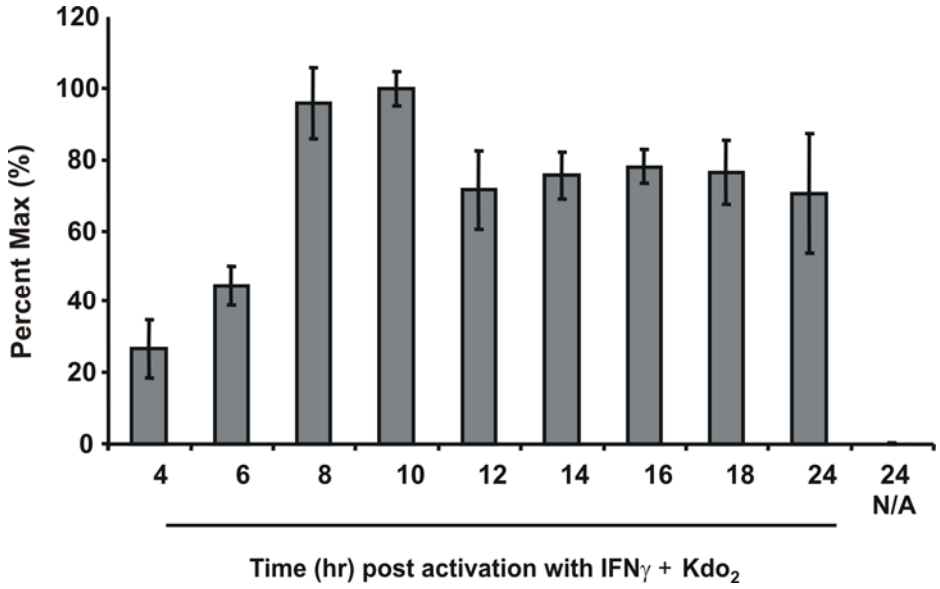

Figure 23. Electrophilic Fatty Acid Derivative-2 is detected 4-6 hours after RAW264.7 cell activation.

RAW264.7 cells were activated with Kdo_2 Lipid A (0.5 μg/ml) and IFNγ (200 U/ml) and EFAD-2 levels were quantified at indicated times post activation.

4.2.3 Electrophilic Fatty Acid Derivatives are α,β-unsaturated keto-derivatives of fatty acids.

Accurate mass TOF data (at an accuracy below 10 ppm), elution profile, and loss of CO_2 upon fragmentation suggested EFAD-2 to be a mono-oxygenated derivative of a 22-carbon fatty acid with a total of five double bonds. The MS/MS spectrum for BME-adducted EFAD-2 (*m/z* 421 $[M-H]^-$) displayed characteristic fragment ions at *m/z* 403 ([M-H-H_2O]), 377 ([M-H-CO_2]), 343 ([M-H-BME]), 325 ([M-H-BME-H_2O]), and 299 ([M-H-BME- CO_2]) (**Fig. 19**), consistent with the fragmentation pattern of BME adducts previously reported[159]. Similarly, EFAD-1 and -3 were identified as mono-oxygenated derivatives of a 22-carbon fatty acid with a total of six and four double bonds, respectively. To elucidate the precursors *in vivo*, fatty acid media supplementation studies were performed. PUFA of the ω-3 and ω-6 series were used for supplementation, and PUFA of different chain lengths and degrees of saturation were chosen based on availability of large pure quantities. Oleic acid (18:1 ω-9) was used as a mono-unsaturated control for fatty acid supplementation, as the ω-9 series is not elongated and desaturated to the same degree as fatty acids of the ω-3 and ω-6 series. The formation of EFAD-2 was significantly increased in activated RAW264.7 cells supplemented with 18:3 ω-3 (α-linolenic acid) and 20:5 ω-3 (EPA) while formation was slightly decreased when the relevant ω-6 species were provided (**Fig. 24**).

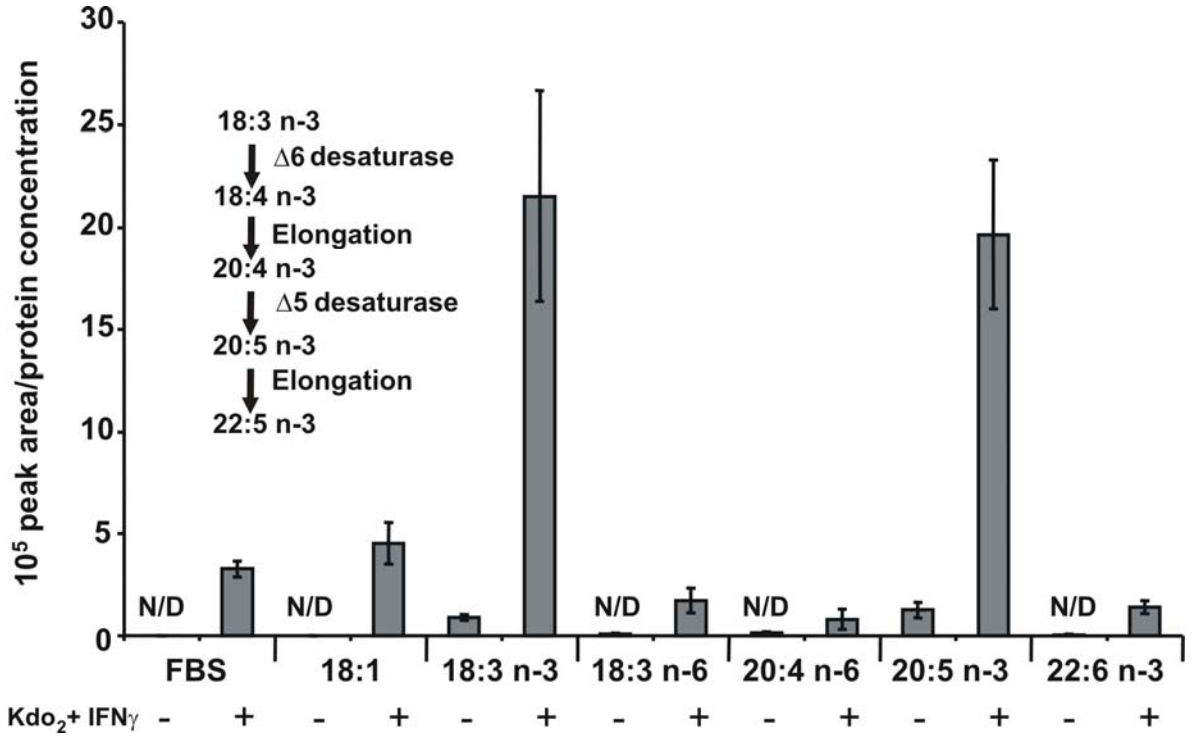

Figure 24. Electrophilic fatty acid derivative-2 is a product of docosapentaenoic acid oxidation.

RAW264.7 cells were grown for 3 days in DMEM and 10% FBS supplemented with 32 μM of the indicated fatty acid. On the third day cells were activated with Kdo_2 Lipid A (0.5 μg/ml) and IFNγ (200 U/ml) and EFAD-2 levels were quantified 21 h post activation.

These results indicated that EFAD-2 was derived from ω-3 PUFAs exclusively. The supplementation of 22:6 ω-3 (DHA) did not increase EFAD-2 levels. This was consistent with the fact that while mammalian cells can desaturate and elongate shorter chain PUFAs, they generally do not resaturate such PUFA as DHA. The formation of EFAD-1 in activated RAW264.7 cells was increased only by the supplementation of 22:6 ω-3 (**Fig. 25**).

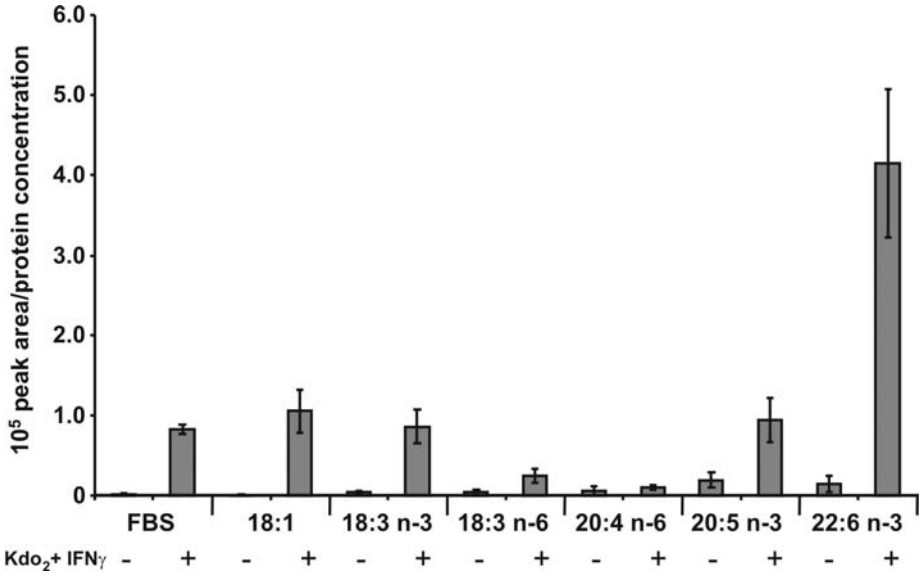

Figure 25. Electrophilic fatty acid derivative-1 is derived from docosahexaenoic acid.

RAW264.7 cells were grown for 3 days in DMEM and 10% FBS supplemented with 32 μM of the indicated fatty acid. On the third day cells were activated with Kdo_2 Lipid A (0.5 μg/ml) and IFNγ (200 U/ml) and EFAD-1 levels were quantified 21 h post activation.

EFAD-3 was increased by both ω-3 and ω-6 fatty acid supplementation, indicating that its precursor could be either ω-3 or ω-6 DTA (**Fig. 26**, see **Appendix B Fig. 49-51** for results for EFADs 4-6).

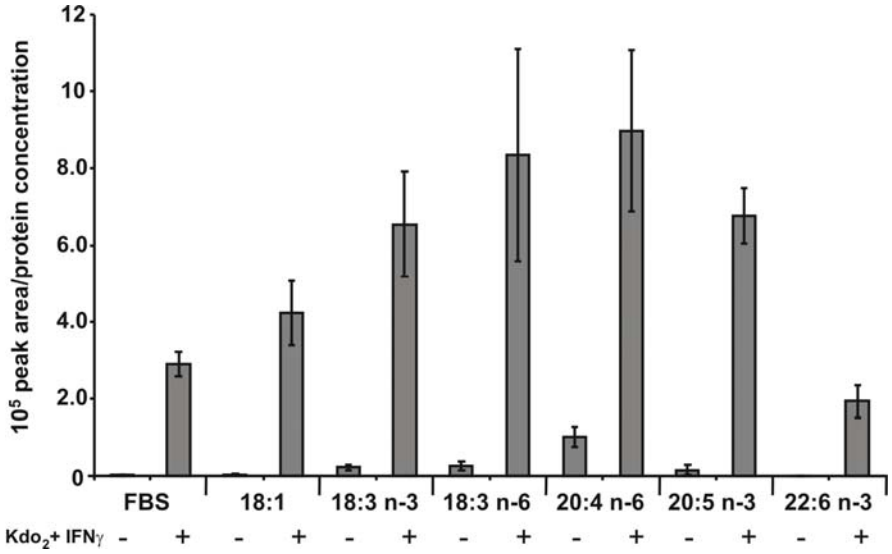

Figure 26. Electrophilic fatty acid derivative-3 is derived from both the ω-6 and ω-3 series of fatty acids.

RAW264.7 cells were grown for 3 days in DMEM and 10% FBS supplemented with 32 μM of the indicated fatty acid. On the third day cells were activated with Kdo_2 Lipid A (0.5 μg/ml) and IFNγ (200 U/ml) and EFAD-3 levels were quantified 21 h post activation.

Overall, this study showed that EFAD-1, EFAD-2, and a percentage of EFAD-3 were derivatives of ω-3 fatty acids DHA, DPA and DTA while EFAD-4 to -6 were synthesized from ω-6 and ω-9 fatty acids (**Table 4**).

In order to confirm that the electrophilic functional group of EFADs was an α,β-unsaturated carbonyl and to exclude the presence of other electrophilic groups (i.e. epoxy group), the Luche reaction was performed **(Fig. 27-29**). This reaction uses $NaBH_4$ (in the presence of $CeCl_3$) to selectively reduce carbonyl groups (but not epoxy or carboxylic acid groups) to the allylic alcohol without loss of regioselectivity (**Fig. 27**)[199].

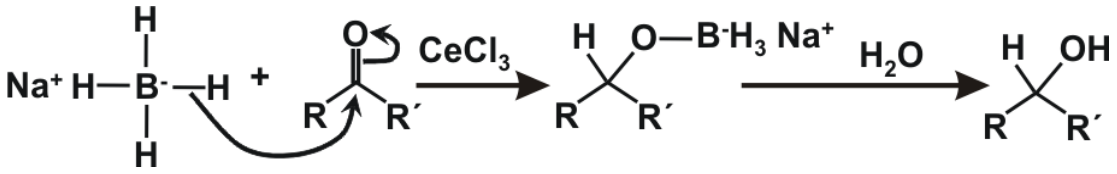

Figure 27. Diagram of $NaBH_4$ reduction of an α,β-unsaturated keto group to an alcohol group.

Lipid extracts from IFNγ and LPS-activated RAW264.7 cell lysates were fractionated using HPLC. The fraction containing EFAD-2 (detected by MRM scan for the loss of CO_2: *m/z* 343/299) was reduced with $NaBH_4$, resulting in a significantly decreased MRM signal for EFAD-2 and the appearance of a previously absent peak at the transition 345/327 (reduced product of EFAD-2, **Fig. 28**).

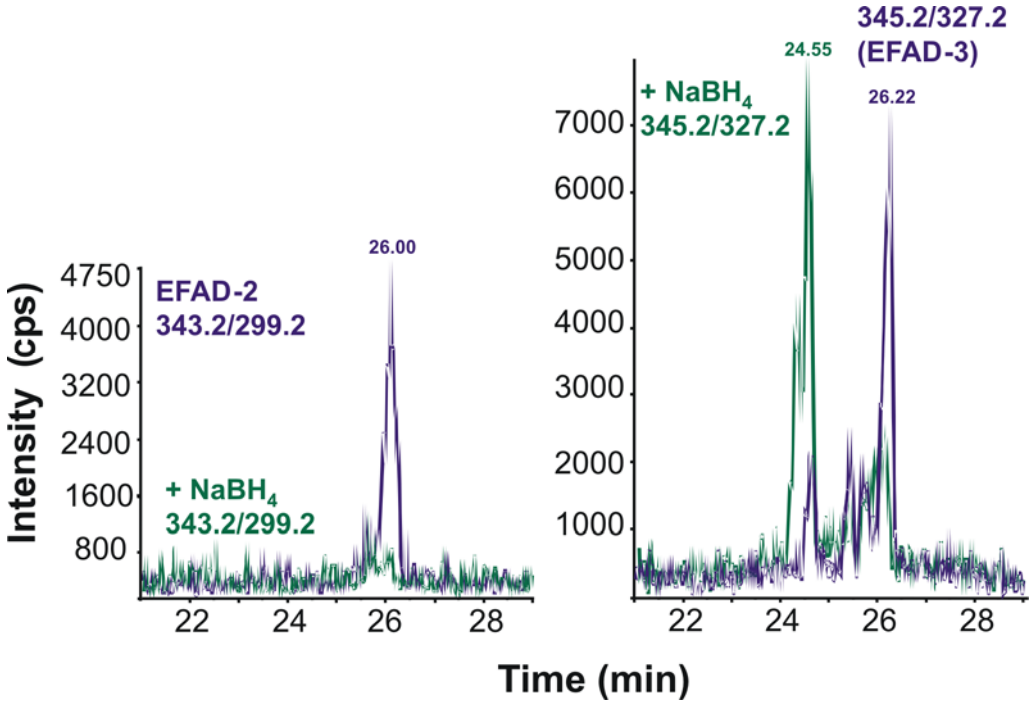

Figure 28. Electrophilic fatty acid derivative-2 can be reduced to the corresponding hydroxy species by $NaBH_4$.

(Left panel) MRM scans monitoring for the *m/z* transition of 343.2/299.2 (keto-DPA losing CO_2) in RAW 264.7 cell lysates purified for EFAD-2 and treated with or without $NaBH_4$. (Right panel) MRM scans monitoring for

the *m/z* transition of 345.2/327.2 (hydroxyl-DPA or keto-DTA losing H_2O) in RAW 264.7 cell lysates purified for EFAD-2 and treated with or without $NaBH_4$.

The reduced (hydroxy) product of EFAD-2 treated with $NaBH_4$ was also detected by MRM following the transition for the loss of CO_2 or H_2O; the MRM transition for loss of water (*m/z* 345/327) (**Fig. 28)**. The *m/z* value of 345 is also the value for parent ion of EFAD-3 (two mass units greater than EFAD-2), thus the transition *m/z* 345/327 gives a signal in the EFAD-2 enriched fraction that is diminished following $NaBH_4$ reduction. Upon treatment with $NaBH_4$ the MRM transition *m/z* 345/327 also displays the appearance of a new signal eluting 2 min before the signal for EFAD-3, suggesting the formation of reduced EFAD-2.

Due to the enhanced fragmentation typical of hydroxy groups during MS/MS, products of the Luche reaction yielded relevant information about the location of the original carbonyl group. In the case of EFAD-2 there is a predominance of reduced carbonyl (hydroxyl) groups located at the 13^{th} or 17^{th} position (**Fig. 34** and **35**). The MS/MS spectrum of the parent ion *m/z* 345.2 typically displays the following fragment ions *m/z* 327 ([M-H]-H_2O) and 283 ([M-H]-H_2O-CO_2). Diagnostic ions for 13-hydroxy-DPA (*m/z* 223, 205 (223-H_2O), and 195) were observed in the EFAD-2 enriched fraction reduced with $NaBH_4$ (**Fig. 29**).

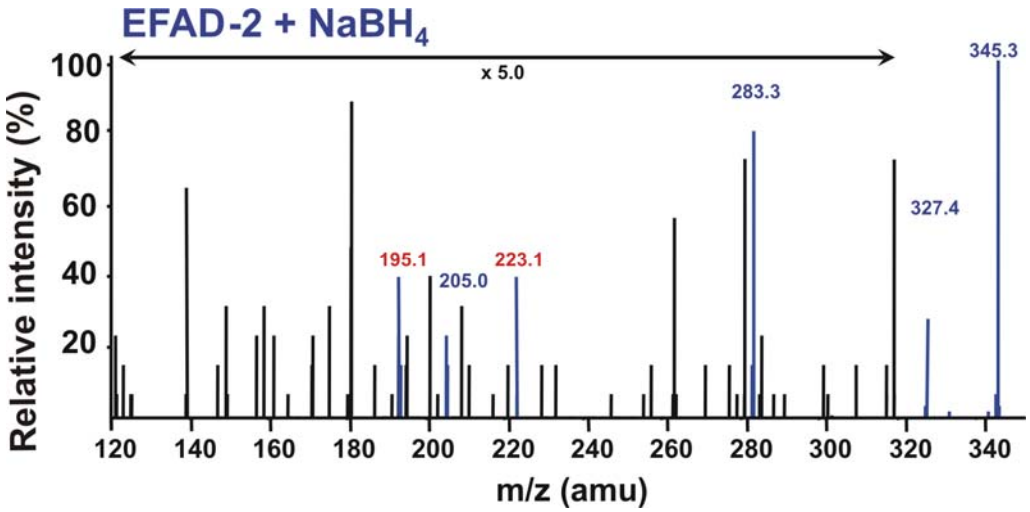

Figure 29. Electrophilic fatty acid derivative-2 reduced by $NaBH_4$ displays a fragmentation pattern indicating a hydroxy group at carbon 13.

EFAD-2 was purified from activated RAW 264.7 cells and reduced with $NaBH_4$ to produce the corresponding hydroxy-derivative, thus providing specific MS/MS fragmentation surrounding the hydroxy group.

The findings of the Luche reaction experiments and the fatty acid supplementation studies finally revealed that EFAD-2 corresponded to 13-oxoDPA, that EFAD-3 was an oxo-derivative of DTA, and that EFAD-5 was an oxo-derivative of 20:3 ω-6 (**Table 4**).

4.2.4 Cyclooxygenase-2 is Responsible for Electrophilic Fatty Acid Derivative Production.

In the process of identifying EFADs as α,β-unsaturated keto-derivatives of PUFA, a series of experiments were performed to determine the mechanisms of their synthesis. First EFAD-2 levels were quantified in RAW264.7 cells activated with Kdo_2 and IFNγ following treatment with a variety of inhibitors (**Fig. 230**, **Appendix B Fig. 55** and **Table 4**).

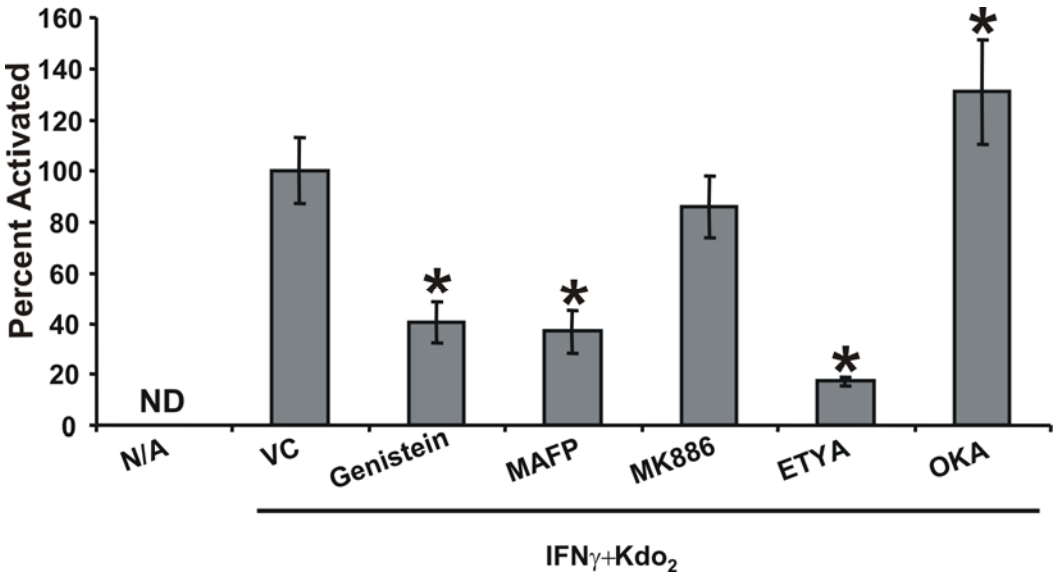

Figure 30. Electrophilic fatty acid derivative-2 formation in RAW264.7 cells is inhibited by genistein, ETYA, and MAFP.

RAW264.7 cells were activated with Kdo_2 Lipid A (0.5 μg/ml) and IFNγ (200 U/ml) in the presence of indicated inhibitors and EFAD-2 levels were quantified 20 h post activation. (a) Inhibitor concentrations were as follows: VC (vehicle control), genistein (25 μM), MAFP (25 μM), MK886 (500 nM), ETYA (25 μM) and OKA (50 nM). Data are expressed as mean ± S.D. (n=4), where * = significantly different (p<0.01) from "Kdo_2 + IFNγ" (one-way ANOVA, post-hoc Tukey's test).

Both Genistein and methyl arachidonyl fluorophosphonate (MAFP) inhibited EFAD-2 production by over 50%. Genistein (25 μM) was chosen as a general tyrosine kinase inhibitor to inhibit LPS and IFNγ signal transduction. MAFP, a selective irreversible inhibitor of both calcium-dependent and calcium-independent cytosolic phospholipase A_2 ($cPLA_2$ and $iPLA_2$), was employed to determine if EFAD precursors were released from complex lipids upon RAW264.7 cell activation. To determine if 5-lipoxygenase (5-LOX) was involved in EFAD formation, MK886 (500 nM) was used to prevent FLAP activation of 5-LOX. MK886 had no significant effect on EFAD-2 formation. Eicosatetraynoic acid (ETYA; 5 μM), a nonspecific

inhibitor of COX and LOX enzymes, strongly inhibited EFAD formation. Finally, the general phosphatase inhibitor, okadaic acid (OKA; 50 nM), caused a slight increase in EFAD formation, which was probably due to the enhancement of signal transduction downstream of LPS and IFNγ.

In order to determine whether the inhibitory effects of ETYA on EFAD formation were due specifically to the inhibition of COX, EFAD-2 levels were quantified in RAW264.7 cells that were activated with Kdo_2 and IFNγ, and treated with COX inhibitors (**Fig. 31**, **Appendix B Fig. 56** and **Table 4**).

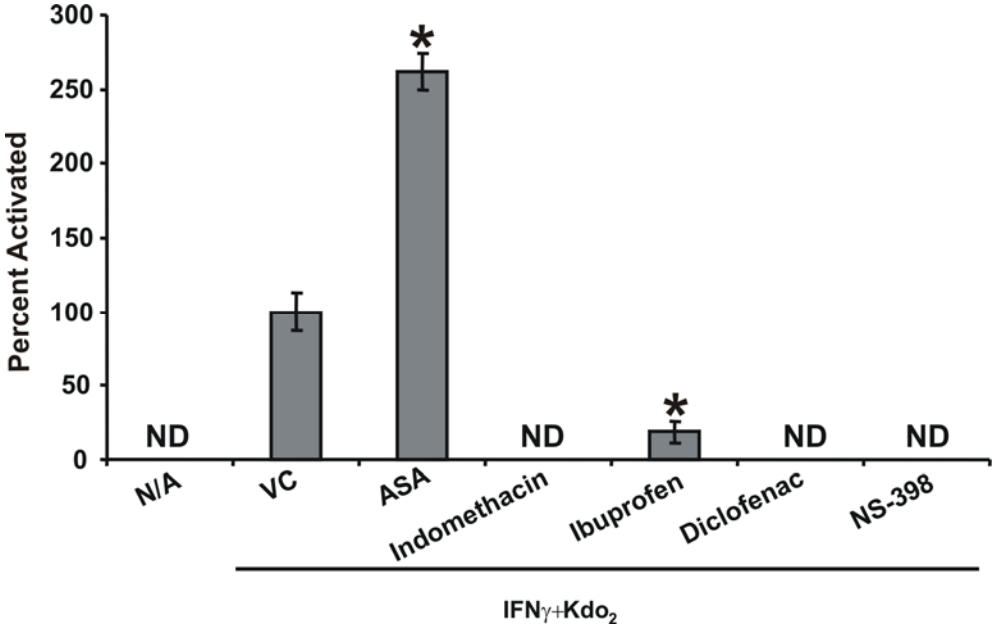

Figure 31. Electrophilic fatty acid derivative-2 formation is dependent on cyclooxygenase-2 activity.

RAW264.7 cells were activated with Kdo_2 Lipid A (0.5 μg/ml) and IFNγ (200 U/ml) in the presence of indicated inhibitors and EFAD-2 levels were quantified 20 h post activation. COX inhibitor concentrations were as follows: VC (vehicle control) aspirin (200 μM), indomethacin (25 μM), ibuprofen (100 μM), diclofenac (1 μM) and NS-398 (4 μM). Data are expressed as mean ± S.D. (n=4), where * = significantly different (p<0.01) from "Kdo_2 + IFNγ" (one-way ANOVA, post-hoc Tukey's test).

COX inhibitors were used at concentrations that were at least 5 times their IC_{50} values, based on previous literature (for a summary see Gierse *et al.*)[161]. Indomethacin (25 μM) and diclofenac (1 μM) were found to completely abolish EFAD formation, while ibuprofen (100 μM) was found to inhibit EFAD formation by more than 80%. Moreover, the selective COX-2 inhibitor, NS-398 (4 μM), a close structural relative of Nimesulide, also abolished EFAD formation. Finally, ASA (200 μM) significantly increased EFAD formation by 2.5 fold. This was consistent with previous reports showing that ASA acetylation of COX-2 Ser530 favors the formation of hydroxy or hydroperoxy derivatives of ω-3 PUFA[131].

The provocative results yielded by the use of COX inhibitors, supported the involvement of COX-2 in EFAD-2 synthesis and motivated the development of an *in vitro* model of enzymatic EFADs synthesis (**Fig. 32** and **Appendix B Fig. 58**).

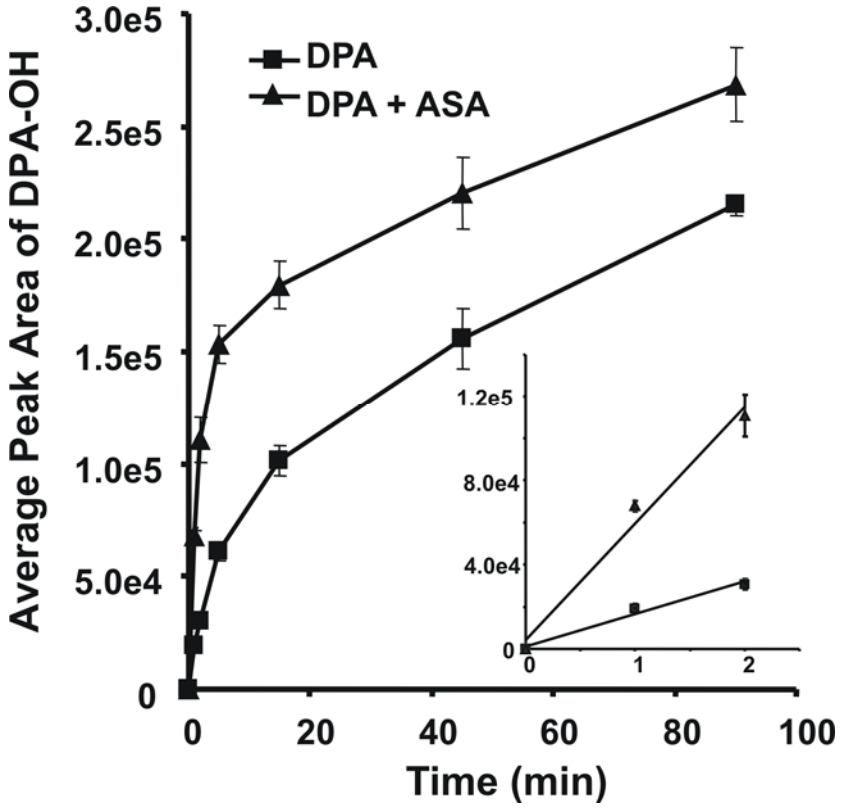

Figure 32. Ovine cyclooxygenase-2 catalyzes the formation of hydroxyl-containing precursors of Electrophilic fatty acid derivative-2 from docosapentaenoic acid *in vitro.*

The hydroxyl-precursors of EFAD-2 were synthesized *in vitro* using purified ovine COX-2 ± aspirin and DPA. The hydroxyl precursors were analyzed (by EPI) and quantified (by following their MRM transitions) at the indicated time points during the reaction by HPLC-ESI-MS/MS.

Purified ovine COX-2 generated the EFAD-2 precursor, hydroxy-DPA (similarly, the EFAD-1 precursor, hydroxy-DHA, was produced from DHA). Similarly, the EFAD-1 precursor, hydroxy-DHA (OH-DHA), was produced from DHA by COX-2 (**Appendix B Fig 61**). ASA increased the rate and extent of formation of hydroxy-DPA and also shifted the population of hydroxy-isomers produced from 13-hydroxy-DPA to 17-hydroxy-DPA (**Fig. 33** and **Fig. 34** and **35**).

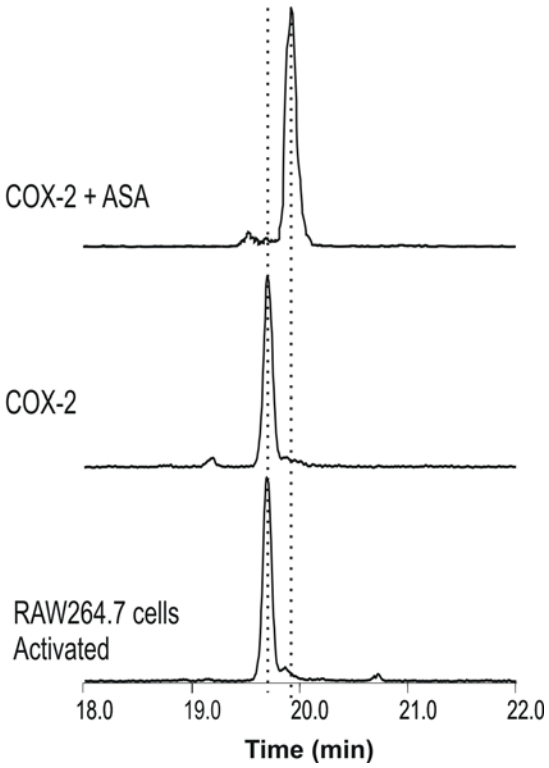

Figure 33. Cyclooxygenase-2 produces hydroxy-docosapentaenoic acid *in vitro* that co-elutes with reduced electrophilic fatty acid derivative-2 purified from activated RAW264.7 cells.

The hydroxyl-precursors of EFAD-2 were synthesized *in vitro* using purified ovine COX-2 ± aspirin and DPA. The hydroxyl precursors were analyzed (by EPI) and quantified (by following their MRM transitions) at the indicated time points during the reaction by HPLC-ESI-MS/MS.

The fragmentation pattern of COX-derived 13-OH-DPA showed the characteristic m/z 195 and 223 ions, corresponding to the hydroxyl group induced fragmentation already observed in RAW264.7 cell extracts upon $NaBH_4$ reduction **(Fig. 29** and **Fig. 34)**. In contrast, when COX-2 was treated with ASA, characteristic ions corresponding to the hydroxyl group at the 17^{th} position were detected **(Fig. 35)**.

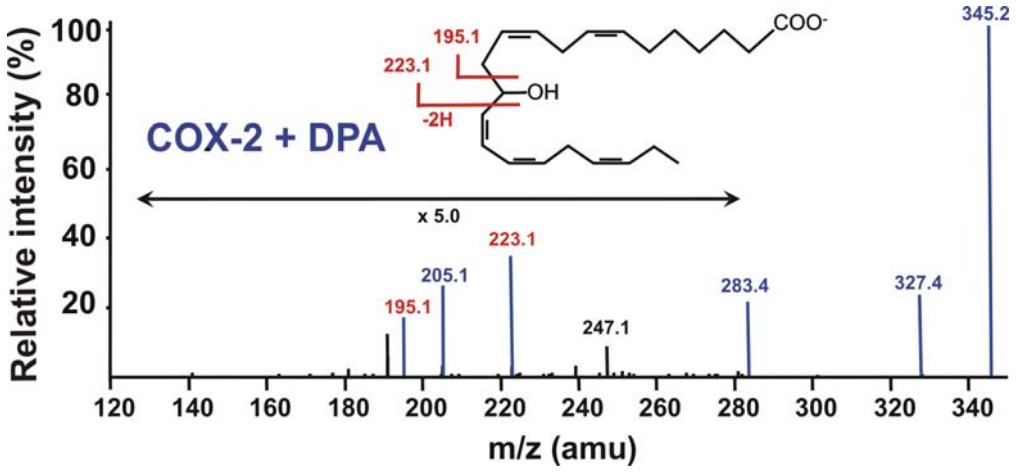

Figure 34. Hydroxy-docosapentaenoic acid produced by incubation of cyclooxygenase-2 and docosapentaenoic acid displays a MS/MS fragmentation pattern indicating a hydroxy group at carbon 13.

DPA was incubated with purified ovine COX-2 *in vitro* and the resulting fragmentation patterns of hydroxy-DPA were analyzed by MS/MS.

Preincubation of COX-2 with ASA produced 17-hydroxy-DPA, which gave the following diagnostic ions: (*m/z* 275, 247, and 203 (247-CO_2). The fragmentation patterns of biological EFADs were confirmed using standards synthesized with purified COX-2.

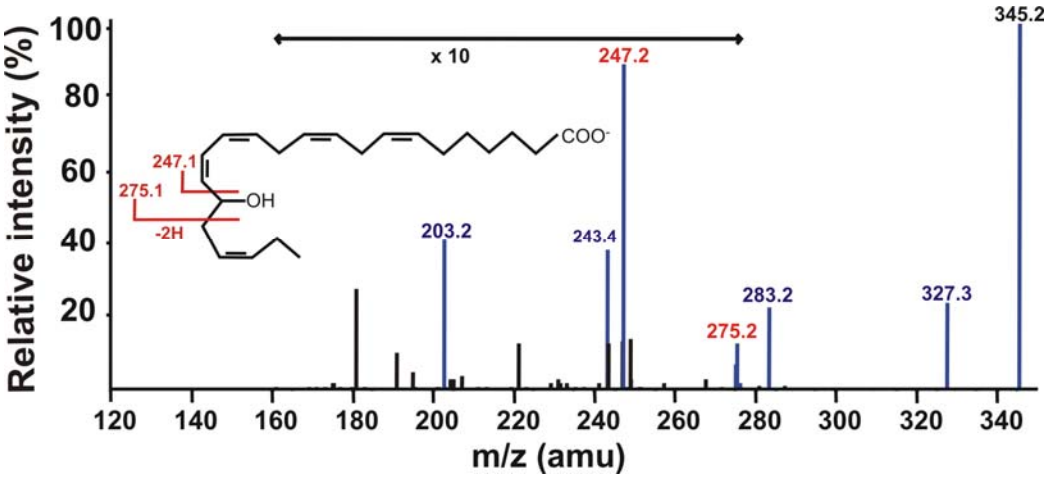

Figure 35. Hydroxy-docosapentaenoic acid produced by incubation of cyclooxygenase-2 with docosapentaenoic acid and acetylsalicylic acid displays a MS/MS fragmentation pattern indicating a hydroxy group at carbon 17.

DPA was incubated with purified ovine COX-2 *in vitro* with aspirin and the resulting fragmentation patterns of hydroxy-DPA were analyzed by MS/MS.

In activated, ASA-treated RAW264.7 cells this shift resulted in the production of 17-oxo-isomers**.** Finally, 17-oxoDPA and 17-oxoDHA were synthesized as standards and found to co-elute with EFAD-2 produced in activated RAW264.7 cells (**Fig. 36**).

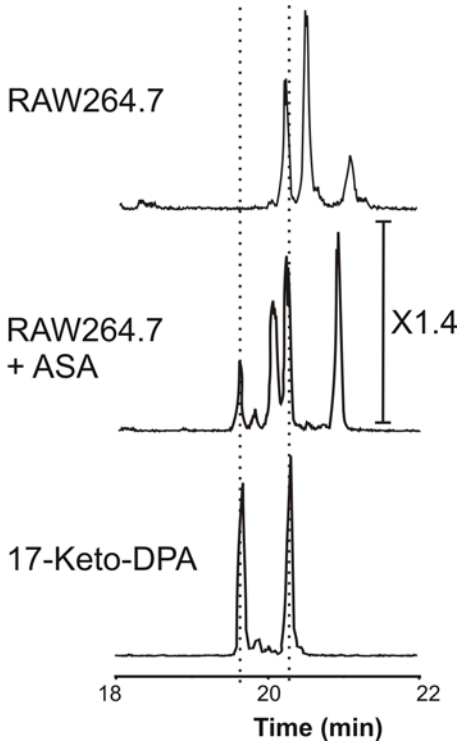

Figure 36. Adducts of β-mercaptoethanol and electrophilic fatty acid derivative-2 produced by activated RAW264.7 cells treated with aspirin co-elute with BME-17-Keto-DPA adduct standards.

RAW264.7 cells were activated with Kdo_2 Lipid A (0.5 μg/ml) and IFNγ (200 U/ml) ± aspirin and compared to a 17-keto-DPA standard. The elution profile of EFAD-2 was monitored by MRM scans following the *m/z* transition of 421.2/343.2 (the BME adduct of EFAD-2 losing BME).

Since COX-2 alone was unable to produce the oxo-group typical of EFADs, a hydroxy-dehydrogenase reaction was necessary in order to complete EFAD biosynthesis in the cells.

Lysates from activated or non-activated RAW264.7 cells were incubated with the EFAD-2 precursors DPA and OH-DPA. When activated and non-activated cells were incubated with OH-DPA in presence of NAD+ there was a time-dependent production of EFAD-2, suggesting that the cells have a constitutively expressed hydroxy-dehydrogenase activity (**Fig. 37**, included with the permission of Chiara Cipollina).

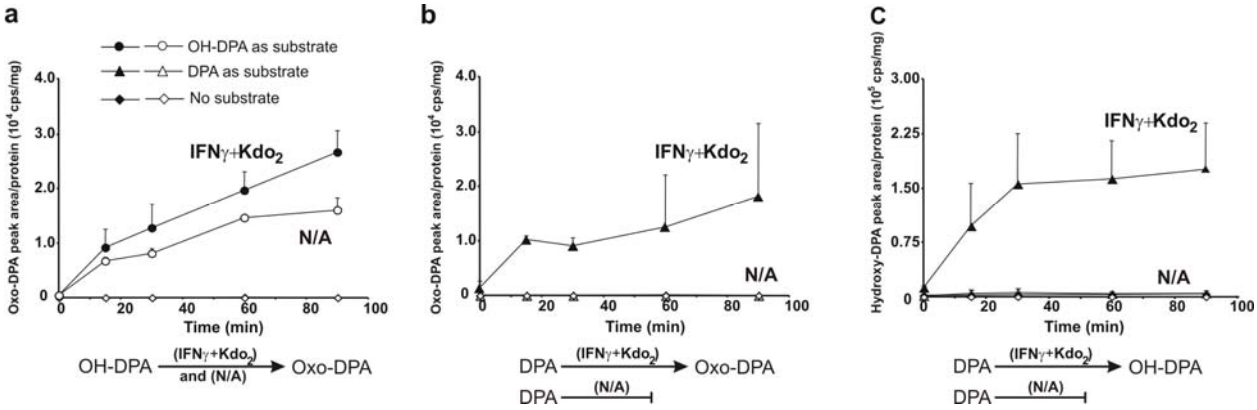

Figure 37. RAW264.7 cells possess an inducible oxygenase activity and a constitutive hydroxy-dehydrogenase activity

RAW264.7 cells were activated with Kdo_2 (0.5 μg/ml) and IFNγ (200 U/ml) or treated with vehicle control and their lysates were collected 20 h post activation. Hydroxy-DPA, DPA, or vehicle was added to the cell lysates and the production of keto-DPA or hydroxy-DPA was monitored over time.

Alternatively, only activated cells displayed a time-dependent production of hydroxy-DPA and EFAD-2 when incubated with DPA. Thus only the metabolism of activated cells was able to convert DPA into oxo-DPA, consistent with the requirement of COX-2 for this conversion. The hydroxy-dehydrogenase activity responsible for the conversion of OH-DPA to its oxo-derivative appeared to be constitutively expressed. Control experiments also confirmed that hydroxy-fatty acid derivatives were not being converted to or formed from the corresponding oxo-derivative during the BME-alkylation with cell lysates (**Appendix B Fig. 48**)

4.2.5 Electrophilic Fatty Acid Derivatives are Produced by Primary Macrophages Isolated from Mouse Bone Marrow.

Since RAW 264.7 cells (and potentially other macrophage cell lines) may experience differences in AA metabolism[200], it was important to demonstrate that the formation of EFADs occurred in primary cell lines as well. Thus, C57BL/6 murine primary hematopoietic stem cells were differentiated to macrophages, activated with Kdo_2 and IFNγ and analyzed for the formation of EFADs. Five out of the six EFAD species (EFAD-1, 2, -3, -5 and -6) were observed which co-eluted with those produced by RAW264.7 cells and with the available standards. Cell lysates were subsequently reacted with BME and lipids were extracted and detected using the same methods as those for the RAW264.7 cells (**Fig. 38** and **Appendix B Fig. 57**).

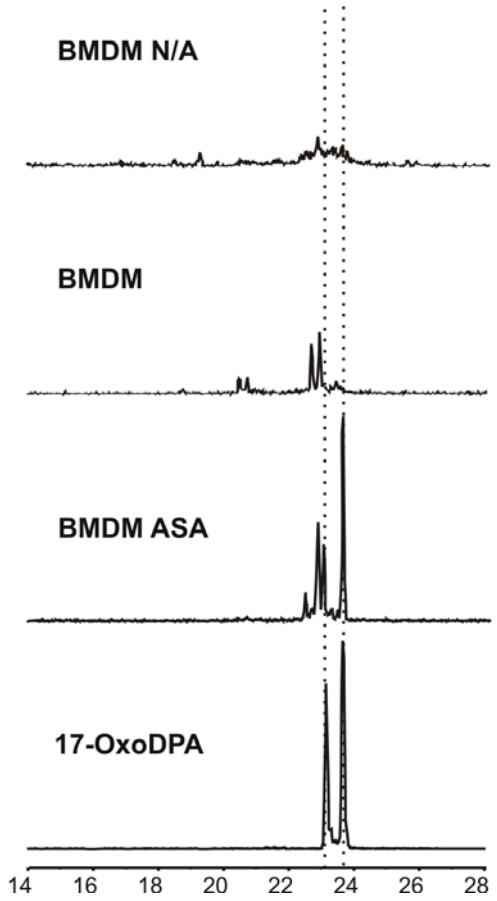

Figure 38. Electrophilic fatty acid derivative-2 is formed in activated primary murine macrophages.

Bone marrow derived macrophages were activated with PMA (3.24 μM), Kdo_2 (0.5 μg/ml), and IFNγ (200 U/ml) and EFADs were detected 10 h post activation.

Similar to what was observed in RAW264.7 cells, when activated bone marrow-derived macrophage (BMDM) cells were treated with ASA the extent of EFAD formation was increased about two to three fold and in the case of EFAD-1 and -2, the isomeric composition shifted from 13-oxo to 17-oxo species.

4.2.6 Electrophilic Fatty Acid Derivatives Adduct to Proteins and GSH.

Many electrophiles (*e.g.* HNE[201], 15d-PGJ_2[17], and NO_2-FA[18]) form adducts with nucleophilic amino acid residues in the cell[202]. In order to confirm EFADs electrophilic nature in the intracellular environment it was important to determine the occurrence and extent of adduction to proteins and small molecule sulfhydryls. Several approaches were used to demonstrate the occurrence of these reactions in activated cells using well-characterized proteins as reporters. First, total EFAD content was quantified and compared with the pool of free EFADs (including EFADs adducted to small molecules such as glutathione, **Fig. 39**). The difference between the two groups gave the percentage of EFADs adducted to proteins (~50%).

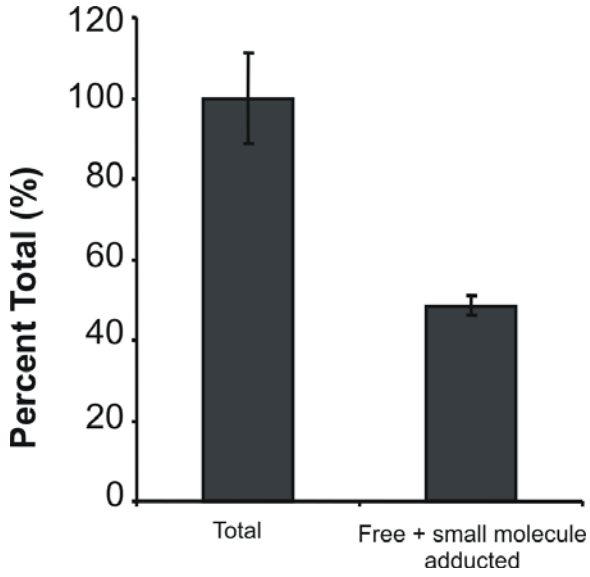

Figure 39. Electrophilic fatty acid derivative-2 adducts to proteins in activated RAW264.7 cells.

RAW264.7 cells were activated with Kdo_2 Lipid A (0.5 μg/ml) and IFNγ (200 U/ml) and harvested 21 h post activation. Cell lysates were then split into two groups: 1) treated directly with BME (500 mM) followed by protein precipitation with acetonitrile and 2) protein precipitation with acetonitrile followed by treatment with BME (500 mM). BME reaction proceeded for 2h and EFAD-2 levels were quantified by RP-HPLC-MS/MS.

Subsequently, the expected difference in reaction kinetics of BME with free and adducted EFADs was used to further confirm the distribution of intracellular EFADs, between free and adduct form. Reaction rates of BME with free electrophiles were measured and were found to be fast, with a pseudo first order reaction rate constant calculated to be between $3x10^{-3}$ and $5\ x10^{-3}$ sec^{-1} for the different α,β-oxo-unsaturated fatty acids tested (15d-PGJ2, EFAD-1, EFAD-2 and oxoETE, data not shown). In contrast, reactions with adducted electrophiles are slower, and depend on the k_{off} reaction rate of the Cys-EFAD and His-EFAD adducts. The time-dependent characteristic of these reactions was used to further confirm the adducted populations present in the cell lysates (**Fig. 40**).

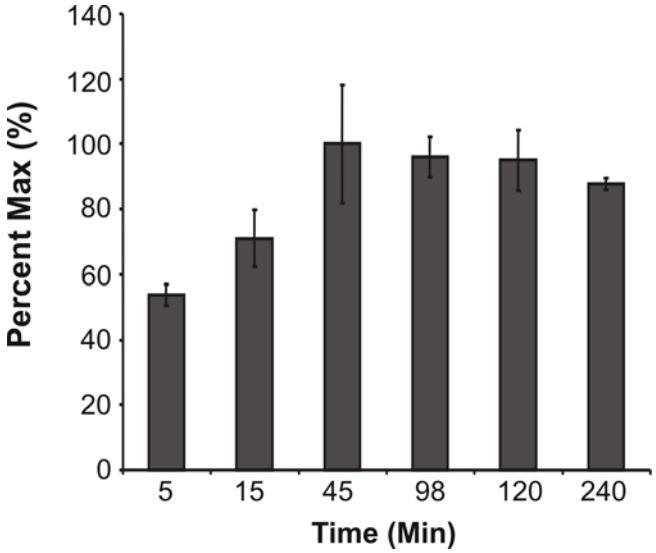

Figure 40. The free population of electrophilic fatty acid derivative-2 reacts with β-mercaptoethanol in the first 5 minutes of the reaction, while the thiol-adducted population takes up 45 minutes to transfer to β-mercaptoethanol.

RAW264.7 cells were activated with Kdo_2 Lipid A (0.5 μg/ml) and IFNγ (200 U/ml) and harvested 21 h post activation. Cell lysates were also monitored for reaction with BME (500 mM) over time.

Fast kinetics with free EFADs and a slower component reaction rate for the displacement of EFADs from adducted proteins were observed. Approximately 50% of the EFADs reacted with BME within the first 5 min, suggesting that protein-adducted EFADs accounted for the remaining ~50% of total EFADs reacted with BME after 45 min. To more specifically test the binding of EFADs to nucleophilic residues in proteins, we tested whether GAPDH was alkylated by EFADs. This enzyme is a well-characterized target for electrophiles and becomes easily inactivated by nitrosylation, oxidation or nucleophilic addition. As expected and based on its electrophilic properties, the EFAD-2 synthetic standard (17-oxo-isoform) readily formed adducts with Cys244, Cys149, His163 and His328 residues of GAPDH *in vitro* (**Appendix B Fig. 63-66**).

Additionally, glutathione adducts of oxo-DHA and oxo-DPA were found both in cell lysates and media of activated RAW264.7 cells, and compared to standards synthesized by reacting GSH and 17-oxo standards in the presence of GST (**Fig. 39**, included with the permission of Chiara Cipollina, **and Appendix B Fig. 59**).

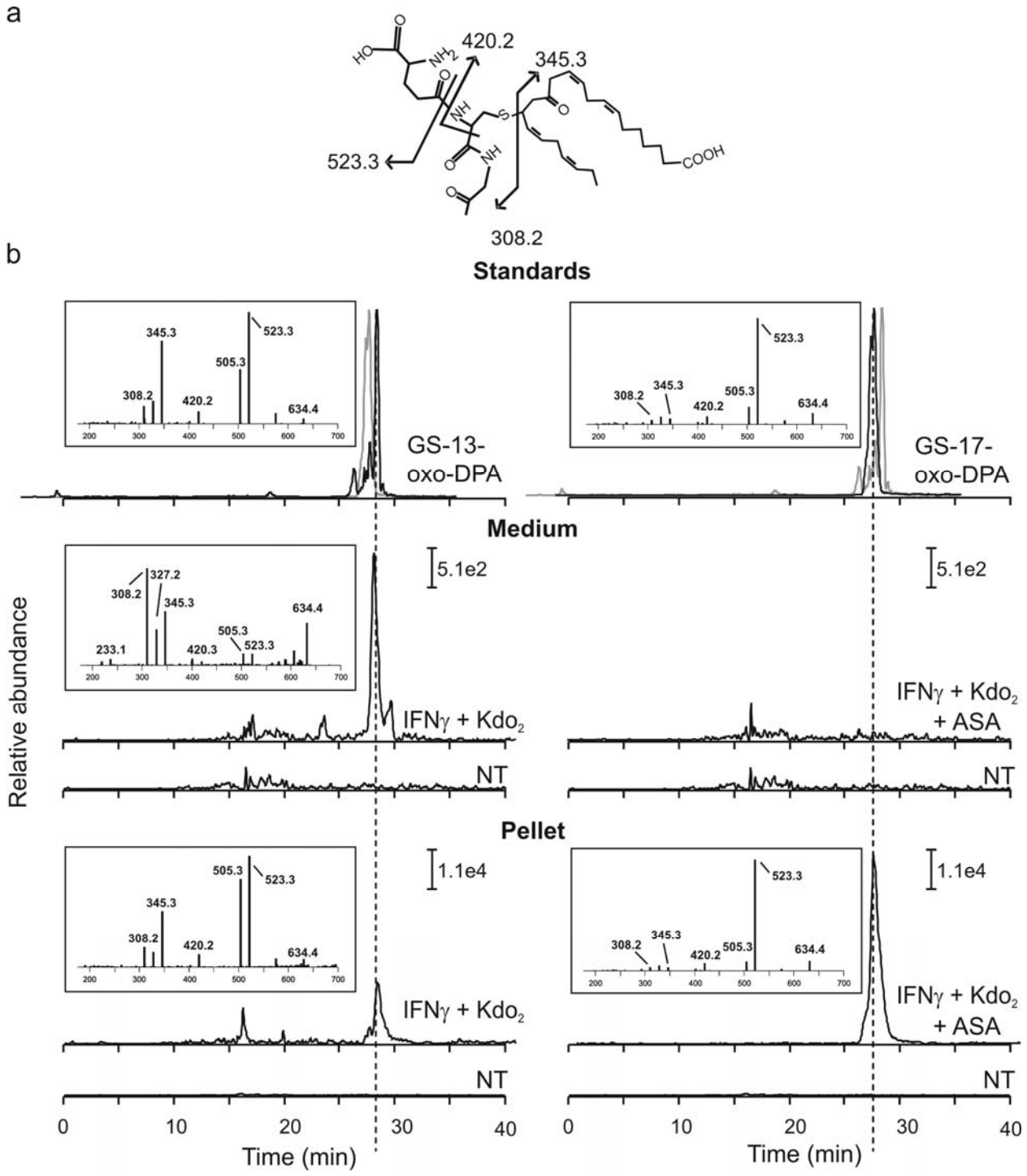

Figure 41. Intracellular and extracellular Glutathione-oxo-docosapentaenoic adducts (*m/z* 634.4) were detected following activation of RAW264.7 cells.

(a) Chemical structure and fragmentation pattern of GS-13-oxo-DPA. (b) Chromatographic profiles and mass spectra of 13- and 17-oxo-DPA derived from synthesized standards (upper panels), cell medium (middle

panel) and cell pellet (lower panel). Differences due to recovery efficiency were taken into account by correcting the signals levels using the internal standard GS-5-oxo-ETE-d7. Fragments 345.3 and 523.3 were selected and monitored as the ones giving the best signal to noise ratio in samples derived from cell media and cell pellets, respectively. Fragment 634.4 derived from loss of H_2O from the parent ion 652.4; m/z 523.3 and m/z 420.3 corresponded to fragments y2 and c1 typical of peptide fragmentation while 345.3 and 308.2 derived from the lipid and the glutathione molecule. m/z 505.3 and m/z 327.2 derived from loss of H_2O from 523.3 and 345.3, respectively. K/I, cells treated with Kdo2-Lipid A and IFNγ; K/I + Asa, cells treated with Kdo2-Lipid A, IFNγ and aspirin; NT, non treated cells.

The fragmentation patterns observed for EFAD-1 and -2 correspond to those obtained with the synthetic standards. Addition of ASA induced an increase in GS-adduct formation, consistent with the concomitant increase in EFADs synthesis. GS-adducts were also found in the extracellular media, with the exception ASA-treated samples, in which extracellular detection was unexpectedly reduced.

4.2.7 Electrophilic Fatty acid Derivatives Activate Cyto-protective and Anti-inflammatory Pathways.

Typically, RES promote the activation of the Nrf2-dependent anti-oxidant response pathway via thiol-dependent modification of the Nrf2 inhibitor Keap1. This allows nuclear translocation of the transcription factor Nrf2 and the expression of its target genes[17]. Consistent with their electrophilic nature, 17-oxo-DHA and 17-oxo-DPA promoted dose-dependent Nrf2 nuclear accumulation and expression of the cytoprotective enzymes heme oxygenase 1 (HO-1) and NAD(P)H:quinone oxidoreductase 1 (NQO-1) at micromolar concentrations (**Appendix B Fig. 60**, included with the permission of Chiara Cipollina).

Besides activating Nrf2-dependent anti-oxidant responses, 17-oxo-DHA and 17-oxo-DPA may play a role in modulating the inflammatory response generated by Kdo_2 and IFNγ treatment. Thus iNOS and COX-2 expression and activities were assessed. EFAD-1 and -2 strongly and dose-dependently repressed iNOS induction and subsequent accumulation of nitrate and nitrite in the cell media **(Appendix B Fig. 61**, included with the permission of Chiara Cipollina**)**. In particular, although the expression of the enzyme seemed to be unaffected when cells were treated with 10 μM concentrations, a clear reduction of nitrite production was still observed. Notably, Cox-2 induction was not affected by EFADs. Among the analyzed cytokines, IL-6, MCP-1 and IL-10 showed the strongest dose-dependent repression following EFAD treatment, with MCP-1 and IL-10 being more affected compared to IL-6 (**Appendix B Fig. 62**, included with the permission of Chiara Cipollina).

Similar results were observed in bone marrow derived macrophages (data not shown). The expression of iNOS and the analyzed pro-inflammatory cytokines is dependent on the activity of NF-kB and Stat-1. Electrophilic lipids can repress the activation of these transcriptional factors either by direct adduction to the NF-kB subunit p65 and to the inhibitor IκBα or via indirect mechanisms. Therefore, we assessed the effect of EFADs on p65 nuclear translocation and DNA binding and on Stat-1 phosphorylation. No significant inhibition was observed (data not shown).

4.2.8 EFADs Act as Peroxisome Proliferator Activated Receptor-γ Ligands.

Oxo fatty acids, such as 15d-PGJ_2[203], 5-oxoEPA, 6-oxoOTE, and the synthetic 4-oxoDHA[173], covalently bind and activate the peroxisome proliferator-activated receptorγ

(PPARγ). Thus PPARγ beta-lactamase reporter assays were performed to determine the ability of 17-oxoDPA and 17-oxoDHA to activate PPARγ **(Fig. 42**). The standards for EFADs 1 and 2 (17-oxoDPA and 17-oxoDHA) displayed slightly greater EC_{50}s (~40 nM) than 15-dPGJ_2 (~25 nM) and EC_{50}s that were orders of magnitude lower than those for 17-hydroxyDPA (>10 μM) or their corresponding native fatty acids (DHA and DPA).

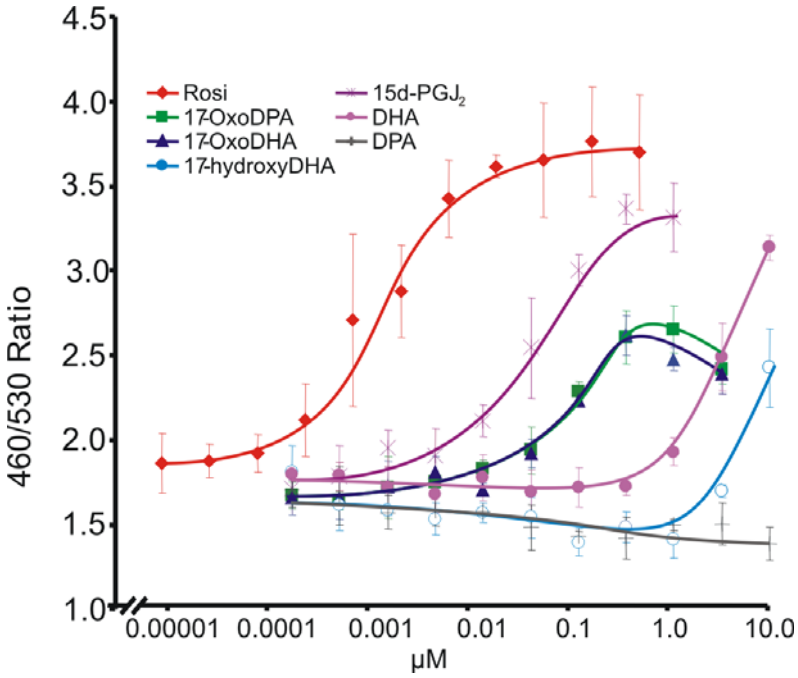

Figure 42. The 17-oxo-standards for electrophilic fatty acid derivatives -1 and -2 are agonists of peroxisome proliferator activated receptor-γ.

PPARγ beta-lactamase reporter assays were performed for Rosiglitazone, 17-oxoDPA, 17-oxoDHA, 15d-PGJ_2, DPA, and DHA with concentrations ranging from 0.5-10,000 nM.

4.3 CONCLUSIONS

Despite current knowledge regarding a wide range of lipid signaling mediators, the question as posed by Harkewicz *et al.* [204] still remains: "are biologically significant eicosanoids [or other fatty acid-derived metabolites] being overlooked?" Herein we address this question by focusing the search for lipid metabolites on those with reversible electrophilic activity and consequently a potential for regulated signaling capabilities. The methods used in this study detected six novel EFADs, as well as oxoETE (data not shown), that were produced following the activation of macrophages with IFNγ and the endotoxin Kdo_2 lipid A. To our knowledge, 5 of these species have not been described before as metabolic products of mammalian cells (however, EFAD-5 may be oxoETrE). Interestingly, 15d-PGJ_2 formation was monitored and not observed in this study; the levels of 15d-PGJ_2 may have been too low for detection.

In taking the search for lipid mediators a step further, the Lipid Metabolites and Pathway Strategy consortium (Lipid MAPS; http://www.lipidmaps.org), has been publishing information focused on the lipid section of the metabolome and "global changes in lipid metabolites" (*i.e.* lipidomics) since 2005. While the methods used to date have identified new lipid metabolites and yielded valuable data on the signaling properties of these metabolites, some of the approaches utilized could be modified to overcome limitations and thus the potential to overlook lipids with unique reactivities or unconventional means of signal transduction Other studies use methods that have focused exclusively on RES; by using MS/MS to detect and study RES-GSH adducts, it is possible to appreciate the *in vivo* signature left by various RES and to obtain structural information on RES of interest by using MS^3 [19]. However, there are also limitations in using this method. For example, RES generated in lipid bilayers may not have the opportunity to interact with GSH, but may still modify membrane associated proteins[13]. This concept has already been

used to characterize enzyme-generated RES produced by the hypersensitive response in tobacco leaves [205].

The recently developed alternative to analyzing only RES-GSH adducts, utilizes an electrophile-alkylation reaction with BME to identify RES that can reversibly adduct to cellular thiols (or other nucleophiles)[159]. Thus, the oxidized lipid species reported in this study were initially discovered exclusively based on their chemical properties: negatively charged small hydrophobic molecules with reversible electrophilic activity. The BME method used herein increased MS/MS sensitivity for RES and standardized the behavior of a variety of RES during MS/MS analysis. For example, oxo-fatty acid derivatives do not fragment as well as the corresponding hydroxy-derivatives, rendering structural identification more difficult. Accordingly, one reason that the species described in this work have not been reported before may be that the typical method of lipid metabolite identification yields largely the expected or the most abundant species; unanticipated lipid species that might be produced and signal at lower concentrations would be relegated to the background of more prominent species in this method. The present work reports previously uncharacterized electrophilic fatty acids, which were primarily derived by oxygenation of ω-3 PUFAs. In particular, EFAD-1 to -3 corresponded to oxoDHA, oxoDPA and oxoDTA (with different isomers being formed depending on the presence of ASA). EFAD-4 to -6 were derived from ω-6 and ω-9 PUFAs. However, the low levels and the presence of several isomers did not allow a detailed structural characterization of these latter species. Subsequent investigation revealed inducible COX-2 was required for EFAD biosynthesis, although additional mechanisms of formation cannot be excluded yet.

While the formation of hydroxy-ETA[206] and hydroxy-DHA[131] by COX-2 has been described previously, further oxidation to the corresponding oxo species has only been observed

for hydroxy-ETA[35]. Moreover, despite the knowledge on 5-oxoETE and KODE, there is a lack of research on similar 22-carbon species. The oxidation of hydroxyl groups on bioactive lipids has been generally viewed as a step in metabolic inactivation, but such a reaction may instead confer novel beneficial biologic activity. The data of this report indicate a bifurcation at the point where hydroxy-derivatives of ω-3 PUFAs could be further oxidized by LOXs to resolvins and neuroprotectins. Furthermore, these monohydroxy-PUFA derivatives are also converted to the corresponding carbonyl species generating bioactive electrophilic lipids.

Although COX-2 was identified as one of the major enzymes responsible for EFAD formation in macrophages, this does not preclude the possibility that other oxygenases or mechanisms are involved in EFAD formation. The autoxidation of DHA and the resulting 10 positional isomers of hydroxy-DHA were identified early in the 1980s[129]. Since then the enzymatic oxidation of PUFA, such as DHA, EPA and ETE, has been described to occur via several pathways and to result in anti-inflammatory or pro-resolution mediators in addition to pro-inflammatory PGs. LOXs, (*i.e.* 5-LOX and in some cases 12-LOX and 15-LOX) can initiate or supplement the oxidation of PUFA. In particular 5-LOXs have been implicated in the production of lipoxins[207], leukotrienes[207], and 5-oxoETE[208] from ETA as well as in the production of resolvins[209] from EPA, and DHA. Cytochrome p450 (CYP) monooxygenases can also catalyze the NADPH-dependent oxidation of PUFA; CYP4F8 catalyzes hydroxylation of both AA and DPA (22:5n-6) mainly at the ω-3 position[191].

Hydroxy-PUFA derivatives, formed by the reactions mentioned above, can be further oxidized to the corresponding oxo-derivatives. Several hydroxy-dehydrogenase enzymes have already been described that could be involved in this second oxidation step of EFAD formation. For example, the enzyme 15-hydroxyprostaglandin dehydrogenase is a candidate for this reaction

since it has been reported to catalyze the formation of 15-oxoETE and the oxidation of RvD1 and RvE1 at position -17[210-212]. The LTB_4 12-hydroxy dehydrogenase/prostaglandin reductase ($LTB_4$12-HD/PGR) can catalyze the $NADP^+$-dependent oxidation of hydroxy-eicosanoids to the corresponding α,β-unsaturated keto derivative[34]. In the case of 5-oxoETE formation, the 5-lipoxygenase product 5-hydroxyeicosatetraenoic acid is further oxidized by 5-hydroxyeicosanoid dehydrogenase (5-HEDH) to 5-oxoETE[35]. As HEDH can catalyze the reaction of 5-HETE to 5-oxoETE in both the forward and reverse direction, the formation of 5-oxoETE is favored by a high $NADP^+$:NADPH ratio (this condition is often symptomatic of cells under oxidative stress). It is interesting to note that while HEDH activity is present in myeloid cells, it is most significantly induced following differentiation to macrophages using PMA[35]. All these reports strongly suggest that dehydrogenase enzymes with homology to those described above are involved in EFAD formation.

The adduction of EFADs to proteins and to GSH is not only the next step in their metabolism, it also demonstrates the role they play as potential modulators of protein function and as electrophilic signal transducers. RES adduction to proteins, such as the covalent modification of GAPDH by NO_2-FA, can alter the protein's activity or subcellular location[18]. RES can also modulate gene expression by covalently binding to transcriptional regulators, as exemplified by NO_2FA adduction to the p65 subunit of NFκB, thus preventing DNA binding[74]. In other cases, RES form covalent adducts with proteins that associate with transcription factors (*e.g.* 15d-PGJ_2 adduction to the Nrf2 inhibitor Keap1[17]). Moreover, RES participate in signaling by forming covalent adducts with GSH; the GSH adduct of 5-oxoETE acts as a potent chemotactic factor for neutrophils and eosinophils[213]. Approximately 50% of the EFADs recovered from activated RAW264.7 cell lysate were adducted to protein, but this value does not

include EFADs that were bound to small molecules such as GSH or EFADs that were irreversibly bound to proteins. Consequently both intracellular and extracellular (secreted) GS-EFAD-2 (and GS-EFAD-1) adducts were identified by RP-HPLC-MS/MS. While both GS-13-oxoDPA and GS-17-oxoDPA adducts were detected intracellularly for RAW264.7 cells, only the GS-13-oxoDPA adduct was detected extracellularly. This observation may be due to several possibilities: treatment of RAW264.7 cells with ASA may affect the secretory pathway, GS-17-oxoDPA may not be secreted as efficiently as GS-13-oxoDPA, or GS-17-oxoDPA may be further metabolized more rapidly than GS-13-oxoDPA once secreted.

In addition to GSH and GAPDH-adduct formation, the modulation of several signaling pathways by EFADs confirmed their role as endogenously produced anti-inflammatory signaling mediators. In view of their electrophilic reactivity, EFADs were initially tested for their ability to participate in some of the signaling pathways that other RES generally modulate. The 17-oxo standards of EFADs-1 and -2 (*i.e.* 17-oxoDHA and 17-oxoDPA) promoted the nuclear accumulation of Nrf2 as well as the expression of two major Nrf2 target genes, HO-1 and NQO-1, thus assisting in the response to oxidative or xenobiotic stress. The 17-oxo standards also acted as agonists of PPARγ, suggesting that EFADs may exert some anti-inflammatory effects through PPARγ activation. This was consistent with previous observations that activation of PPARγ by low concentrations of the synthetic ligand Rosiglitazone, inhibits the expression of a small set of IFNγ and LPS-dependent genes in primary mouse macrophages[214]. Additionally, 17-oxoDPA and 17-oxoDHA inhibited IFNγ and LPS-induced cytokine production in a dose-dependent manner in RAW264.7 cells. Further evidence concerning the anti-inflammatory signaling properties of EFADs was the dose-dependent inhibition of iNOS expression and activity by 17-oxoDPA and 17-oxoDHA following macrophage activation with IFNγ and Kdo_2.

Surprisingly, EFAD-1 and -2 did not affect NF-κB DNA binding activity, p65 nuclear translocation, nor STAT-1 phosphorylation suggesting that the inhibition of cytokine and iNOS expression was independent of these signaling pathways (data not shown). Additionally, COX-2 induction in response to Kdo_2 and IFNγ was not affected. Overall these findings suggest that EFADs may exert their anti-inflammatory actions via pathways other than NF-κB and STAT-1. The activation of PPARγ may be a possibility, especially since the activation of PPARγ differentially inhibits iNOS and COX-2 and generates a pattern of cytokine expression similar to what we have observed without affecting NF-κB activation[214]. Additional evidence supporting a role for EFADs as signaling mediators was the observation that 17-oxoDPA and 17-oxoDHA covalently bind Cys and His residues in GAPDH, giving a similar pattern to that previously observed for NO_2-FA[18]. Finally, preliminary data indicate that EFAD-1 and -2 may promote a cytoprotective response via the activation of the heat shock response, possibly by inducing activation of the transcription factor Hsf1 and the subsequent transcription of target genes, such as Hsp70 and Hsp40[69,215]. This would represent a further mechanism through which EFADs may exert their beneficial actions. Overall, while recognized signaling pathways that are modulated by electrophiles were tested, it is probable that EFADs each have their own unique signaling profiles and receptors. Further investigation is currently underway to elucidate these profiles.

The study of fatty acids modified by oxidative processes is a well-established field that includes several families of classic (*e.g.* PGs, TXs, and hydroperoxy and hydroxy fatty acid products of auto-oxidation) and relatively new lipids (*e.g.* resolvins, lipoxins, oxoETEs, neuroprostanes and NO_2-FA). Many of these lipids act as signaling molecules that assist in mediating essential homeostatic or pathological processes. Others are currently considered inactive metabolites of lipid mediators or by-products of oxidative stress. Initially, oxidized

PUFA derivatives were considered to be simply degradation products of an oxidizing environment or pro-inflammatory signaling mediators. This view has changed significantly in the past 20 years as new species of and roles for oxidized PUFA emerged. Numerous studies have associated the consumption of ω-3 PUFA with reduced risk of heart disease[123], colon cancer and neurocognitive disorders[121]. DHA and EPA have been the particular focus of these studies, but the mechanisms by which they exert their anti-inflammatory effects in various diseases are still unclear. It is becoming more apparent that some of the protective actions of ω-3 PUFA are mediated by their oxidized derivatives formed during periods of oxidative stress or during the resolution phase of inflammation[131,216].

Overall, the EFADs described in this study are bioactive lipids derived from omega-3 fatty acids and are produced via COX-2 catalysis, which is enhanced by ASA. The emerging beneficial roles of COX-2 and omega-3 fatty acids in resolution of inflammation and their crucial role in cardiovascular homeostasis indicate that COX-2-derived EFADs may contribute to mediating these actions. The ASA-dependent enhancement of EFAD biosynthesis further strengthens this hypothesis suggesting that the protective and anti-inflammatory effects of EFADs observed in cellular models may participate in transducing some of the beneficial actions of omega-3 fatty acids, COX-2, and ASA in human health.

5.0 DISCUSSION

Fatty acid-derived RES, formed by oxidative, inflammatory, and detoxification events, proceed to mediate aspects involved in the progression or resolution of these events. Many diseases with an inflammatory component have been observed to have significantly increased RES levels. For example, cyclopentenone neuroprostanes are found in frontal cortex brain tissue samples from Alzheimer's Disease patients at ~3 times normal levels of age-matched controls[73]. Furthermore, increased levels of oxoETEs are detected in the lungs of patients with severe pulmonary hypertension[217]. Even the formation of NO_2-FA has been shown to be increased in mitochondria during ischemia reperfusion[218]. Thus, all three of these electrophilic lipid derivatives display potent anti-inflammatory effects that may be involved in the modulation of if not protection from the inflammatory events that form them. Both NO_2-FA and EFADs were found to activate the transcription of PPARγ-dependent genes in the mid nM range, as determined by a PPARγ reporter assay in HEK293H cells, suggesting a role in macrophage differentiation and cytokine expression. However, many points of interest remain in terms of how these hydrophobic and reactive species are transported through hydrophilic and thiol rich environments and how they may be related to other lipid-derived signaling mediators.

5.1 POTENTIAL MECHANISMS OF TRANSPORT OF ELECTROPHILIC FATTY ACID DERIVATIVES

Both NO_2-FA and EFADs activate PPARγ and modulate the activities of other transcription factors such as Nrf2 in cell culture, but the routes of transport for these hydrophobic and reactive molecules remain unidentified. Carrier proteins must be involved in the transport of these compounds through the aqueous extracellular medium and the nucleophilic environment of the cytoplasm. It is likely that serum albumin is one of the carrier proteins involved in the extracellular transport of electrophilic lipids. Human serum albumin (HSA) constitutes approximately 50% of all human serum proteins and has been extensively studied. HSA is primarily involved in the transport of free fatty acids but it also plays important roles in maintaining the colloid osmotic pressure of the blood, metal cation transport, binding and transporting acidic drugs including the salicylates and ibuprofen, and to a lesser degree binding hormones such as estrogen and thyroid hormones[219]. Several of the hydrophobic binding sites of HSA accommodate a wide variety of fatty acid ligands and 1 mol of HSA typically binds from 2 to 7 mol fatty acids depending on fatty acid chain length and degree of saturation[220-222]. Additionally, the binding to albumin allows transport of hydrophobic molecules through aqueous milieus and promotes the transfer of the molecule into cellular membranes, as is the case with cannabinergic compounds[223].

An additional feature of HSA that makes it a strong candidate for the transport of electrophilic lipids is that it contains a thiol that is capable of reacting with electrophiles. The reduced form of HSA (mercaptoalbumin) possesses a free thiol Cys34, which has a pK_a of 5.0. This value is considerably lower than the pK_a of GSH (9.2) and facilitates reaction with electrophiles[224]. Accordingly, Cys34 of HSA has been documented to form adducts with

endogenous thiols, electrophiles such as HNE[225] and thiol reactive drugs including bucillamine derivatives, which are anti-rheumatic drugs[224]. Thus the abundance of serum albumin in the blood and the presence of a reactive cysteine support a role for the transport of NO_2-FA and EFADs in cell culture and *in vivo*. It is important to note that if an electrophilic lipid has formed a covalent adduct to Cys34 of HSA, the dissociation rate may be especially slow. However, electrophilic lipids may still be released from HSA upon conformational changes induced by interaction with lipid membranes or target proteins.

Another carrier protein that could be involved in the transport of NO_2-FA and EFADs is adipocyte fatty acid binding protein (A-FABP, aP2). Fatty acid binding proteins (FABPs) are members of a family of intracellular lipid binding proteins including cellular retinoic acid binding proteins (CRABPs) and nine isotypes of FABPs[226]. All intracellular lipid binding proteins have similar three-dimensional folds with the entrance to a β-barrel ligand-binding pocket surrounded by two α -helices[222]. While significantly different in structure from albumin, FABPs can also bind a wide variety of fatty acid ligands and are thought to be involved in fatty acid transport to nuclear receptors and possibly sequestration within the cell. In particular, A-FABP is expressed in adipocytes and macrophages, and it is significantly up-regulated upon treatment of U937 cells with PMA, which differentiates these monocyte-like human histiocytic lymphoma cells into a macrophage-like phenotype[227]. Interestingly, the ligand binding site of A-FABP contains a reactive free thiol on Cys117[228]. As Cys117 is located near lysine residues in a ligand binding pocket that is lined equally with hydrophobic and polar/charged amino acid residues, the pK_a of Cys117 should be low enough to react with electrophilic lipids; the pK_a of cysteine thiols can be lowered by proximity of positively charged groups of basic amino acid

residues, including histidine, lysine, and arginine)[222,229]. The reactivity of Cys117 of A-FABP suggests that adduction with electrophilic ligands is possible.

A-FABP has been shown to be responsible for the delivery of fatty acid ligands selectively to PPARγ[226]. When A-FABP is over-expressed, PPARγ transcriptional activity increased in the absence of ligand and increased most significantly in the presence of linoleic acid, 15d-PGJ_2, or Troglitazone. Furthermore, coprecipitation experiments identify that A-FABP interacts primarily with PPARγ[227]. Finally, kinetic analysis indicates that A-FABP facilitates ligand binding to PPARγ by delivering and channeling its ligand directly to the PPARγ ligand binding domain. Thus it is expected that NO_2-FA and EFADs are delivered to PPARγ by A-FABP and that other intracellular lipid binding proteins are involved in delivering these electrophilic lipids to other receptors.

5.2 ELECTROPHILIC FATTY ACID DERIVATIVES COMPARED TO OTHER LIPID SIGNALING MEDIATORS

The EFADs reported herein are chemically related to oxoETEs and other α,β-unsaturated carbonyl compounds, though in terms of origin they are also closely related to prostanoids and resolvins formed by COX-2. These relationships may indicate the actions and mechanisms of EFADs in modulating cell signaling and inflammation.

5.2.1 Electrophilic Fatty Acid Derivatives and Resolvins Share the Same Origin But Have Different Destinies

In exploring a path of formation for D series resolvins, Serhan *et al.* observed that the *in vivo* addition of ASA (500 μg) and DHA to TNFα-induced murine air pouch exudates abolished prostanoid production, while at the same time increasing the formation of a series of 17*R*-hydroxy-DHA compounds[131]. The di- and tri-hydroxy-docosanoids of this series are members of the resolvin family. Human recombinant COX-2 was also reported to produce primarily 13-hydroxy-DHA and to convert to the production of 17*R*-hydroxy-DHA upon pre-incubation with ASA. The COX-2 change in regioselectivity for DHA was also confirmed in this study during the identification of EFAD formation. Moreover, during EFAD synthesis the position of the oxygen is maintained during the conversion of the hydroxy to the carbonyl group. The authors also observed that COX inhibitors other than ASA, including indomethacin, acetaminophen, and NS-398 (a COX-2 selective inhibitor) reduced the formation of 13-hydroxy-DHA *in vitro* and completely inhibited the formation of 17-hydroxy-DHA. Again this finding is consistent with the inhibitor studies used to elucidate the path of biosynthesis for the EFADs.

In terms of signaling, 13- or 17*R*-hydroxy-DHA dose-dependently inhibited (with an apparent IC_{50} of approximately 50 pM) IL-1β transcription in microglial cells stimulated with TNFα[131]. Unlike other oxidized products of EPA and AA, Serhan *et al.* found that the monohydroxy-DHA isomers did not decrease polymorphonuclear neutrophilic leukocytes (PMN) transmigration *in vitro*. However, monohydroxy-DHA derivatives significantly reduced PMN recruitment in zymosan-induced peritonitis and a dermal air pouch model of inflammation in mice. The authors claim that these effects are due to the conversion of monohydroxy-DHA to di-

and tri-hydroxy-DHA products by human and murine leukocytes. Based on the path of EFAD synthesis demonstrated in this work, it is very possible that the anti-inflammatory actions of monohydroxy-DHA described above are due at least in part to the conversion of monohydroxy-DHA to EFAD-1.

5.2.2 Electrophilic Fatty Acid Derivatives and Other Reactive Electrophilic Species

EFADs are softer electrophiles compared to NO_2-FA. As α,β-unsaturated oxo-derivatives of fatty acids, the rate of EFAD reaction with GSH should be similar to that of 15d-PGJ_2 and PGA_2, which both have a second-order rate constant ~0.7 $M^{-1}s^{-1}$ for reaction with GSH[24]. In contrast NO_2-FA react much more rapidly with GSH; the second-order rate constant for OA-NO_2 reaction with GSH is ~183 $M^{-1}s^{-1}$[24]. In the case of GSH, the reaction rates for both electrophiles may not represent what is observed *in vivo* because catalysis by GSTs would essentially equalize the abilities of RES with different reactivities to form adducts with GSH. However, these reaction rates are important to consider in terms of overall reactivity with nucleophilic biomolecules such as cysteine residues of proteins. Ultimately, the reaction rate of a particular RES would determine its ability to effect signaling or cell damage by the formation of adducts with cellular nucleophiles.

As RES that are more similar to EFAD-1, cyclopentenone neuroprostanes (A_4/J_4-NPs) are derived from DHA oxidation and possess an electrophilic α,β-unsaturated keto group. However, unlike EFAD-1, A_4/J_4-NPs are formed by non-enzymatic lipid peroxidation in which an endoperoxide intermediate of DHA may go through a series of reduction, rearrangement, and dehydration reactions to produce a cyclopentane ring with various functional groups[33,73,230]. The synthetic 14-A_4-NP demonstrates anti-inflammatory properties in RAW264.7 macrophages that

are attributed to its electrophilic reactivity with Cys179 of IKKβ; the mutation of Cys179 reduced A_4-NP inhibition of NF-κB-mediated transcription[73]. While EFADs 1 and 2 were not observed to inhibit NF-κB p65 subunit nuclear translocation or NF-κB DNA binding, they significantly inhibited iNOS expression and •NO production. Similarly, the inhibition of iNOS expression by A_4-NP was demonstrated to be dependent on its electrophilic moiety; the formation of GSH adducts or the reduction of the keto group with $NaBH_4$ both significantly diminished the ability of A_4-NP to inhibit LPS-induced •NO production (as measured by nitrite levels in the media)[73]. Despite its ability to activate PPARγ, the anti-inflammatory effects of A_4-NP appear to be PPARγ-independent. However, it is important to note that this conclusion was only based on the inability of PPARγ antagonists (GW9662 and T0070907) to reverse A_4-NP-mediated inhibition of LPS-induced nitrite production[73]. If this conclusion is true, the similarities of EFADs with cyclopentenone neuroprostanes may indicate that their effects are also PPARγ-independent in RAW264.7 cells.

6.0 CONCLUSIONS

The electrophilic fatty acid derivatives discovered and characterized in this work (*i.e.* NO_2-FA and EFADs) are naturally-occurring electrophilic products of redox reactions, and can modulate a variety of cellular signaling processes including the transcriptional activity of the peroxisome proliferator-activated receptor-γ (PPARγ). NO_2-FA act as partial agonists of PPARγ at nM concentrations and covalently bind PPARγ via Michael addition with an LBD thiol. Similarly, EFADs activated PPARγ-dependent gene transcription at nM concentrations. Furthermore, NO_2-FA displayed selective and partial PPARγ modulator characteristics by inducing coregulator protein interactions to different extents than those induced by the TZD Rosiglitazone.

A newly discovered ω-3 PUFA-derived class of RES is formed upon macrophage activation by IFNγ and LPS (RAW264.7 and THP-1 cell lines and primary macrophages). Two major EFADs were identified as 13- and 17-keto derivatives of docosapentaenoic acid (DPA) and docosahexaenoic acid (DHA). Purified cyclooxygenase-2 (COX-2) product profiles and treatment of activated macrophages with COX-2 inhibitors revealed that EFAD synthesis was first catalyzed by inducible COX-2 (yielding a hydroxy-PUFA derivative), followed by a yet-to-be-identified dehydrogenase catalyzing oxidation of the hydroxy- to the oxo-derivative. EFAD production was increased 2.5 fold in ASA-treated activated macrophages. Quantitative analysis indicated that EFADs are highly abundant electrophiles in activated macrophages, reaching intracellular concentrations as high as 350 nM. Importantly, EFADs form reversible covalent

adducts with both proteins and small molecule thiols in activated macrophages, supporting a capability for post-translational protein modification-mediated cell signaling. It was confirmed that synthetic isomers of EFAD-1 and -2 (17-oxoDHA and 17-oxoDPA respectively) adduct GSH *in vivo*, as well as GAPDH *in vitro*. Furthermore, these synthetic isomers activated the Keap1/Nrf2 pathway and inhibited cytokine production and iNOS expression in activated macrophages. In aggregate, the inducible COX-2-dependent formation of ω-3-derived EFADs, their enhanced production with ASA-acetylation of COX-2, and their electrophilic signaling capabilities suggest that these species are acting as autocrine signaling modulators of inflammation *in vivo*.

APPENDIX A

ADDITIONAL DATA FOR CHAPTER 3

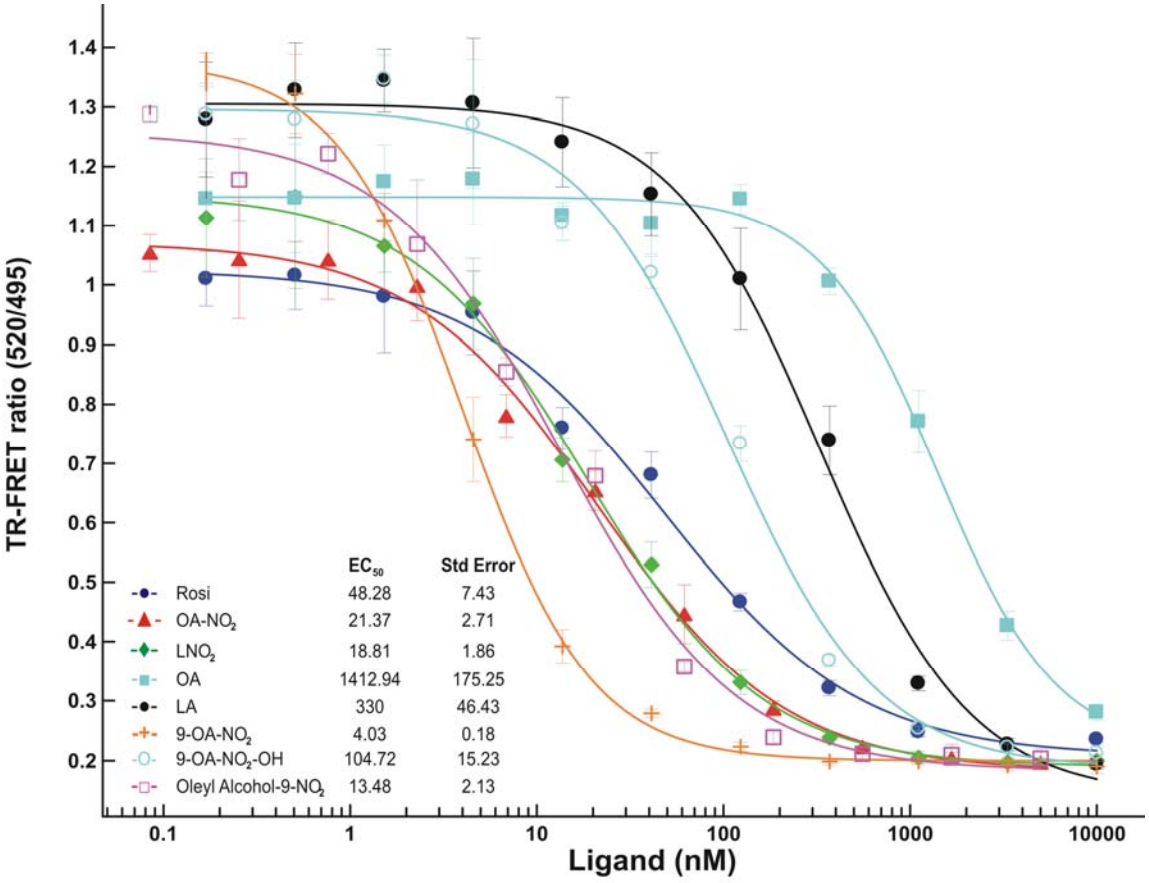

Figure 43. Peroxisome proliferator activated receptor γ competitive binding assay for nitroalkene derivatives of oleic acid and linoleic acid.

Ligand binding curves with ligand concentrations ranging from 0.17-10,000 nM and containing 125 μM DTT. Curve fitting equations and EC_{50}s were determined by XLfit4 and are displayed in inset.

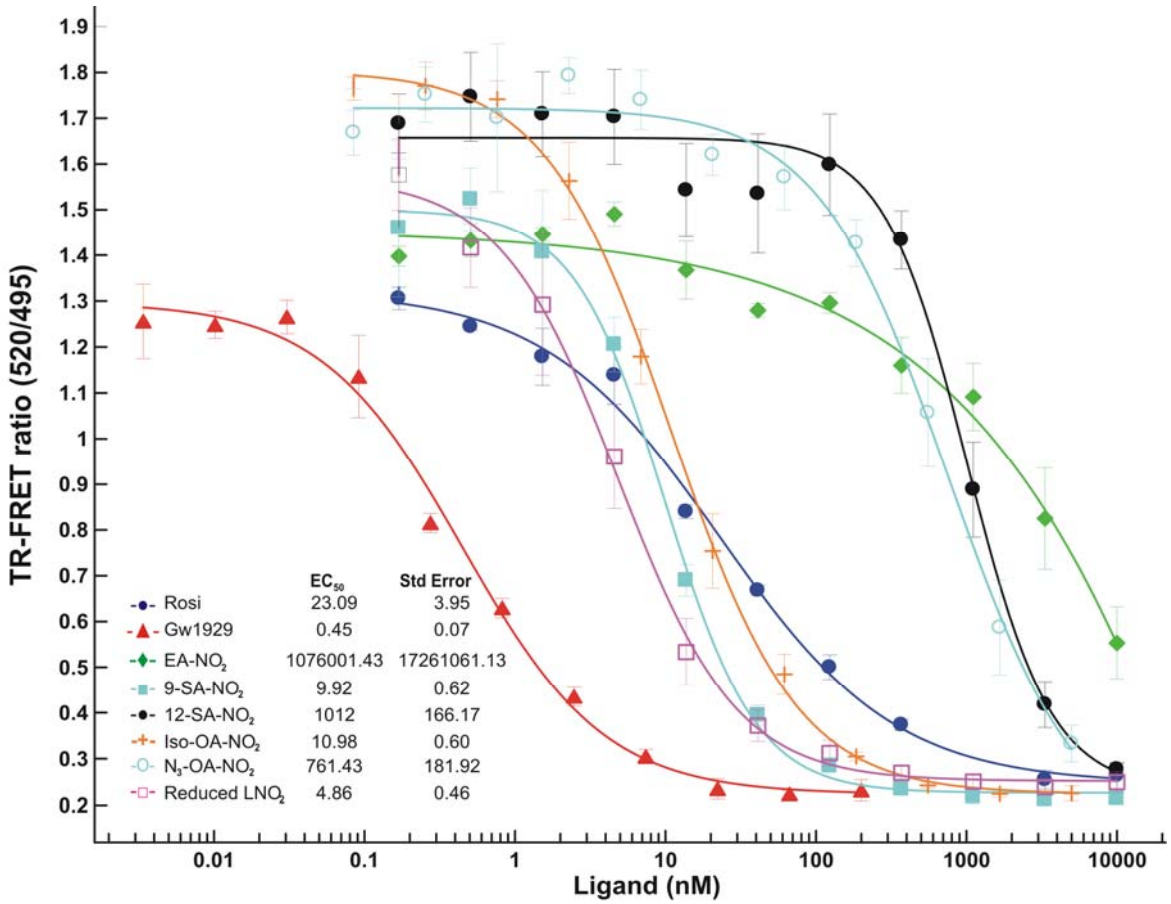

Figure 44. Peroxisome proliferator activated receptor γ competitive binding assay for nitroalkene derivatives of fatty acids.

Ligand binding curves with liand concentrations ranging from 0.17-10,000 nM and containing 125 μM DTT. Curve fitting equations and EC_{50}s were determined by XLfit4 and are displayed in inset.

APPENDIX B

ADDITIONAL DATA FOR CHAPTER 4

B.1 CONTROL EXPERIMENTS

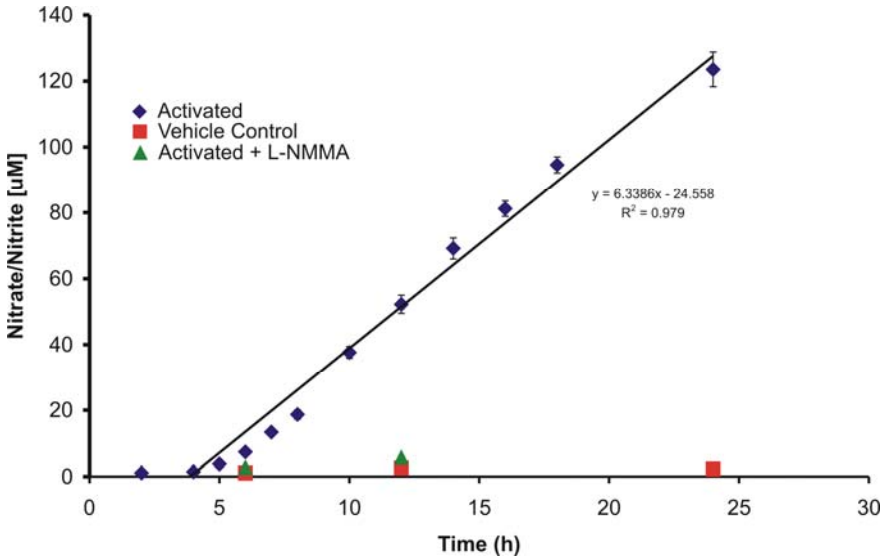

Figure 45. Activation of RAW264.7 cells with IFNγ and LPS gives the expected induction and rate of NO production as measured by the Griess reaction.

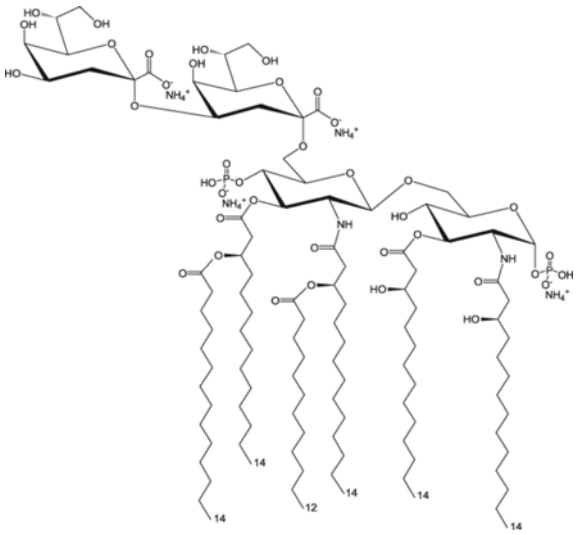

Figure 46. Structure of Kdo_2-lipid A.

Kdo_2-lipid A (di[3-deoxy-D-*manno*-octulosonic acid]-lipid A) is a commercially available synthetic endotoxin[198,231,232].

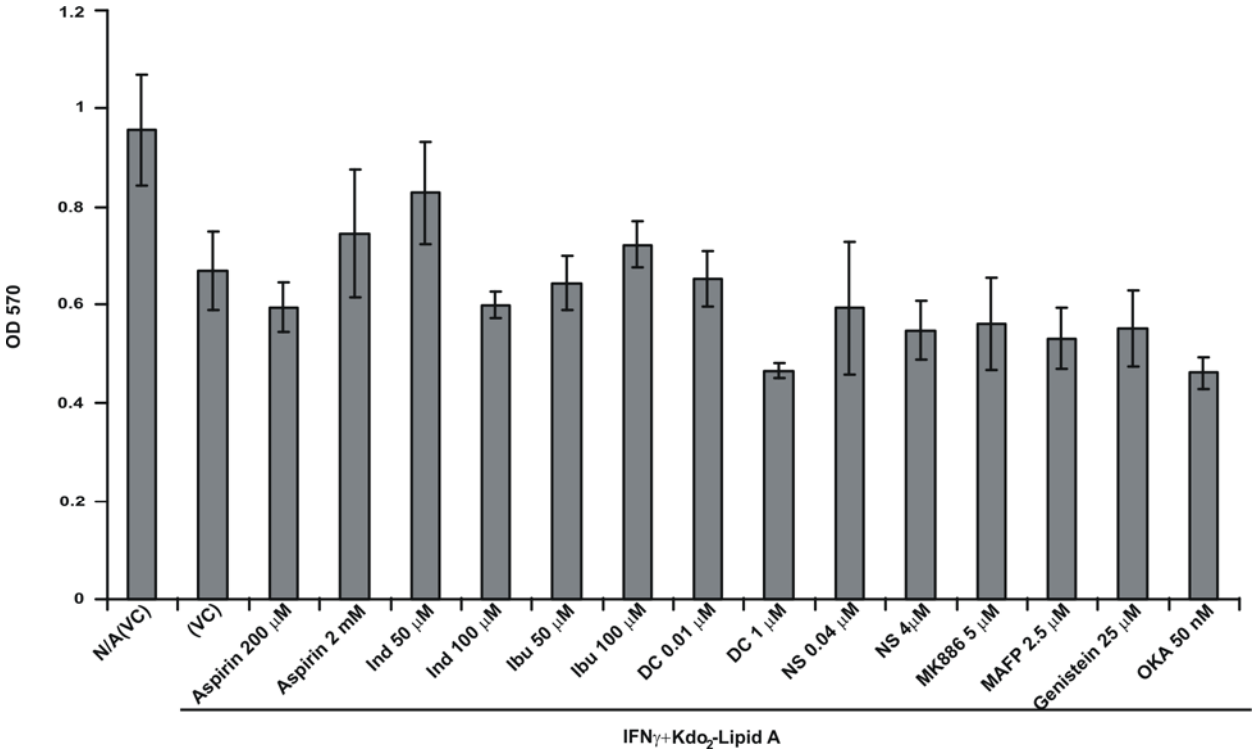

Figure 47. MTT assay to determine cell viability with various compounds.

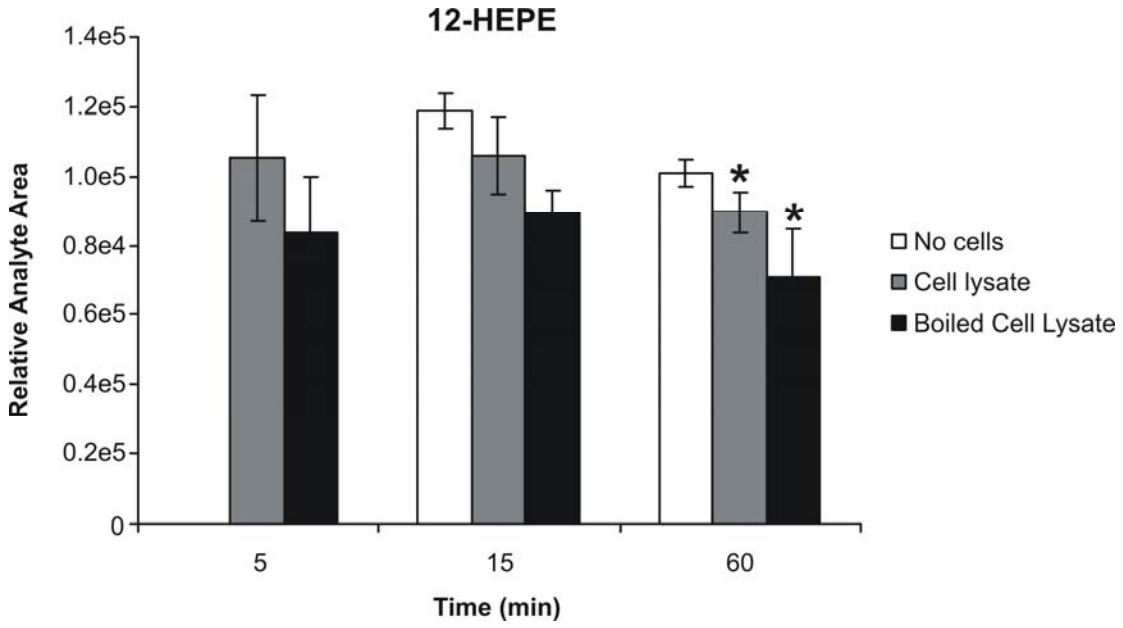

Figure 48. There is no significant enzymatic conversion or formation of 12-hydroxy-eicosapentaenoic acid during reaction with BME.

Activated RAW264.7 cell lysates were split in two groups and one group was boiled for 10 min to eliminate enzymatic activity. Both groups of lysates and a series of blanks (50 mM phosphate buffer, pH7.4) were then spiked with 12-HEPE (500 ng/ml) and 5-oxoETE-d7 internal standard (5 ng/ml) and BME (500 mM) and reacted for 1 h at 37°C. 12-HEPE was quantified by MRM following the loss of CO_2. Data are expressed as mean $\pm$ S.D. (n=5), where * = significantly different (p<0.05) from "no cells" control (one-way ANOVA, post-hoc Tukey's test).

B.2 ADDITIONAL DATA FOR ELECTROPHILIC FATTY ACID DERIVATIVES 1-6

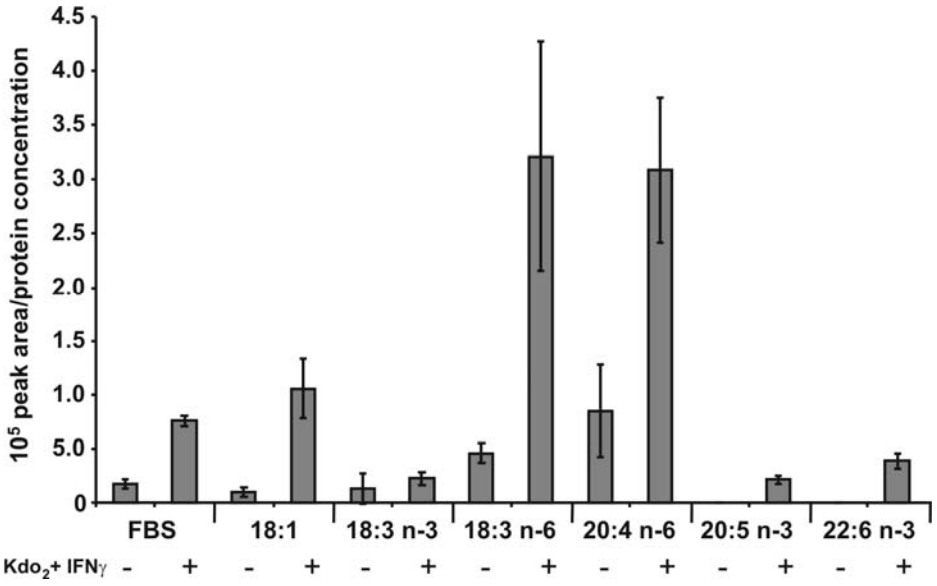

Figure 49. Electrophilic fatty acid derivative-4 is derived from the ω-6 series of fatty acids.

RAW264.7 cells were grown for 3 days in DMEM and 10% FBS supplemented with 32 μM of the indicated fatty acid. On the third day cells were activated with Kdo_2 Lipid A (0.5 μg/ml) and IFNγ (200 U/ml) and EFAD-4 levels were quantified 21 h post activation.

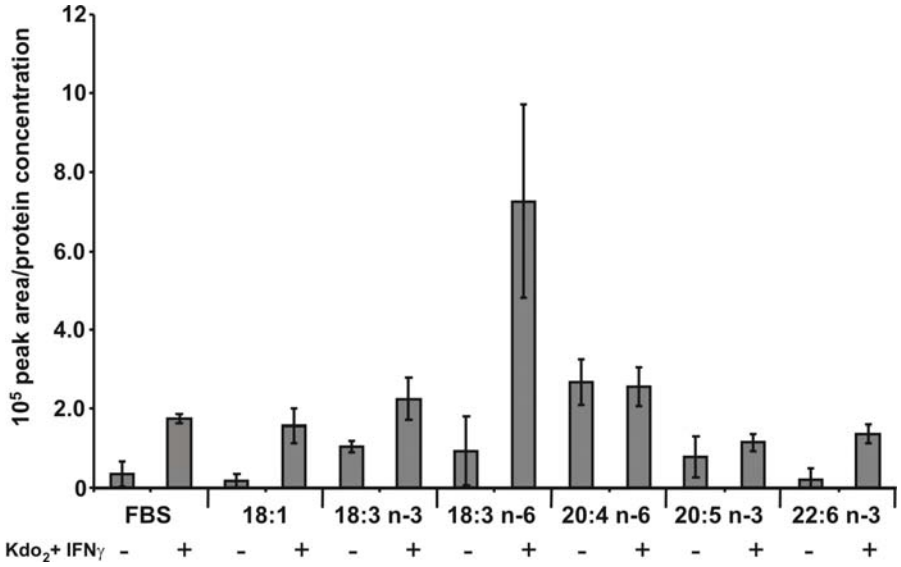

Figure 50. Electrophilic fatty acid derivative-5 is derived from the ω-6 series of fatty acids.

RAW264.7 cells were grown for 3 days in DMEM and 10% FBS supplemented with 32 μM of the indicated fatty acid. On the third day cells were activated with Kdo_2 Lipid A (0.5 μg/ml) and IFNγ (200 U/ml) and EFAD-5 levels were quantified 21 h post activation.

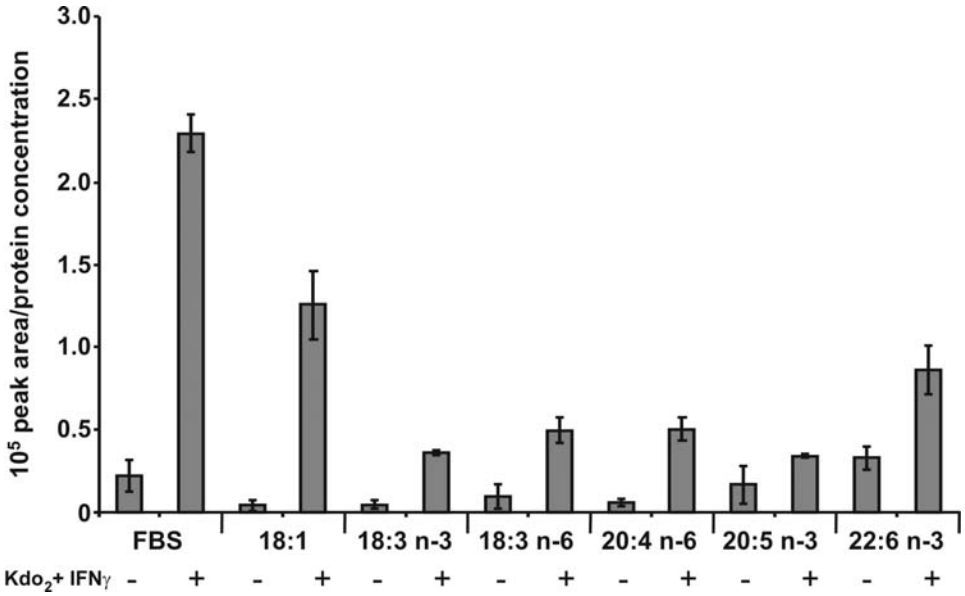

Figure 51. Electrophilic fatty acid derivative-6 is derived from the ω-9 series of fatty acids.

RAW264.7 cells were grown for 3 days in DMEM and 10% FBS supplemented with 32 μM of the indicated fatty acid. On the third day cells were activated with Kdo_2 Lipid A (0.5 μg/ml) and IFNγ (200 U/ml) and EFAD-6 levels were quantified 21 h post activation.

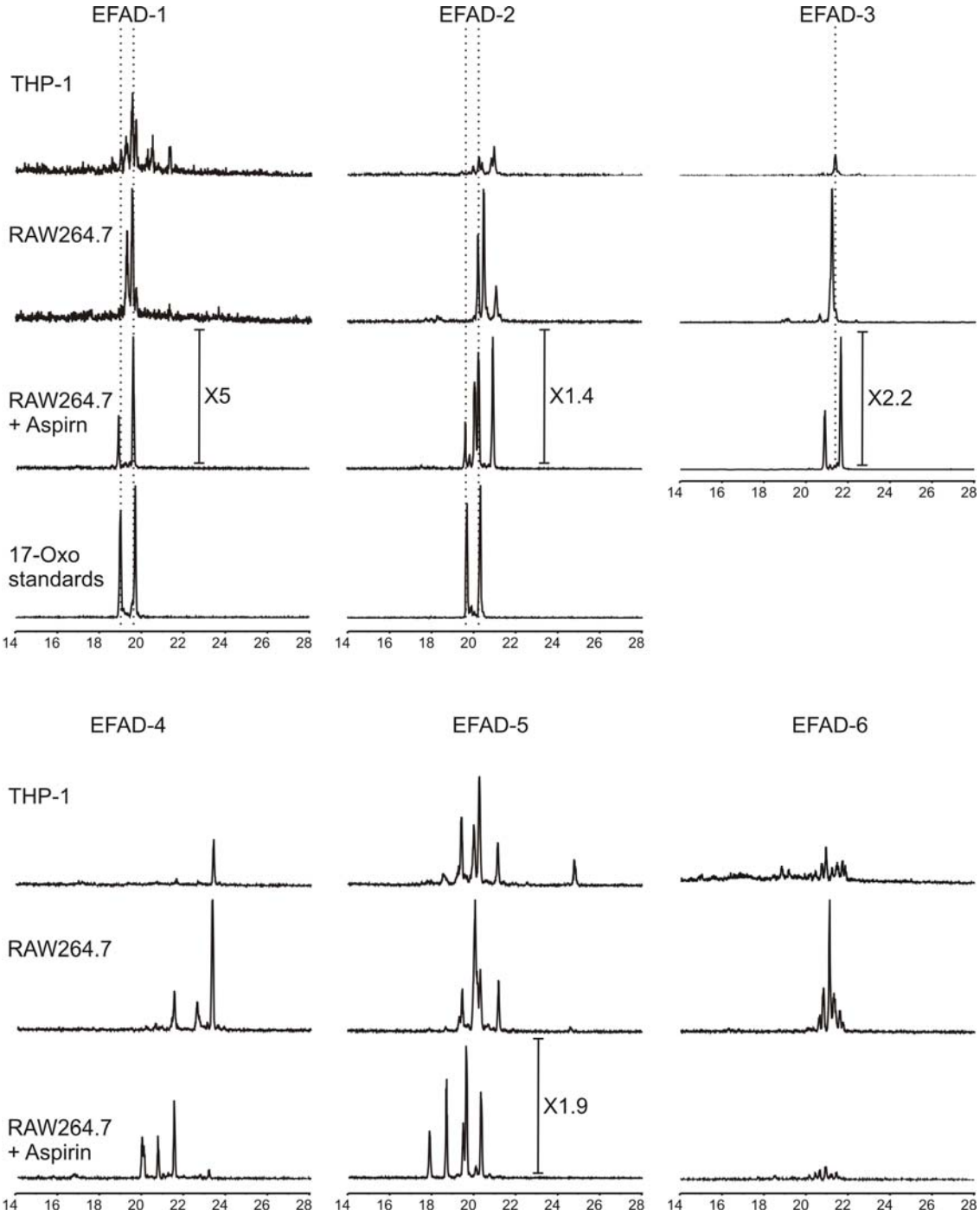

Figure 52. Electrophilic fatty acid derivatives produced by THP-1 cells coelute with those produced by RAW264.7 cells.

THP-1 cells were differentiated with PMA (86 nM) for 16 h, activated with Kdo_2 (0.5 μg/ml) and IFNγ (200 U/ml), and EFAD levels were detected 8 h post activation. MRM scans following the neutral loss of 78 were used to detect EFAD-BME adducts.

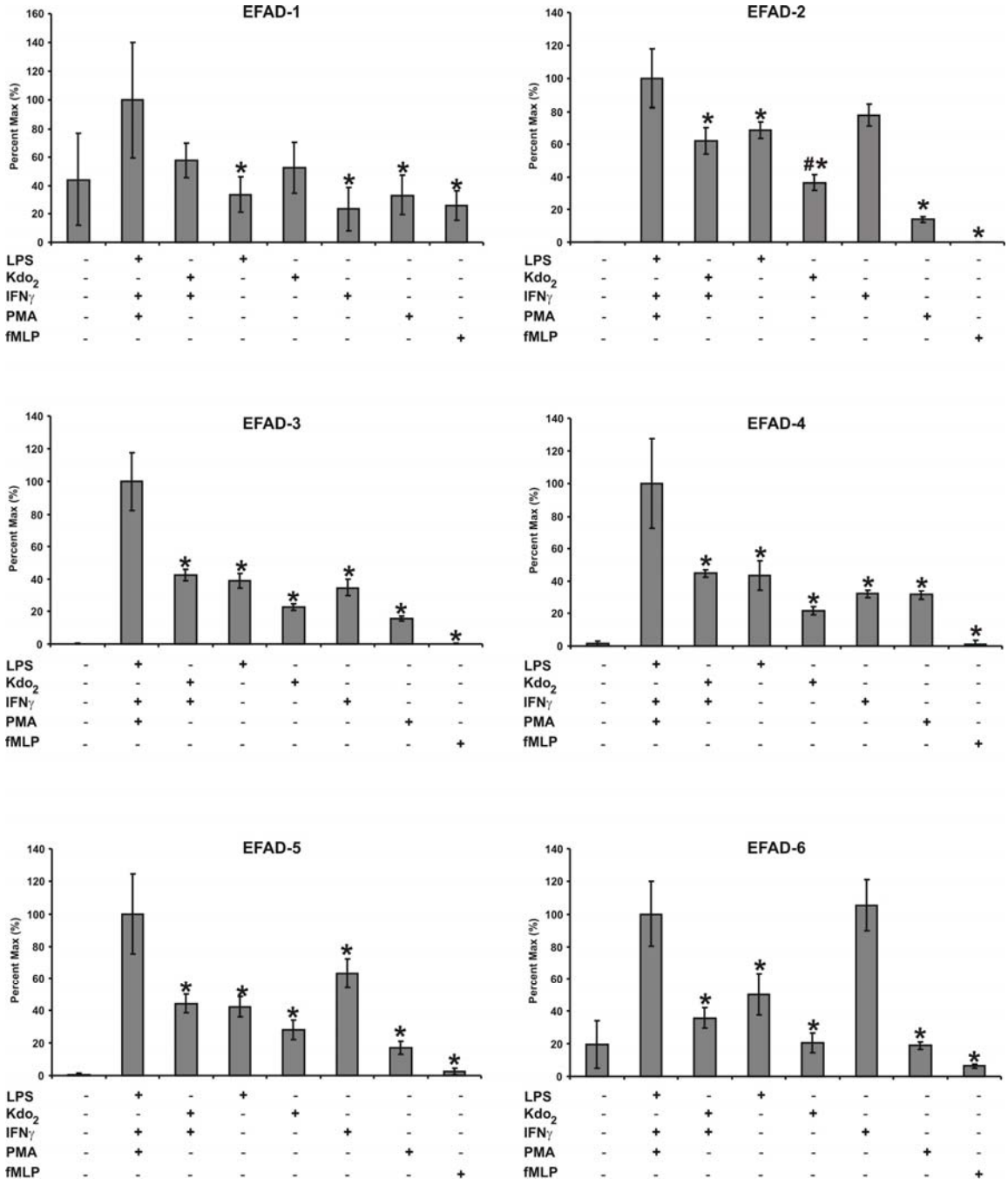

Figure 53. EFAD production is induced by Type 1 macrophage polarization of RAW264.7 cells.

RAW264.7 cells were activated with the indicated compounds and EFAD levels were quantified 20 h post activation. Compound concentrations are as follows: LPS (0.5 μg/ml), Kdo_2 Lipid A (0.5 μg/ml), IFNγ (200 U/ml), PMA (3.24 μM), and fMLP (1 μM). Data are expressed as mean ± S.D. (n=4), where * = significantly different ($p<0.01$) from "PMA + IFNγ + LPS," and # = a significant difference ($p<0.01$) between LPS and "Kdo_2 + IFNγ" (one-way ANOVA, post-hoc Tukey's test).

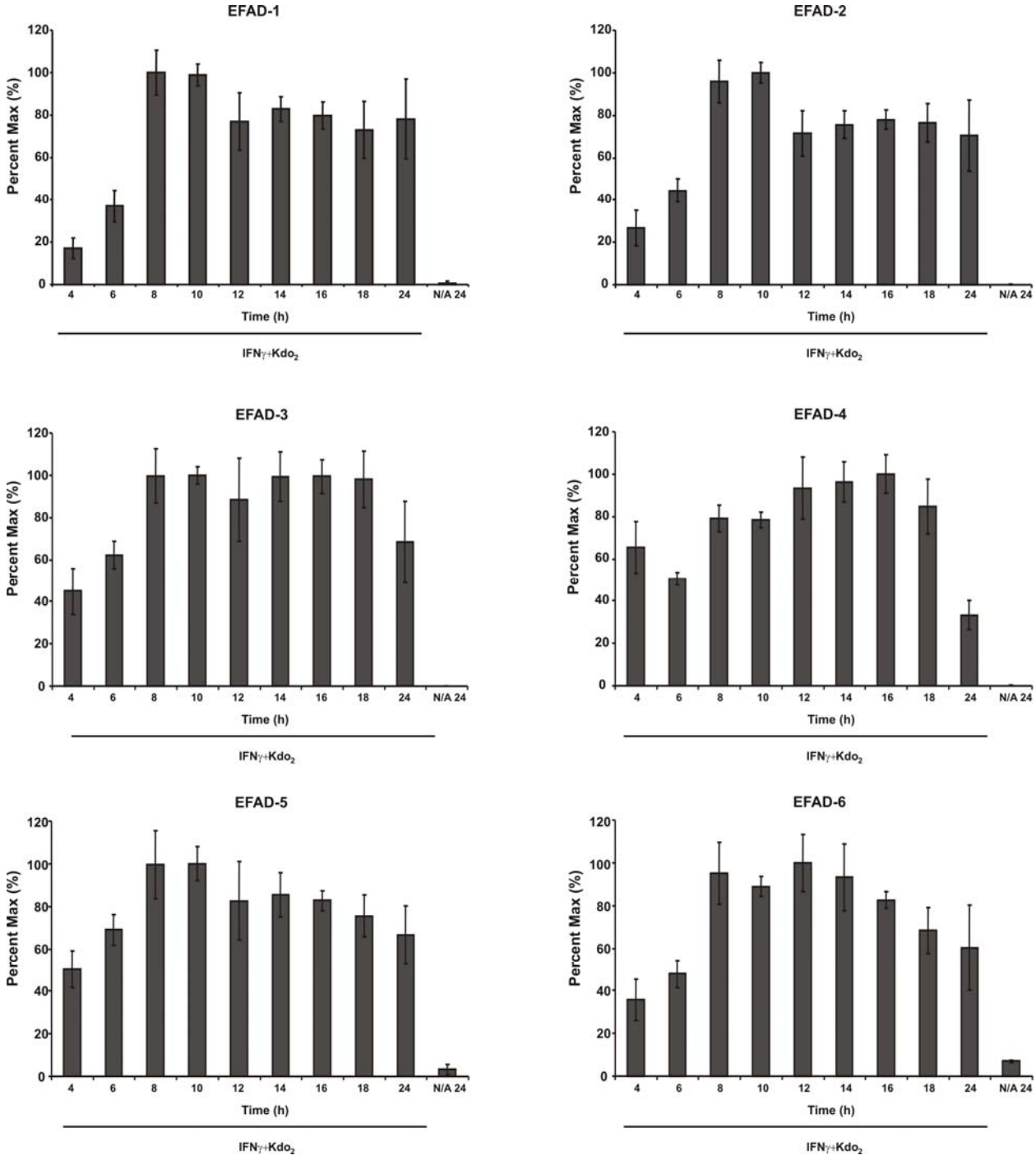

Figure 54. EFAD levels generally peak 8-10 h post activation and remain relatively stable up to 20 h.

RAW264.7 cells were activated with Kdo_2 Lipid A (0.5 μg/ml) and IFNγ (200 U/ml) and EFAD levels were quantified at indicated times post activation.

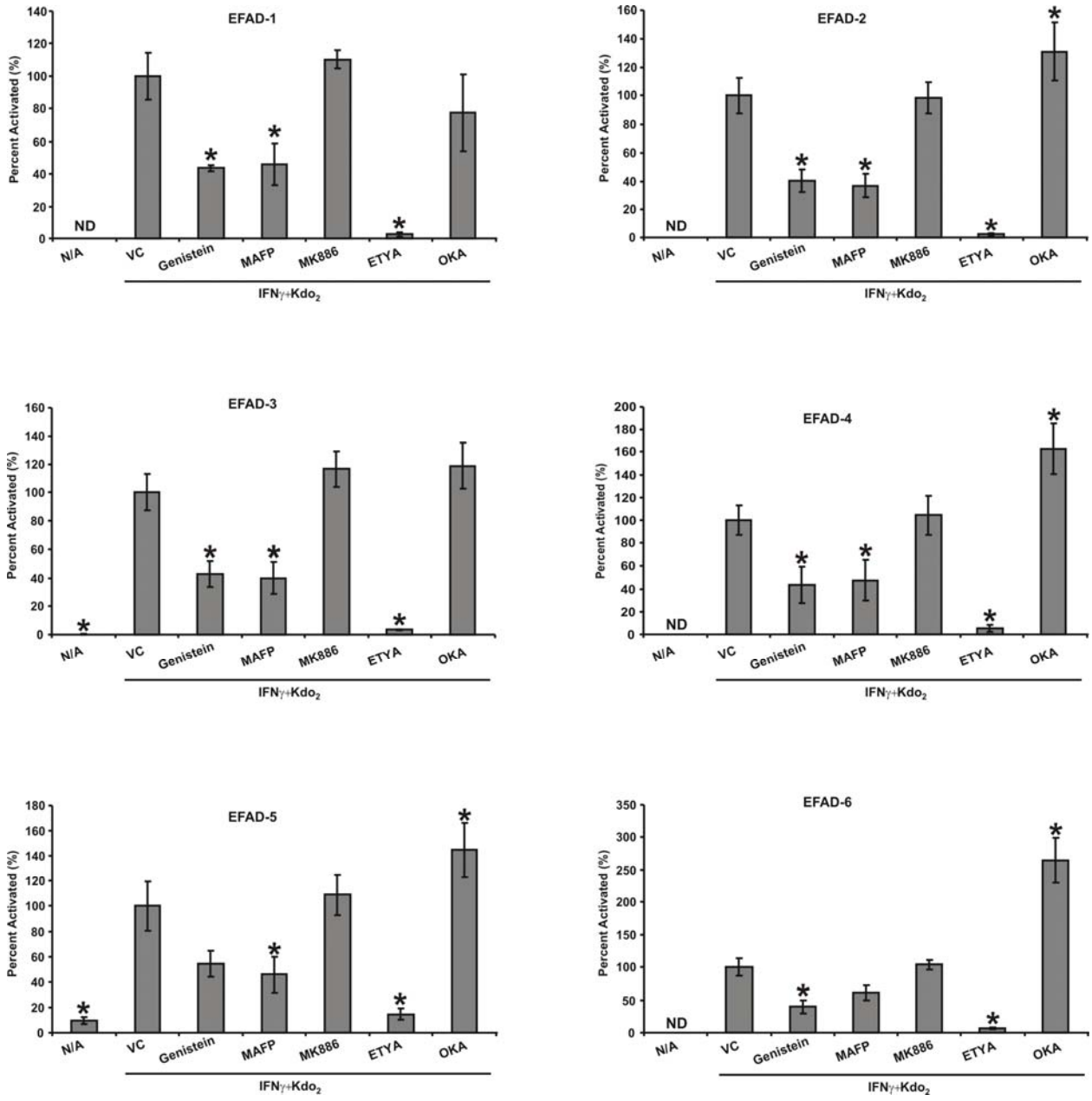

Figure 55. EFAD formation is dependent on PLA_2 and COX enzymes.

RAW264.7 cells were activated with Kdo_2 Lipid A (0.5 μg/ml) and IFNγ (200 U/ml) in the presence of indicated inhibitors and EFAD-2 levels were quantified 21 h post activation. Inhibitor concentrations were as follows: genistein (25 μM), MAFP (25 μM), MK886 (500 nM), ETYA (25 μM) and OKA (50 nM) (a-e). Data are expressed as mean ± S.D. (n=4), where * = significantly different (p<0.01) from "Kdo_2 + IFNγ" (one-way ANOVA, post-hoc Tukey's test).

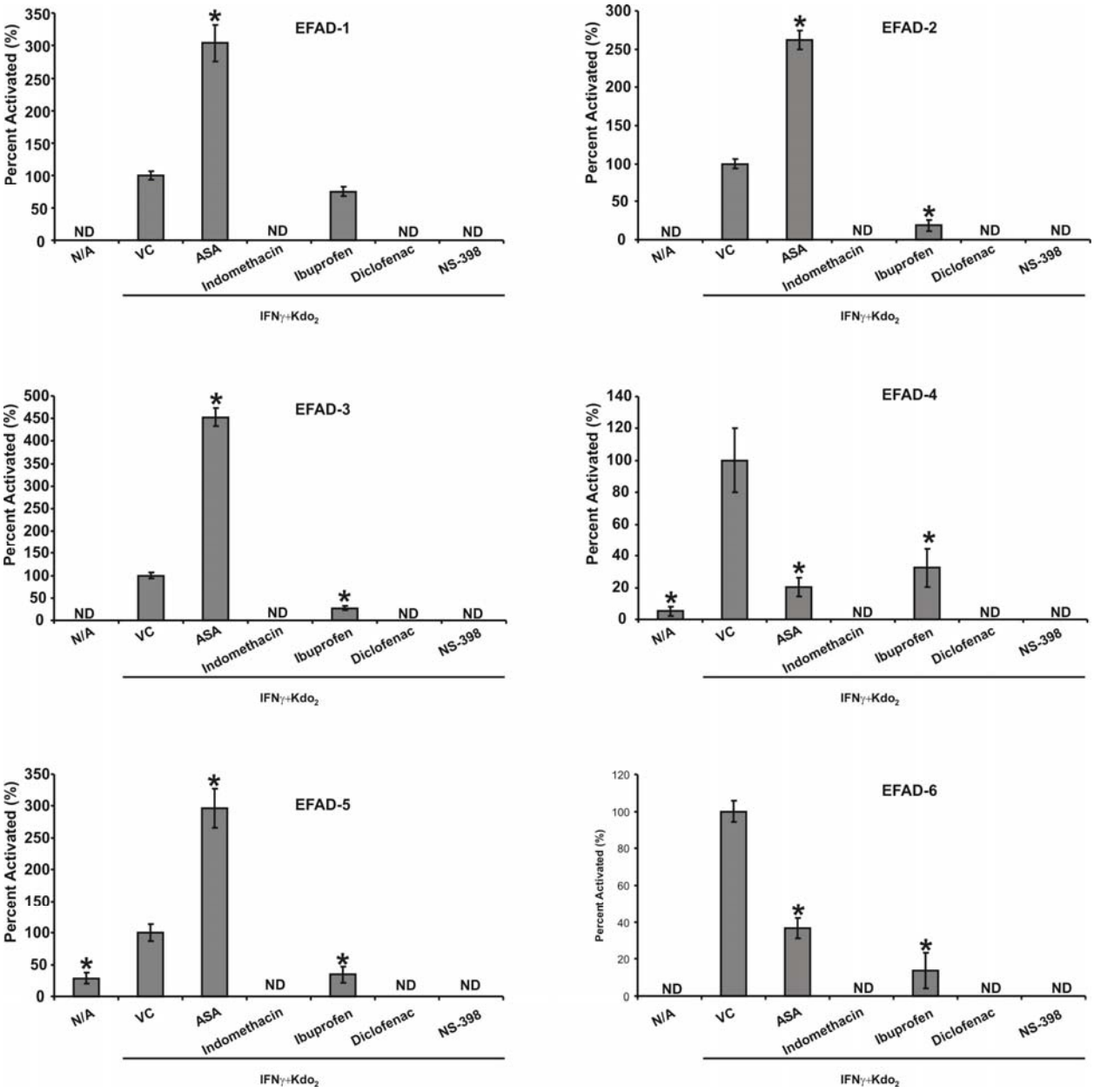

Figure 56. EFAD formation requires COX-2.

RAW264.7 cells were activated with Kdo_2 Lipid A (0.5 μg/ml) and IFNγ (200 U/ml) in the presence of indicated COX inhibitors and EFAD-2 levels were quantified 21 h post activation. COX inhibitor concentrations were as follows: aspirin (200 μM), indomethacin (25 μM), ibuprofen (100 μM), diclofenac (1 μM) and NS-398 (4 μM) (a-e). Data are expressed as mean ± S.D. (n=4), where * = significantly different (p<0.01) from "Kdo_2 + IFNγ" (one-way ANOVA, post-hoc Tukey's test).

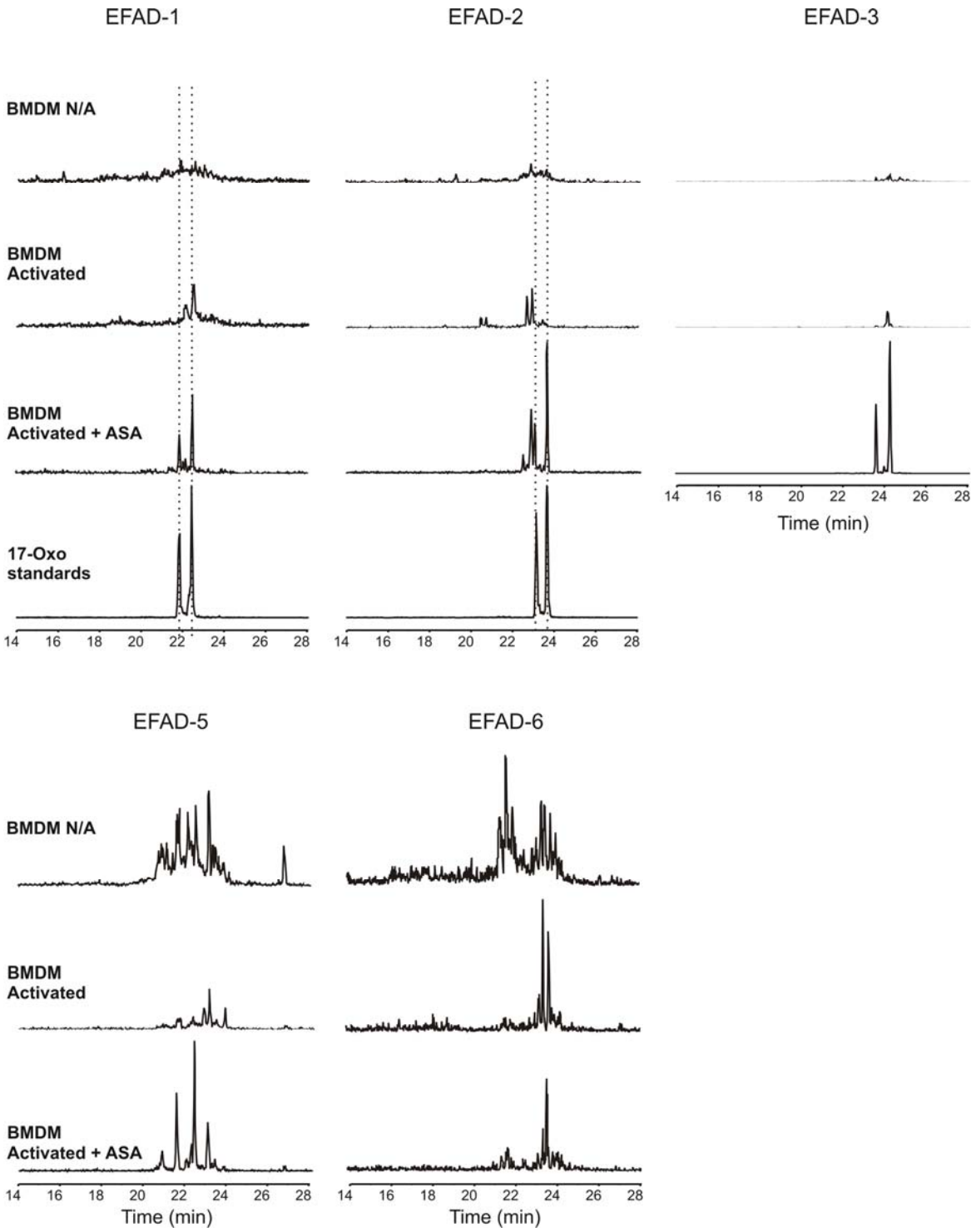

Figure 57. Electrophilic fatty acid derivatives produced by bone marrow-derived macrophages coelute with those produced by RAW264.7 cells.

BMDMs were activated with PMA (50 ng/ml), IFNγ (200 U/ml) and (0.5 μg/ml) and were harvested 24 h post activation. MRM scans following the neutral loss of 78 were used to detect EFAD-BME adducts.

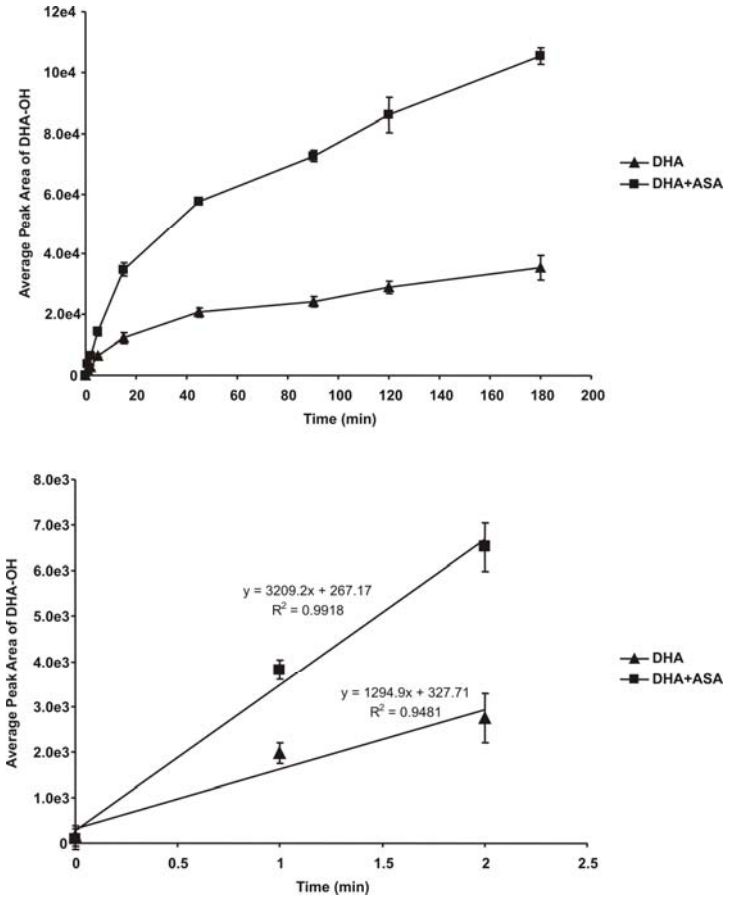

Figure 58. COX-2 can form the precursor of EFAD-1 from DHA.

The hydroxyl-precursors of EFAD-1 were synthesized *in vitro* using purified ovine COX-2 ± aspirin and DHA. The hydroxyl precursors were analyzed (by EPI) and quantified (by following their MRM transitions) at the indicated time points during the reaction by HPLC-ESI-MS/MS.

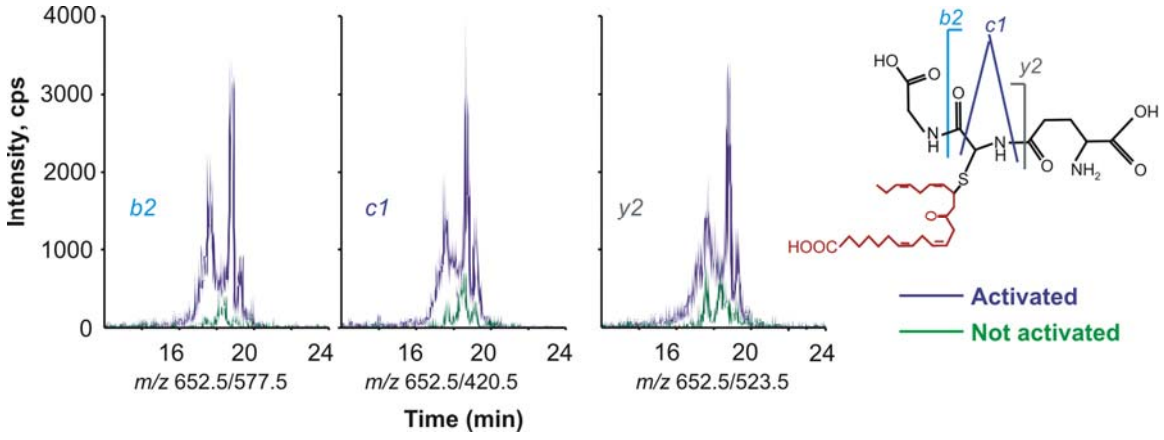

Figure 59. EFAD-2 GSH adducts were initially detected in the cell pellets of activated RAW264.7 cells.

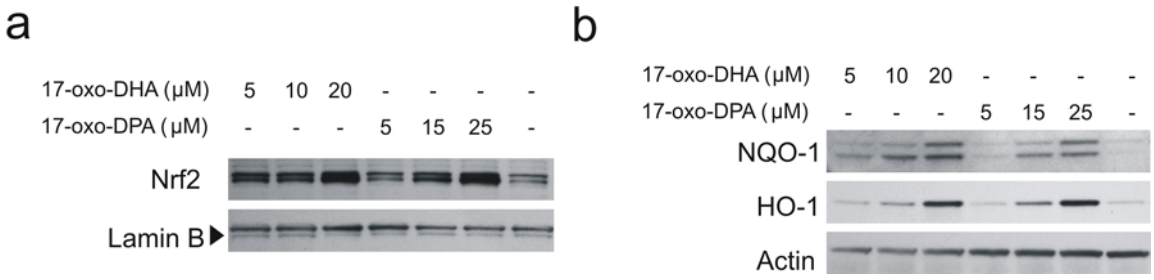

Figure 60. The 17-oxo standards activate the transcription of Nrf2-dependent genes.

RAW264.7 cells were treated with increasing concentration of 17-oxo-DHA and 17-oxo-DPA. (**a**) Cells were harvested 1h after treatment and Nrf2 levels were quantified in nuclear extracts. (**b**) Cells were harvested 18h after treatment and HO-1 and NQO-1 levels were measured by western blot.

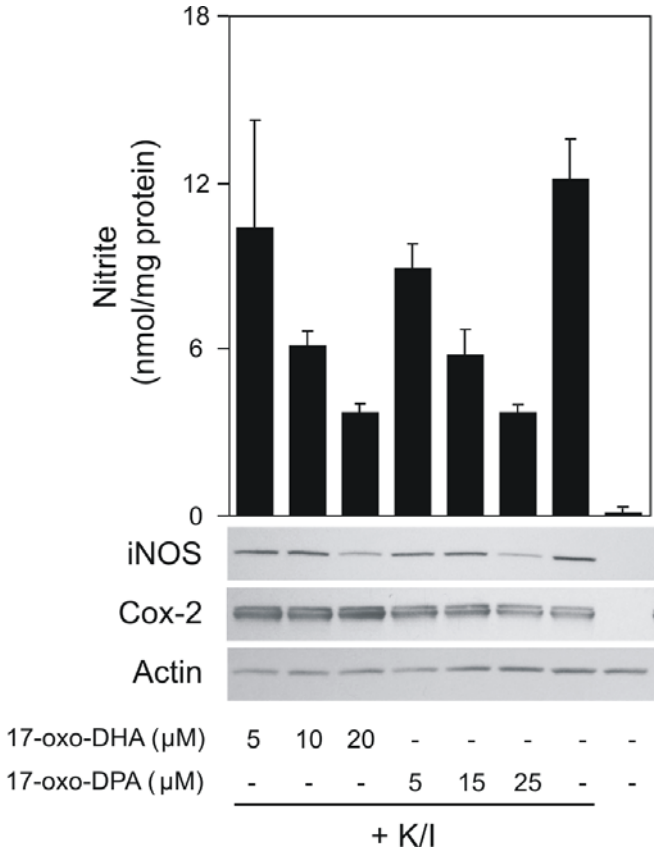

Figure 61. The 17-oxo standards inhibit inducible nitric oxide synthase expression and subsequent nitrite accumulation in the media.

RAW264.7 cells were treated with increasing concentration of 17-oxo-DHA and 17-oxo-DPA for 6h and Kdo_2 Lipid A + IFNγ were added. Samples were collected at 12h. Nitrite levels were measured in the cell media and normalized by the total protein content; iNOS and Cox-2 levels were measured in total cell lysates.

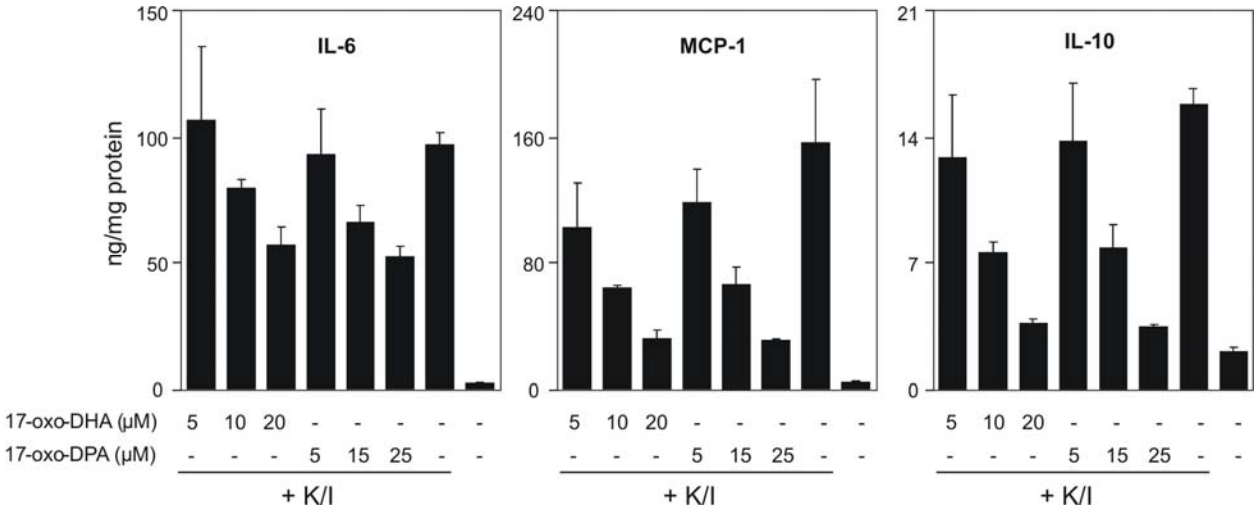

Figure 62. The 17-oxo standards inhibit cytokine production in activated RAW264.7 cells.

RAW264.7 cells were treated with increasing concentration of 17-oxo-DHA and 17-oxo-DPA for 6h and Kdo_2 Lipid A + IFNγ were added. Samples were collected at 12h. IL-6, MCP-1 and IL-10 levels were measured in the cell media and normalized by the total protein content.

Peptide 1				
	17-oxoDPA-adducted		non adducted	
aa	b	y	b	y
V	100.08	-	100.08	-
P	197.13	1745.02	197.13	1457.74
T	298.18	1647.97	298.18	1360.69
P	395.23	1546.92	395.23	1259.64
N	509.27	1449.87	509.27	1162.59
V	608.34	1335.82	608.34	1048.55
S	695.37	1236.76	695.37	949.48
V	794.44	1149.72	794.44	862.45
V	893.51	1050.66	893.51	763.38
D	1008.54	951.59	1008.54	664.31
L	1121.62	836.56	1121.62	549.28
T	1222.67	723.48	1222.67	436.2
C* (244)	1369.96	622.43	1362.7	336.15
R	-	175.12	-	175.12

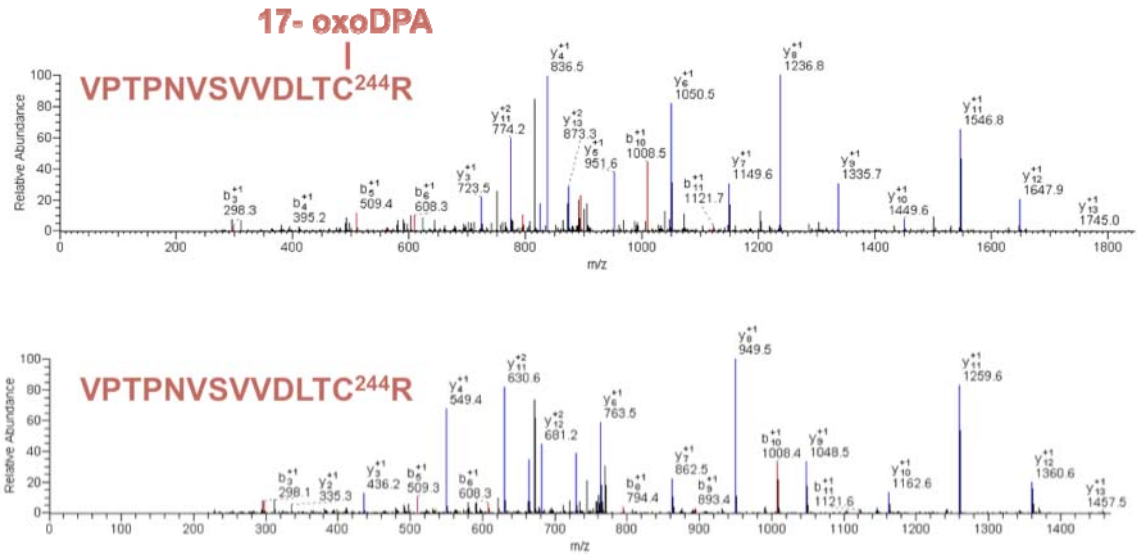

Figure 63. Mass spectrometric analysis of *in vitro* reaction of glyceraldehyde-3-phosphate dehydrogenase with 17-oxodocosapentaenoic acid; alkylation at cysteine 244.

Four residues were detected and confirmed as being targets for EFAD-2 (17-oxoDPA) in treated rabbit GAPDH. Upper panels show EFAD-2 modified peptides and lower panels show spectra from corresponding native peptide.

Peptide 2				
	17-oxoDPA-adducted		non adducted	
aa	b	y	b	y
V	100.08	-	100.08	-
I	213.16	2863.61	213.16	2519.31
H*	694.52	2750.52	350.22	2406.22
D	809.55	2269.16	465.25	2269.16
H	946.60	2154.14	602.30	2154.14
F	1093.67	2017.08	749.37	2017.08
G	1150.69	1870.01	806.39	1870.01
I	1263.78	1812.99	919.48	1812.99
V	1362.85	1699.90	1018.55	1699.90
E	1491.89	1600.84	1147.59	1600.84
G	1548.91	1471.79	1204.61	1471.79
L	1661.99	1414.77	1317.69	1414.77
M	1793.04	1301.69	1448.74	1301.69
T	1894.08	1170.65	1549.78	1170.65
T	1995.13	1069.60	1650.83	1069.60
V	2094.20	968.55	1749.90	968.55
H	2231.26	869.48	1886.96	869.48
A	2302.30	732.43	1958.00	732.43
I	2415.38	661.39	2071.08	661.39
T	256.43	548.30	2172.13	548.30
A	2587.46	447.26	2243.16	447.26
T	2688.51	376.22	2344.21	376.22
Q	2816.57	275.17	2472.27	275.17
K		147.11		147.11

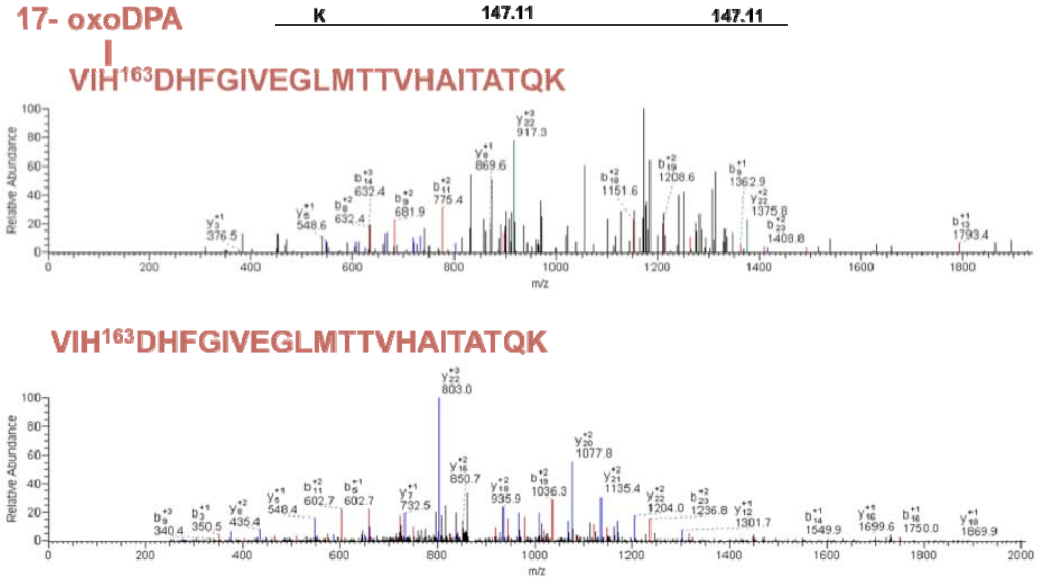

Figure 64. Mass spectrometric analysis of *in vitro* reaction of glyceraldehyde-3-phosphate dehydrogenase with 17-oxodocosapentaenoic acid; alkylation at histidine 163.

Four residues were detected and confirmed as being targets for EFAD-2 (17-oxoDPA) in treated rabbit GAPDH. Upper panels show EFAD-2 modified peptides and lower panels show spectra from corresponding native peptide.

Peptide 3				
	17-oxoDPA -adducted		non adducted	
aa	b	y	b	y
I	114.09	-	114.09	-
V	213.60	1994.10	213.16	1706.82
S	300.19	1895.03	300.19	1607.75
N	414.23	1808.00	414.23	1520.72
A	485.27	1693.96	485.27	1406.68
S	572.30	1622.92	572.30	1335.64
C#	1019.61	1535.89	732.33	1248.61
T	1120.66	1088.58	833.38	1088.58
T	1221.71	987.53	934.43	987.53
N	1335.75	886.48	1048.47	886.48
C*	1495.78	772.44	1208.50	772.44
L	1608.87	612.41	1321.59	612.41
A	1679.90	499.32	1392.62	499.32
P	1776.96	428.29	1489.68	428.29
L	1890.04	331.23	1602.76	331.23
A	1961.08	218.15	1673.80	218.15
K	-	147.11	-	147.11

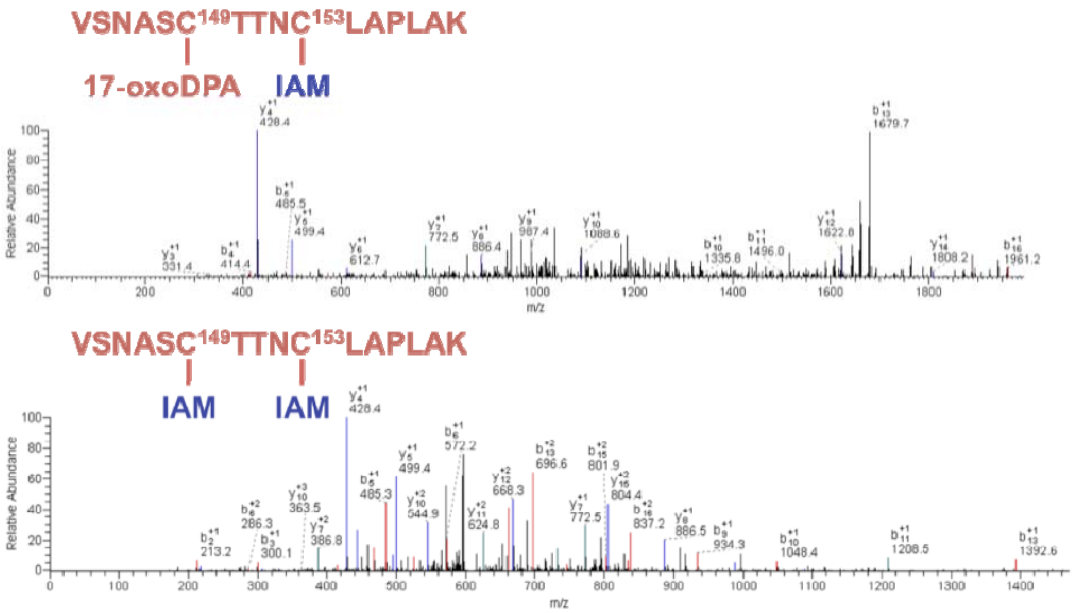

Figure 65. Mass spectrometric analysis of *in vitro* reaction of glyceraldehyde-3-phosphate dehydrogenase with 17-oxodocosapentaenoic acid; alkylation at cysteine 149.

Four residues were detected and confirmed as being targets for EFAD-2 (17-oxoDPA) in treated rabbit GAPDH. Upper panels show EFAD-2 modified peptides and lower panels show spectra from corresponding native peptide.

Peptide 4				
	17-oxoDPA-adducted		non adducted	
aa	b	y	b	y
V	100.80	-	100.80	-
V	199.14	1474.87	199.14	1130.57
D	314.17	1375.80	314.17	1031.50
L	427.26	1260.77	427.26	916.47
M	558.30	1147.69	558.30	803.39
V	657.36	1016.65	657.36	672.35
H#	1138.72	917.58	794.42	573.28
M	1269.76	436.22	925.46	436.22
A	1340.80	305.18	996.50	305.18
S	1427.83	234.14	1083.53	234.14
K	-	147.11	-	147.11

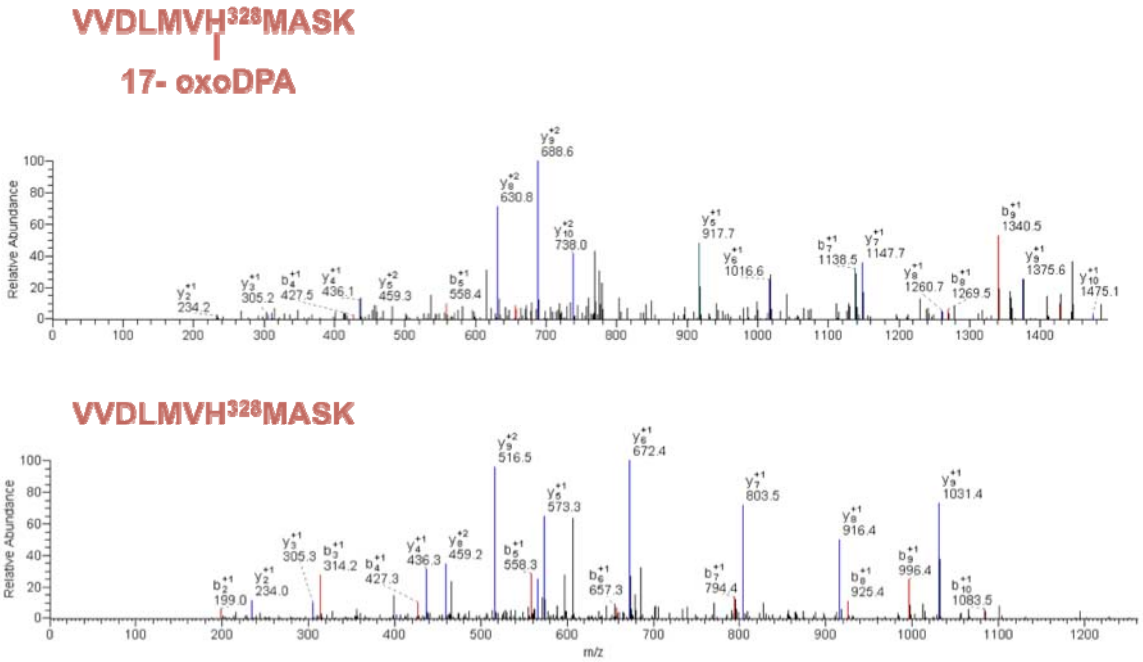

Figure 66. Mass spectrometric analysis of *in vitro* reaction of glyceraldehyde-3-phosphate dehydrogenase with 17-oxodocosapentaenoic acid; alkylation at histidine 328.

Four residues were detected and confirmed as being targets for EFAD-2 (17-oxoDPA) in treated rabbit GAPDH. Upper panels show EFAD-2 modified peptides and lower panels show spectra from corresponding native peptide.

BIBLIOGRAPHY

1. LoPachin, R.M., Barber, D.S. & Gavin, T. Molecular mechanisms of the conjugated alpha,beta-unsaturated carbonyl derivatives: relevance to neurotoxicity and neurodegenerative diseases. *Toxicol Sci* **104**, 235-249 (2008).
2. Mantovani, A.*, et al.* The chemokine system in diverse forms of macrophage activation and polarization. *Trends in Immunology* **25**, 677-686 (2004).
3. Mantovani, A., Sica, A. & Locati, M. New vistas on macrophage differentiation and activation. *Eur J Immunol* **37**, 14-16 (2007).
4. Dale, D.C., Boxer, L. & Liles, W.C. The phagocytes: neutrophils and monocytes. *Blood* **112**, 935-945 (2008).
5. Schroder, K., Sweet, M.J. & Hume, D.A. Signal integration between IFNgamma and TLR signalling pathways in macrophages. *Immunobiology* **211**, 511-524 (2006).
6. Itoh, K., Tong, K.I. & Yamamoto, M. Molecular mechanism activating Nrf2-Keap1 pathway in regulation of adaptive response to electrophiles. *Free Radic Biol Med* **36**, 1208-1213 (2004).
7. Moos, P.J., Edes, K., Cassidy, P., Massuda, E. & Fitzpatrick, F.A. Electrophilic prostaglandins and lipid aldehydes repress redox-sensitive transcription factors p53 and hypoxia-inducible factor by impairing the selenoprotein thioredoxin reductase. *J Biol Chem* **278**, 745-750 (2003).
8. Marnett, L.J. Oxy radicals, lipid peroxidation and DNA damage. *Toxicology* **181-182**, 219-222 (2002).
9. Feng, Z., Hu, W., Hu, Y. & Tang, M.S. Acrolein is a major cigarette-related lung cancer agent: Preferential binding at p53 mutational hotspots and inhibition of DNA repair. *Proc Natl Acad Sci U S A* **103**, 15404-15409 (2006).
10. Kumagai, T.*, et al.* A lipid peroxidation-derived inflammatory mediator: identification of 4-hydroxy-2-nonenal as a potential inducer of cyclooxygenase-2 in macrophages. *J Biol Chem* **279**, 48389-48396 (2004).
11. Calingasan, N.Y., Uchida, K. & Gibson, G.E. Protein-bound acrolein: a novel marker of oxidative stress in Alzheimer's disease. *J Neurochem* **72**, 751-756 (1999).
12. Beauchamp, R.O., Jr., Andjelkovich, D.A., Kligerman, A.D., Morgan, K.T. & Heck, H.D. A critical review of the literature on acrolein toxicity. *Crit Rev Toxicol* **14**, 309-380 (1985).
13. Farmer, E.E. & Davoine, C. Reactive electrophile species. *Current Opinion in Plant Biology* **10**, 380-386 (2007).
14. Lin, D., Saleh, S. & Liebler, D.C. Reversibility of covalent electrophile-protein adducts and chemical toxicity. *Chem Res Toxicol* **21**, 2361-2369 (2008).

15. Hong, F., Sekhar, K.R., Freeman, M.L. & Liebler, D.C. Specific patterns of electrophile adduction trigger Keap1 ubiquitination and Nrf2 activation. *J Biol Chem* **280**, 31768-31775 (2005).
16. Liebler, D.C. Protein damage by reactive electrophiles: targets and consequences. *Chem Res Toxicol* **21**, 117-128 (2008).
17. Levonen, A.-L., *et al.* Cellular mechanisms of redox cell signalling: role of cysteine modification in controlling antioxidant defences in response to electrophilic lipid oxidation products. *Biochem J* **378**, 373-382 (2004).
18. Batthyany, C., *et al.* Reversible post-translational modification of proteins by nitrated fatty acids in vivo. *J Biol Chem* **281**, 20450-20463 (2006).
19. Davoine, C., Douki, T., Iacazio, G., Montillet, J.L. & Triantaphylides, C. Conjugation of keto fatty acids to glutathione in plant tissues. Characterization and quantification by HPLC-tandem mass spectrometry. *Anal Chem* **77**, 7366-7372 (2005).
20. Zhu, P., Oe, T. & Blair, I.A. Determination of cellular redox status by stable isotope dilution liquid chromatography/mass spectrometry analysis of glutathione and glutathione disulfide. *Rapid Commun Mass Spectrom* **22**, 432-440 (2008).
21. Ishikawa, K. & Maruyama, Y. Heme oxygenase as an intrinsic defense system in vascular wall: implication against atherogenesis. *J Atheroscler Thromb* **8**, 63-70 (2001).
22. Falletti, O. & Douki, T. Low glutathione level favors formation of DNA adducts to 4-hydroxy-2(E)-nonenal, a major lipid peroxidation product. *Chem Res Toxicol* **21**, 2097-2105 (2008).
23. Holtzclaw, W.D., Dinkova-Kostova, A.T. & Talalay, P. Protection against electrophile and oxidative stress by induction of phase 2 genes: the quest for the elusive sensor that responds to inducers. *Advances in Enzyme Regulation, Vol 44* **44**, 335-367 (2004).
24. Baker, L.M., *et al.* Nitro-fatty acid reaction with glutathione and cysteine. Kinetic analysis of thiol alkylation by a Michael addition reaction. *J Biol Chem* **282**, 31085-31093 (2007).
25. Benesch, R.E., Lardy, H.A. & Benesch, R. The sulfhydryl groups of crystalline proteins. I. Some albumins, enzymes, and hemoglobins. *J Biol Chem* **216**, 663-676 (1955).
26. Copley, S.D., Novak, W.R. & Babbitt, P.C. Divergence of function in the thioredoxin fold suprafamily: evidence for evolution of peroxiredoxins from a thioredoxin-like ancestor. *Biochemistry* **43**, 13981-13995 (2004).
27. Oe, T., Arora, J.S., Lee, S.H. & Blair, I.A. A novel lipid hydroperoxide-derived cyclic covalent modification to histone H4. *J Biol Chem* **278**, 42098-42105 (2003).
28. Zhang, W.H., Liu, J., Xu, G., Yuan, Q. & Sayre, L.M. Model studies on protein side chain modification by 4-oxo-2-nonenal. *Chem Res Toxicol* **16**, 512-523 (2003).
29. Weber, H., Chetelat, A., Reymond, P. & Farmer, E.E. Selective and powerful stress gene expression in Arabidopsis in response to malondialdehyde. *Plant J* **37**, 877-888 (2004).
30. Yamada, S., *et al.* Immunochemical detection of a lipofuscin-like fluorophore derived from malondialdehyde and lysine. *J Lipid Res* **42**, 1187-1196 (2001).
31. Esterbauer, H., Gebicki, J., Puhl, H. & Jurgens, G. The role of lipid peroxidation and antioxidants in oxidative modification of LDL. *Free Radic Biol Med* **13**, 341-390 (1992).
32. Stevens, J.F. & Maier, C.S. Acrolein: sources, metabolism, and biomolecular interactions relevant to human health and disease. *Mol Nutr Food Res* **52**, 7-25 (2008).

33. Fam, S.S., *et al.* Formation of highly reactive A-ring and J-ring isoprostane-like compounds (A4/J4-neuroprostanes) in vivo from docosahexaenoic acid. *J Biol Chem* **277**, 36076-36084 (2002).
34. Dick, R.A., Kwak, M.K., Sutter, T.R. & Kensler, T.W. Antioxidative function and substrate specificity of NAD(P)H-dependent alkenal/one oxidoreductase. A new role for leukotriene B4 12-hydroxydehydrogenase/15-oxoprostaglandin 13-reductase. *J Biol Chem* **276**, 40803-40810 (2001).
35. Erlemann, K.R., *et al.* Regulation of 5-hydroxyeicosanoid dehydrogenase activity in monocytic cells. *Biochem J* **403**, 157-165 (2007).
36. Liu, J., *et al.* Analysis of protein covalent modification by xenobiotics using a covert oxidatively activated tag: raloxifene proof-of-principle study. *Chem Res Toxicol* **18**, 1485-1496 (2005).
37. Chen, Q., *et al.* Cytochrome P450 3A4-mediated bioactivation of raloxifene: irreversible enzyme inhibition and thiol adduct formation. *Chem Res Toxicol* **15**, 907-914 (2002).
38. Zhou, S., Chan, E., Duan, W., Huang, M. & Chen, Y.Z. Drug bioactivation, covalent binding to target proteins and toxicity relevance. *Drug Metab Rev* **37**, 41-213 (2005).
39. Farmer, E.E. Surface-to-air signals. *Nature* **411**, 854-856 (2001).
40. Reilly, C.A. & Yost, G.S. Metabolism of capsaicinoids by P450 enzymes: a review of recent findings on reaction mechanisms, bio-activation, and detoxification processes. *Drug Metab Rev* **38**, 685-706 (2006).
41. Chanda, S., Bashir, M., Babbar, S., Koganti, A. & Bley, K. In vitro hepatic and skin metabolism of capsaicin. *Drug Metab Dispos* **36**, 670-675 (2008).
42. Cebi, M. & Koert, U. Reactivity recognition by TRPA1 channels. *Chembiochem* **8**, 979-980 (2007).
43. Zhang, Y., Kensler, T.W., Cho, C.G., Posner, G.H. & Talalay, P. Anticarcinogenic activities of sulforaphane and structurally related synthetic norbornyl isothiocyanates. *Proc Natl Acad Sci U S A* **91**, 3147-3150 (1994).
44. Yano, T., *et al.* The effect of 6-methylthiohexyl isothiocyanate isolated from Wasabia japonica (wasabi) on 4-(methylnitrosamino)-1-(3-pyridyl)-1-buatnone-induced lung tumorigenesis in mice. *Cancer Lett* **155**, 115-120 (2000).
45. Haridas, V., *et al.* Triterpenoid electrophiles (avicins) activate the innate stress response by redox regulation of a gene battery. *Journal of Clinical Investigation* **113**, 65-73 (2004).
46. Haridas, V., *et al.* Avicins: triterpenoid saponins from Acacia victoriae (Bentham) induce apoptosis by mitochondrial perturbation. *Proc Natl Acad Sci U S A* **98**, 5821-5826 (2001).
47. Mujoo, K., *et al.* Triterpenoid saponins from Acacia victoriae (Bentham) decrease tumor cell proliferation and induce apoptosis. *Cancer Res* **61**, 5486-5490 (2001).
48. Dinkova-Kostova, A.T., *et al.* Extremely potent triterpenoid inducers of the phase 2 response: Correlations of protection against oxidant and inflammatory stress. *Proceedings of the National Academy of Sciences of the United States of America* **102**, 4584-4589 (2005).
49. Ito, Y., *et al.* The novel triterpenoid CDDO induces apoptosis and differentiation of human osteosarcoma cells by a caspase-8 dependent mechanism. *Mol Pharmacol* **59**, 1094-1099 (2001).

50. Pedersen, I.M., *et al.* The triterpenoid CDDO induces apoptosis in refractory CLL B cells. *Blood* **100**, 2965-2972 (2002).
51. Suh, N., *et al.* Novel triterpenoids suppress inducible nitric oxide synthase (iNOS) and inducible cyclooxygenase (COX-2) in mouse macrophages. *Cancer Res* **58**, 717-723 (1998).
52. Jung, G., Breitmaier, E. & Voelter, W. [Dissociation equilibrium of glutathione. A Fourier transform-13C-NMR spectroscopic study of pH-dependence and of charge densities]. *Eur J Biochem* **24**, 438-445 (1972).
53. Barry Halliwell, J.M.C.G. Antioxidant defenses: endogenous and diet derived. in *Free Radicals in Biology and Medicine* 111 (Oxford University Press Inc., New York, 2007).
54. Townsend, D.M., Tew, K.D. & Tapiero, H. The importance of glutathione in human disease. *Biomed Pharmacother* **57**, 145-155 (2003).
55. Bhuyan, D.K., Master, R.W. & Bhuyan, K.C. Crosslinking of aminophospholipids in cellular membranes of lens by oxidative stress in vitro. *Biochim Biophys Acta* **1285**, 21-28 (1996).
56. Chung, F.L., Young, R. & Hecht, S.S. Formation of cyclic 1,N2-propanodeoxyguanosine adducts in DNA upon reaction with acrolein or crotonaldehyde. *Cancer Res* **44**, 990-995 (1984).
57. Stein, S., Lao, Y., Yang, I.Y., Hecht, S.S. & Moriya, M. Genotoxicity of acetaldehyde- and crotonaldehyde-induced 1,N2-propanodeoxyguanosine DNA adducts in human cells. *Mutat Res* **608**, 1-7 (2006).
58. Yang, I.Y., *et al.* Mutagenesis by acrolein-derived propanodeoxyguanosine adducts in human cells. *Biochemistry* **41**, 13826-13832 (2002).
59. Nath, R.G. & Chung, F.L. Detection of exocyclic 1,N2-propanodeoxyguanosine adducts as common DNA lesions in rodents and humans. *Proc Natl Acad Sci U S A* **91**, 7491-7495 (1994).
60. Lee, S.H., Williams, M.V., Dubois, R.N. & Blair, I.A. Cyclooxygenase-2-mediated DNA damage. *J Biol Chem* **280**, 28337-28346 (2005).
61. Lakshmana Rao, P.V., Vijayaraghavan, R. & Bhaskar, A.S. Sulphur mustard induced DNA damage in mice after dermal and inhalation exposure. *Toxicology* **139**, 39-51 (1999).
62. Aldini, G., *et al.* Identification of actin as a 15-deoxy-Delta12,14-prostaglandin J2 target in neuroblastoma cells: mass spectrometric, computational, and functional approaches to investigate the effect on cytoskeletal derangement. *Biochemistry* **46**, 2707-2718 (2007).
63. Shibata, T., *et al.* Thioredoxin as a molecular target of cyclopentenone prostaglandins. *J Biol Chem* **278**, 26046-26054 (2003).
64. Halliwell, B.G., John M.C. Antioxidant defenses: endogenous and diet derived. in *Free Radicals in Biology and Medicine* 111 (Oxford University Press Inc., New York, 2007).
65. Mustacich, D. & Powis, G. Thioredoxin reductase. *Biochem J* **346 Pt 1**, 1-8 (2000).
66. Fisher, A.A., *et al.* Quinone electrophiles selectively adduct "electrophile binding motifs" within cytochrome c. *Biochemistry* **46**, 11090-11100 (2007).
67. Carbone, D.L., Doorn, J.A., Kiebler, Z., Sampey, B.P. & Petersen, D.R. Inhibition of Hsp72-mediated protein refolding by 4-hydroxy-2-nonenal. *Chem Res Toxicol* **17**, 1459-1467 (2004).

68. Carbone, D.L., Doorn, J.A., Kiebler, Z., Ickes, B.R. & Petersen, D.R. Modification of heat shock protein 90 by 4-hydroxynonenal in a rat model of chronic alcoholic liver disease. *J Pharmacol Exp Ther* **315**, 8-15 (2005).
69. Jacobs, A.T. & Marnett, L.J. Heat shock factor 1 attenuates 4-Hydroxynonenal-mediated apoptosis: critical role for heat shock protein 70 induction and stabilization of Bcl-XL. *J Biol Chem* **282**, 33412-33420 (2007).
70. Soh, Y., *et al.* Selective activation of the c-Jun N-terminal protein kinase pathway during 4-hydroxynonenal-induced apoptosis of PC12 cells. *Mol Pharmacol* **58**, 535-541 (2000).
71. Sampey, B.P., Carbone, D.L., Doorn, J.A., Drechsel, D.A. & Petersen, D.R. 4-Hydroxy-2-nonenal adduction of extracellular signal-regulated kinase (Erk) and the inhibition of hepatocyte Erk-Est-like protein-1-activating protein-1 signal transduction. *Mol Pharmacol* **71**, 871-883 (2007).
72. Codreanu, S.G., Adams, D.G., Dawson, E.S., Wadzinski, B.E. & Liebler, D.C. Inhibition of protein phosphatase 2A activity by selective electrophile alkylation damage. *Biochemistry* **45**, 10020-10029 (2006).
73. Musiek, E.S., *et al.* Electrophilic cyclopentenone neuroprostanes are anti-inflammatory mediators formed from the peroxidation of the omega-3 polyunsaturated fatty acid docosahexaenoic acid. *J Biol Chem* **283**, 19927-19935 (2008).
74. Cui, T., *et al.* Nitrated fatty acids: Endogenous anti-inflammatory signaling mediators. *J Biol Chem* **281**, 35686-35698 (2006).
75. Nerland, D.E. The antioxidant/electrophile response element motif. *Drug Metab Rev* **39**, 235-248 (2007).
76. Williams, R.T. Comparative patterns of drug metabolism. *Fed Proc* **26**, 1029-1039 (1967).
77. Itoh, K., *et al.* Keap1 represses nuclear activation of antioxidant responsive elements by Nrf2 through binding to the amino-terminal Neh2 domain. *Genes Dev* **13**, 76-86 (1999).
78. Li, W. & Kong, A.N. Molecular mechanisms of Nrf2-mediated antioxidant response. *Mol Carcinog* **48**, 91-104 (2009).
79. Kang, M.I., Kobayashi, A., Wakabayashi, N., Kim, S.G. & Yamamoto, M. Scaffolding of Keap1 to the actin cytoskeleton controls the function of Nrf2 as key regulator of cytoprotective phase 2 genes. *Proc Natl Acad Sci U S A* **101**, 2046-2051 (2004).
80. Zhang, D.D. & Hannink, M. Distinct cysteine residues in Keap1 are required for Keap1-dependent ubiquitination of Nrf2 and for stabilization of Nrf2 by chemopreventive agents and oxidative stress. *Mol Cell Biol* **23**, 8137-8151 (2003).
81. Baker, P.R., *et al.* Fatty acid transduction of nitric oxide signaling: multiple nitrated unsaturated fatty acid derivatives exist in human blood and urine and serve as endogenous peroxisome proliferator-activated receptor ligands. *J Biol Chem* **280**, 42464-42475 (2005).
82. Baker, P.R., Schopfer, F.J., Sweeney, S. & Freeman, B.A. Red cell membrane and plasma linoleic acid nitration products: synthesis, clinical identification, and quantitation. *Proc Natl Acad Sci U S A* **101**, 11577-11582 (2004).
83. Lima, E.S., Di Mascio, P. & Abdalla, D.S.P. Cholesteryl nitrolinoleate, a nitrated lipid present in human blood plasma and lipoproteins. *J Lipid Res* **44**, 1660-1666 (2003).
84. Wright, M.M., *et al.* Fatty acid transduction of nitric oxide signaling: nitrolinoleic acid potently activates endothelial heme oxygenase 1 expression. *Proc Natl Acad Sci U S A* **103**, 4299-4304 (2006).

85. Schopfer, F.J., *et al.* Fatty acid transduction of nitric oxide signaling. Nitrolinoleic acid is a hydrophobically stabilized nitric oxide donor. *J Biol Chem* **280**, 19289-19297 (2005).
86. Ichikawa, T., *et al.* Nitroalkenes suppress lipopolysaccharide-induced signal transducer and activator of transcription signaling in macrophages: A critical role of mitogen-activated protein kinase phosphatase 1. *Endocrinology* **149**, 4086-4094 (2008).
87. Kalyanaraman, B. Nitrated lipids: a class of cell-signaling molecules. *Proc Natl Acad Sci U S A* **101**, 11527-11528 (2004).
88. Rubbo, H., *et al.* Nitric oxide inhibition of lipoxygenase-dependent liposome and low-density lipoprotein oxidation: termination of radical chain propagation reactions and formation of nitrogen-containing oxidized lipid derivatives. *Arch Biochem Biophys* **324**, 15-25 (1995).
89. Rubbo, H., *et al.* Nitric oxide regulation of superoxide and peroxynitrite-dependent lipid peroxidation. Formation of novel nitrogen-containing oxidized lipid derivatives. *J Biol Chem* **269**, 26066-26075 (1994).
90. O'Donnell, V.B., *et al.* 15-Lipoxygenase catalytically consumes nitric oxide and impairs activation of guanylate cyclase. *J Biol Chem* **274**, 20083-20091 (1999).
91. Tsikas, D., *et al.* Specific GC-MS/MS stable-isotope dilution methodology for free 9- and 10-nitro-oleic acid in human plasma challenges previous LC-MS/MS reports. *J Chromatogr B Analyt Technol Biomed Life Sci* (2009).
92. Balazy, M., *et al.* Vicinal nitrohydroxyeicosatrienoic acids: vasodilator lipids formed by reaction of nitrogen dioxide with arachidonic acid. *J Pharmacol Exp Ther* **299**, 611-619 (2001).
93. Lima, E.S., *et al.* Nitrated lipids decompose to nitric oxide and lipid radicals and cause vasorelaxation. *Free Radic Biol Med* **39**, 532-539 (2005).
94. Lim, D.G., *et al.* Nitrolinoleate, a nitric oxide-derived mediator of cell function: synthesis, characterization, and vasomotor activity. *Proc Natl Acad Sci U S A* **99**, 15941-15946 (2002).
95. Schopfer, F.J., *et al.* Nitrolinoleic acid: an endogenous peroxisome proliferator-activated receptor gamma ligand. *Proc Natl Acad Sci U S A* **102**, 2340-2345 (2005).
96. Kelley, E.E., *et al.* Nitro-oleic acid: A novel and irreversible inhibitor of xanthine oxidoreductase. *J Biol Chem, doi: 10.1074/jbc.M802402200* (2008).
97. Villacorta, L., *et al.* Nitro-linoleic acid inhibits vascular smooth muscle cell proliferation via the Keap1/Nrf2 signaling pathway. *Am J Physiol Heart Circ Physiol* **293**, H770-776 (2007).
98. Altiok, S., Xu, M. & Spiegelman, B.M. PPARgamma induces cell cycle withdrawal: inhibition of E2F/DP DNA-binding activity via down-regulation of PP2A. *Genes Dev* **11**, 1987-1998 (1997).
99. Chawla, A., Schwarz, E.J., Dimaculangan, D.D. & Lazar, M.A. Peroxisome proliferator-activated receptor (PPAR) gamma: adipose-predominant expression and induction early in adipocyte differentiation. *Endocrinology* **135**, 798-800 (1994).
100. Ricote, M., Li, A.C., Willson, T.M., Kelly, C.J. & Glass, C.K. The peroxisome proliferator-activated receptor-gamma is a negative regulator of macrophage activation. *Nature* **391**, 79-82 (1998).
101. Finegood, D.T., *et al.* Beta-cell mass dynamics in Zucker diabetic fatty rats. Rosiglitazone prevents the rise in net cell death. *Diabetes* **50**, 1021-1029 (2001).

102. Guilherme, A., Virbasius, J.V., Puri, V. & Czech, M.P. Adipocyte dysfunctions linking obesity to insulin resistance and type 2 diabetes. *Nat Rev Mol Cell Biol* **9**, 367-377 (2008).
103. Halabi, C.M., *et al.* Interference with PPAR gamma function in smooth muscle causes vascular dysfunction and hypertension. *Cell Metab* **7**, 215-226 (2008).
104. Barroso, I., *et al.* Dominant negative mutations in human PPARgamma associated with severe insulin resistance, diabetes mellitus and hypertension. *Nature* **402**, 880-883 (1999).
105. Feige, J.N., Gelman, L., Michalik, L., Desvergne, B. & Wahli, W. From molecular action to physiological outputs: peroxisome proliferator-activated receptors are nuclear receptors at the crossroads of key cellular functions. *Progress in lipid research* **45**, 120-159 (2006).
106. Yu, C.Y., *et al.* Binding analyses between human PPAR gamma-LBD and ligands - Surface plasmon resonance biosensor assay correlating with circular dichroic spectroscopy determination and molecular docking. *European Journal of Biochemistry* **271**, 386-397 (2004).
107. Krey, G., *et al.* Fatty acids, eicosanoids, and hypolipidemic agents identified as ligands of peroxisome proliferator-activated receptors by coactivator-dependent receptor ligand assay. *Molecular Endocrinology* **11**, 779-791 (1997).
108. Xu, H.E., *et al.* Molecular recognition of fatty acids by peroxisome proliferator-activated receptors. *Molecular Cell* **3**, 397-403 (1999).
109. Straus, D.S. & Glass, C.K. Cyclopentenone prostaglandins: New insights on biological activities and cellular targets. *Medicinal Research Reviews* **21**, 185-210 (2001).
110. Forman, B.M., *et al.* 15-Deoxy-delta 12, 14-prostaglandin J2 is a ligand for the adipocyte determination factor PPAR gamma. *Cell* **83**, 803-812 (1995).
111. Nagy, L., Tontonoz, P., Alvarez, J.G.A., Chen, H.W. & Evans, R.M. Oxidized LDL regulates macrophage gene expression through ligand activation of PPAR gamma. *Cell* **93**, 229-240 (1998).
112. Liu, Y., *et al.* The antiinflammatory effect of laminar flow: The role of PPAR gamma, epoxyeicosatrienoic acids, and soluble epoxide hydrolase. *Proceedings of the National Academy of Sciences of the United States of America* **102**, 16747-16752 (2005).
113. McIntyre, T.M., *et al.* Identification of an intracellular receptor for lysophosphatidic acid (LPA): LPA is a transcellular PPAR gamma agonist. *Proceedings of the National Academy of Sciences of the United States of America* **100**, 131-136 (2003).
114. Lehmann, J.M., *et al.* An Antidiabetic Thiazolidinedione Is a High-Affinity Ligand for Peroxisome Proliferator-Activated Receptor Gamma(Ppar-Gamma). *Journal of Biological Chemistry* **270**, 12953-12956 (1995).
115. Young, P.W., *et al.* Identification of high-affinity binding sites for the insulin sensitizer rosiglitazone (BRL-49653) in rodent and human adipocytes using a radioiodinated ligand for peroxisomal proliferator-activated receptor gamma. *Journal of Pharmacology and Experimental Therapeutics* **284**, 751-759 (1998).
116. Lehmann, J.M., *et al.* An antidiabetic thiazolidinedione is a high affinity ligand for peroxisome proliferator-activated receptor gamma (PPAR gamma). *J Biol Chem* **270**, 12953-12956 (1995).

117. Gerstein, H.C., *et al.* Effect of rosiglitazone on the frequency of diabetes in patients with impaired glucose tolerance or impaired fasting glucose: a randomised controlled trial. *Lancet* **368**, 1096-1105 (2006).
118. Lehrke, M. & Lazar, M.A. The many faces of PPARgamma. *Cell* **123**, 993-999 (2005).
119. Connor, W.E. Importance of n-3 fatty acids in health and disease. *Am J Clin Nutr* **71**, 171S-175S (2000).
120. Neuringer, M., Anderson, G.J. & Connor, W.E. The essentiality of n-3 fatty acids for the development and function of the retina and brain. *Annu Rev Nutr* **8**, 517-541 (1988).
121. Morris, M.C., Evans, D.A., Tangney, C.C., Bienias, J.L. & Wilson, R.S. Fish consumption and cognitive decline with age in a large community study. *Arch Neurol* **62**, 1849-1853 (2005).
122. Fedor, D. & Kelley, D.S. Prevention of insulin resistance by n-3 polyunsaturated fatty acids. *Curr Opin Clin Nutr Metab Care* **12**, 138-146 (2009).
123. Dietary supplementation with n-3 polyunsaturated fatty acids and vitamin E after myocardial infarction: results of the GISSI-Prevenzione trial. Gruppo Italiano per lo Studio della Sopravvivenza nell'Infarto miocardico. *Lancet* **354**, 447-455 (1999).
124. Duda, M.K., *et al.* Fish oil, but not flaxseed oil, decreases inflammation and prevents pressure overload-induced cardiac dysfunction. *Cardiovasc Res* **81**, 319-327 (2009).
125. Fradet, V., Cheng, I., Casey, G. & Witte, J.S. Dietary omega-3 fatty acids, cyclooxygenase-2 genetic variation, and aggressive prostate cancer risk. *Clin Cancer Res* **15**, 2559-2566 (2009).
126. Harris, W.S., Assaad, B. & Poston, W.C. Tissue omega-6/omega-3 fatty acid ratio and risk for coronary artery disease. *Am J Cardiol* **98**, 19i-26i (2006).
127. Gibney, M.J. & Hunter, B. The effects of short- and long-term supplementation with fish oil on the incorporation of n-3 polyunsaturated fatty acids into cells of the immune system in healthy volunteers. *Eur J Clin Nutr* **47**, 255-259 (1993).
128. Reynaud, D., Thickitt, C.P. & Pace-Asciak, C.R. Facile preparation and structural determination of monohydroxy derivatives of docosahexaenoic acid (HDoHE) by alpha-tocopherol-directed autoxidation. *Anal Biochem* **214**, 165-170 (1993).
129. VanRollins, M. & Murphy, R.C. Autooxidation of docosahexaenoic acid: analysis of ten isomers of hydroxydocosahexaenoate. *J Lipid Res* **25**, 507-517 (1984).
130. Serhan, C.N., *et al.* Novel functional sets of lipid-derived mediators with antiinflammatory actions generated from omega-3 fatty acids via cyclooxygenase 2-nonsteroidal antiinflammatory drugs and transcellular processing. *J Exp Med* **192**, 1197-1204 (2000).
131. Serhan, C.N., *et al.* Resolvins: a family of bioactive products of omega-3 fatty acid transformation circuits initiated by aspirin treatment that counter proinflammation signals. *J Exp Med* **196**, 1025-1037 (2002).
132. Simmons, D.L., Botting, R.M. & Hla, T. Cyclooxygenase isozymes: the biology of prostaglandin synthesis and inhibition. *Pharmacol Rev* **56**, 387-437 (2004).
133. Tilley, S.L., Coffman, T.M. & Koller, B.H. Mixed messages: modulation of inflammation and immune responses by prostaglandins and thromboxanes. *J Clin Invest* **108**, 15-23 (2001).
134. Arita, M., *et al.* Resolvin E1, an endogenous lipid mediator derived from omega-3 eicosapentaenoic acid, protects against 2,4,6-trinitrobenzene sulfonic acid-induced colitis. *Proc Natl Acad Sci U S A* **102**, 7671-7676 (2005).

135. Arita, M., *et al.* Stereochemical assignment, antiinflammatory properties, and receptor for the omega-3 lipid mediator resolvin E1. *J Exp Med* **201**, 713-722 (2005).
136. Mollace, V., Muscoli, C., Masini, E., Cuzzocrea, S. & Salvemini, D. Modulation of prostaglandin biosynthesis by nitric oxide and nitric oxide donors. *Pharmacol Rev* **57**, 217-252 (2005).
137. Smith, W.L.a.M., R.C. The eicosanoids: cyclooxygenase, lipoxygenase, and epoxygenase pathways. in *Biochemistry of Lipids, Lipoproteins and Membranes, 4th edition*, Vol. 36 (ed. Vance, D.E.a.V., J.E.) 341-369 (Elsevier, Amsterdam, 2004).
138. Brash, A.R. Arachidonic acid as a bioactive molecule. *J Clin Invest* **107**, 1339-1345 (2001).
139. Bishop-Bailey, D. & Hla, T. Endothelial cell apoptosis induced by the peroxisome proliferator-activated receptor (PPAR) ligand 15-deoxy-Delta12, 14-prostaglandin J2. *J Biol Chem* **274**, 17042-17048 (1999).
140. Rossi, A., *et al.* Anti-inflammatory cyclopentenone prostaglandins are direct inhibitors of IkappaB kinase. *Nature* **403**, 103-108 (2000).
141. Garavito, R.M., Malkowski, M.G. & DeWitt, D.L. The structures of prostaglandin endoperoxide H synthases-1 and -2. *Prostaglandins Other Lipid Mediat* **68-69**, 129-152 (2002).
142. Morita, I., *et al.* Different intracellular locations for prostaglandin endoperoxide H synthase-1 and -2. *J Biol Chem* **270**, 10902-10908 (1995).
143. Ren, Y., *et al.* Topology of prostaglandin H synthase-1 in the endoplasmic reticulum membrane. *Arch Biochem Biophys* **323**, 205-214 (1995).
144. Song, I. & Smith, W.L. C-terminal Ser/Pro-Thr-Glu-Leu tetrapeptides of prostaglandin endoperoxide H synthases-1 and -2 target the enzymes to the endoplasmic reticulum. *Arch Biochem Biophys* **334**, 67-72 (1996).
145. Liou, J.Y., Deng, W.G., Gilroy, D.W., Shyue, S.K. & Wu, K.K. Colocalization and interaction of cyclooxygenase-2 with caveolin-1 in human fibroblasts. *J Biol Chem* **276**, 34975-34982 (2001).
146. Liou, J.Y., *et al.* Colocalization of prostacyclin synthase with prostaglandin H synthase-1 (PGHS-1) but not phorbol ester-induced PGHS-2 in cultured endothelial cells. *J Biol Chem* **275**, 15314-15320 (2000).
147. Malkowski, M.G., Ginell, S.L., Smith, W.L. & Garavito, R.M. The productive conformation of arachidonic acid bound to prostaglandin synthase. *Science* **289**, 1933-1937 (2000).
148. Thuresson, E.D., *et al.* Prostaglandin endoperoxide H synthase-1: the functions of cyclooxygenase active site residues in the binding, positioning, and oxygenation of arachidonic acid. *J Biol Chem* **276**, 10347-10357 (2001).
149. Rouzer, C.A. & Marnett, L.J. Mechanism of free radical oxygenation of polyunsaturated fatty acids by cyclooxygenases. *Chem Rev* **103**, 2239-2304 (2003).
150. Kim, S.F., Huri, D.A. & Snyder, S.H. Inducible nitric oxide synthase binds, S-nitrosylates, and activates cyclooxygenase-2. *Science* **310**, 1966-1970 (2005).
151. Kalgutkar, A.S., Crews, B.C. & Marnett, L.J. Design, synthesis, and biochemical evaluation of N-substituted maleimides as inhibitors of prostaglandin endoperoxide synthases. *J Med Chem* **39**, 1692-1703 (1996).
152. Kennedy, T.A., Smith, C.J. & Marnett, L.J. Investigation of the role of cysteines in catalysis by prostaglandin endoperoxide synthase. *J Biol Chem* **269**, 27357-27364 (1994).

153. Rome, L.H. & Lands, W.E. Structural requirements for time-dependent inhibition of prostaglandin biosynthesis by anti-inflammatory drugs. *Proc Natl Acad Sci U S A* **72**, 4863-4865 (1975).
154. Guo, Q., Wang, L.H., Ruan, K.H. & Kulmacz, R.J. Role of Val509 in time-dependent inhibition of human prostaglandin H synthase-2 cyclooxygenase activity by isoform-selective agents. *J Biol Chem* **271**, 19134-19139 (1996).
155. Davies, J.Q. & Gordon, S. Isolation and culture of murine macrophages. *Methods Mol Biol* **290**, 91-103 (2005).
156. Alvarez, M.N., Piacenza, L., Irigoin, F., Peluffo, G. & Radi, R. Macrophage-derived peroxynitrite diffusion and toxicity to Trypanosoma cruzi. *Arch Biochem Biophys* **432**, 222-232 (2004).
157. Alvarez, M.N., Trujillo, M. & Radi, R. Peroxynitrite formation from biochemical and cellular fluxes of nitric oxide and superoxide. *Methods in Enzymology* **359**, 353-366 (2002).
158. Landino, L.M., Crews, B.C., Timmons, M.D., Morrow, J.D. & Marnett, L.J. Peroxynitrite, the coupling product of nitric oxide and superoxide, activates prostaglandin biosynthesis. *Proc Natl Acad Sci U S A* **93**, 15069-15074 (1996).
159. Schopfer, F.J.*, et al.* Detection and quantification of protein adduction by electrophilic fatty acids: mitochondrial generation of fatty acid nitroalkene derivatives. *Free Radic Biol Med* **46**, 1250-1259 (2009).
160. Fujimoto, Y., Uno, E. & Sakuma, S. Effects of reactive oxygen and nitrogen species on cyclooxygenase-1 and-2 activities. *Prostaglandins Leukotrienes and Essential Fatty Acids* **71**, 335-340 (2004).
161. Gierse, J.K. & Koboldt, C.M. Current Protocols in Pharmacology. in *Cyclooxygenase Assays* (ed. S.J., E.) (John Wiley and Sons, Inc., 1998).
162. Bligh, E.G. & Dyer, W.J. A rapid method of total lipid extraction and purification. *Can J Biochem Physiol* **37**, 911-917 (1959).
163. Cerghizan, A., Bala, C., Nita, C. & Hancu, N. Practical aspects of the control of cardiovascular risk in type 2 diabetes mellitus and the metabolic syndrome. *Exp Clin Cardiol* **12**, 83-86 (2007).
164. Hajer, G.R., van Haeften, T.W. & Visseren, F.L. Adipose tissue dysfunction in obesity, diabetes, and vascular diseases. *European heart journal* (2008).
165. Tontonoz, P. & Spiegelman, B.M. Fat and beyond: the diverse biology of PPARgamma. *Annual review of biochemistry* **77**, 289-312 (2008).
166. McGuire, D.K. & Inzucchi, S.E. New drugs for the treatment of diabetes mellitus: part I: Thiazolidinediones and their evolving cardiovascular implications. *Circulation* **117**, 440-449 (2008).
167. Tsikas, D.*, et al.* Specific GC-MS/MS stable-isotope dilution methodology for free 9- and 10-nitro-oleic acid in human plasma challenges previous LC-MS/MS reports. *J Chromatogr B Analyt Technol Biomed Life Sci* **877**, 2895-2908 (2009).
168. Tsikas, D., Zoerner, A.A., Mitschke, A. & Gutzki, F.M. Nitro-fatty acids occur in human plasma in the picomolar range: a targeted nitro-lipidomics GC-MS/MS study. *Lipids* **44**, 855-865 (2009).
169. Freeman, B.A.*, et al.* Nitro-fatty acid formation and signaling. *J Biol Chem* **283**, 15515-15519 (2008).

170. Nadtochiy, S.M., Baker, P.R., Freeman, B.A. & Brookes, P.S. Mitochondrial nitroalkene formation and mild uncoupling in ischaemic preconditioning: implications for cardioprotection. *Cardiovasc Res* (2008).
171. Batthyany, C., *et al.* Reversible post-translational modification of proteins by nitrated fatty acids in vivo. *J of Biol Chem* **281**, 20450-20463 (2006).
172. Young, P.W., *et al.* Identification of high-affinity binding sites for the insulin sensitizer rosiglitazone (BRL-49653) in rodent and human adipocytes using a radioiodinated ligand for peroxisomal proliferator-activated receptor gamma. *J Pharmacol Exp Ther* **284**, 751-759 (1998).
173. Itoh, T., *et al.* Structural basis for the activation of PPARgamma by oxidized fatty acids. *Nat Struct Mol Biol*, 924-931 (2008).
174. Nissen, S.E. & Wolski, K. Effect of rosiglitazone on the risk of myocardial infarction and death from cardiovascular causes. *N Engl J Med* **356**, 2457-2471 (2007).
175. Nissen, S.E., Wolski, K. & Topol, E.J. Effect of muraglitazar on death and major adverse cardiovascular events in patients with type 2 diabetes mellitus. *Jama* **294**, 2581-2586 (2005).
176. Nettles, K.W. Insights into PPARgamma from structures with endogenous and covalently bound ligands. *Nat Struct Mol Biol* **15**, 893-895 (2008).
177. Zhang, F., Lavan, B.E. & Gregoire, F.M. Selective modulators of PPAR-gamma activity: Molecular aspects related to obesity and side-effects. *PPAR Res* **2007**, 32696 (2007).
178. Li, Y., *et al.* Molecular recognition of nitrated fatty acids by PPAR gamma. *Nat Struct Mol Biol* **15**, 865-867 (2008).
179. Li, Y., *et al.* T2384, a novel antidiabetic agent with unique peroxisome proliferator-activated receptor gamma binding properties. *J Biol Chem* **283**, 9168-9176 (2008).
180. Wigren, J., *et al.* Differential recruitment of the coactivator proteins CREB-binding protein and steroid receptor coactivator-1 to peroxisome proliferator-activated receptor gamma/9-cis-retinoic acid receptor heterodimers by ligands present in oxidized low-density lipoprotein. *J Endocrinol* **177**, 207-214 (2003).
181. Feige, J.N. & Auwerx, J. Transcriptional coregulators in the control of energy homeostasis. *Trends Cell Biol* **17**, 292-301 (2007).
182. Guan, Y., *et al.* Thiazolidinediones expand body fluid volume through PPARgamma stimulation of ENaC-mediated renal salt absorption. *Nature medicine* **11**, 861-866 (2005).
183. Khanderia, U., Pop-Busui, R. & Eagle, K.A. Thiazolidinediones in type 2 diabetes: a cardiology perspective. *The Annals of pharmacotherapy* **42**, 1466-1474 (2008).
184. Serhan, C.N., Chiang, N. & Van Dyke, T.E. Resolving inflammation: dual anti-inflammatory and pro-resolution lipid mediators. *Nat Rev Immunol* **8**, 349-361 (2008).
185. Kim, E.H. & Surh, Y.J. 15-deoxy-Delta12,14-prostaglandin J2 as a potential endogenous regulator of redox-sensitive transcription factors. *Biochem Pharmacol* **72**, 1516-1528 (2006).
186. Daikh, B.E., Laethem, R.M. & Koop, D.R. Stereoselective epoxidation of arachidonic acid by cytochrome P-450s 2CAA and 2C2. *J Pharmacol Exp Ther* **269**, 1130-1135 (1994).
187. Zeldin, D.C., *et al.* Biochemical characterization of the human liver cytochrome P450 arachidonic acid epoxygenase pathway. *Arch Biochem Biophys* **330**, 87-96 (1996).

188. Fer, M., *et al.* Metabolism of eicosapentaenoic and docosahexaenoic acids by recombinant human cytochromes P450. *Arch Biochem Biophys* **471**, 116-125 (2008).
189. Node, K., *et al.* Anti-inflammatory properties of cytochrome P450 epoxygenase-derived eicosanoids. *Science* **285**, 1276-1279 (1999).
190. Harmon, S.D., *et al.* Oxygenation of omega-3 fatty acids by human cytochrome P450 4F3B: effect on 20-hydroxyeicosatetraenoic acid production. *Prostaglandins Leukot Essent Fatty Acids* **75**, 169-177 (2006).
191. Stark, K., Wongsud, B., Burman, R. & Oliw, E.H. Oxygenation of polyunsaturated long chain fatty acids by recombinant CYP4F8 and CYP4F12 and catalytic importance of Tyr-125 and Gly-328 of CYP4F8. *Arch Biochem Biophys* **441**, 174-181 (2005).
192. Blewett, A.J., Varma, D., Gilles, T., Libonati, J.R. & Jansen, S.A. Development and validation of a high-performance liquid chromatography-electrospray mass spectrometry method for the simultaneous determination of 23 eicosanoids. *J Pharm Biomed Anal* **46**, 653-662 (2008).
193. Arita, M., Clish, C.B. & Serhan, C.N. The contributions of aspirin and microbial oxygenase to the biosynthesis of anti-inflammatory resolvins: novel oxygenase products from omega-3 polyunsaturated fatty acids. *Biochem Biophys Res Commun* **338**, 149-157 (2005).
194. Satoh, T., *et al.* Activation of the Keap1/Nrf2 pathway for neuroprotection by electrophillic phase II inducers. *Proc Natl Acad Sci U S A* **103**, 768-773 (2006).
195. Dinkova-Kostova, A.T., Cory, A.H., Bozak, R.E., Hicks, R.J. & Cory, J.G. Bis(2-hydroxybenzylidene)acetone, a potent inducer of the phase 2 response, causes apoptosis in mouse leukemia cells through a p53-independent, caspase-mediated pathway. *Cancer Lett* **245**, 341-349 (2007).
196. Thornalley, P.J. Isothiocyanates: mechanism of cancer chemopreventive action. *Anticancer Drugs* **13**, 331-338 (2002).
197. Mochizuki, M., *et al.* Role of 15-deoxy delta(12,14) prostaglandin J2 and Nrf2 pathways in protection against acute lung injury. *Am J Respir Crit Care Med* **171**, 1260-1266 (2005).
198. Raetz, C.R., *et al.* Kdo2-Lipid A of Escherichia coli, a defined endotoxin that activates macrophages via TLR-4. *J Lipid Res* **47**, 1097-1111 (2006).
199. Jean-Louis Luche, L.R.-H.a.P.C. Reduction of natural enones in the presence of cerium trichloride. *J. Chem. Soc., Chem. Commun.*, 601-602 (1978).
200. Rouzer, C.A., *et al.* Lipid profiling reveals arachidonate deficiency in RAW264.7 cells: Structural and functional implications. *Biochemistry* **45**, 14795-14808 (2006).
201. Ishikawa, T., Esterbauer, H. & Sies, H. Role of cardiac glutathione transferase and of the glutathione S-conjugate export system in biotransformation of 4-hydroxynonenal in the heart. *J Biol Chem* **261**, 1576-1581 (1986).
202. Murphy, R.C. & Zarini, S. Glutathione adducts of oxyeicosanoids. *Prostaglandins Other Lipid Mediat* **68-69**, 471-482 (2002).
203. Waku, T., Shiraki, T., Oyama, T. & Morikawa, K. Atomic structure of mutant PPARgamma LBD complexed with 15d-PGJ2: novel modulation mechanism of PPARgamma/RXRalpha function by covalently bound ligands. *FEBS Lett* **583**, 320-324 (2009).

204. Harkewicz, R., Fahy, E., Andreyev, A. & Dennis, E.A. Arachidonate-derived dihomoprostaglandin production observed in endotoxin-stimulated macrophage-like cells. *J Biol Chem* **282**, 2899-2910 (2007).
205. Davoine, C., *et al.* Adducts of oxylipin electrophiles to glutathione reflect a 13 specificity of the downstream lipoxygenase pathway in the tobacco hypersensitive response. *Plant Physiology* **140**, 1484-1493 (2006).
206. Schwartzman, M.L., Falck, J.R., Yadagiri, P. & Escalante, B. Metabolism of 20-hydroxyeicosatetraenoic acid by cyclooxygenase. Formation and identification of novel endothelium-dependent vasoconstrictor metabolites. *J Biol Chem* **264**, 11658-11662 (1989).
207. Samuelsson, B., Dahlen, S.E., Lindgren, J.A., Rouzer, C.A. & Serhan, C.N. Leukotrienes and lipoxins: structures, biosynthesis, and biological effects. *Science* **237**, 1171-1176 (1987).
208. Powell, W.S. & Rokach, J. Biochemistry, biology and chemistry of the 5-lipoxygenase product 5-oxo-ETE. *Prog Lipid Res* **44**, 154-183 (2005).
209. Serhan, C.N., Gotlinger, K., Hong, S. & Arita, M. Resolvins, docosatrienes, and neuroprotectins, novel omega-3-derived mediators, and their aspirin-triggered endogenous epimers: an overview of their protective roles in catabasis. *Prostaglandins Other Lipid Mediat* **73**, 155-172 (2004).
210. Wei, C., Zhu, P., Shah, S.J. & Blair, I.A. 15-Oxo-Eicosatetraenoic Acid, a Metabolite of Macrophage 15-Hydroxyprostaglandin Dehydrogenase that Inhibits Endothelial Cell Proliferation. *Mol Pharmacol* (2009).
211. Arita, M., *et al.* Metabolic inactivation of resolvin E1 and stabilization of its anti-inflammatory actions. *J Biol Chem* **281**, 22847-22854 (2006).
212. Sun, Y.P., *et al.* Resolvin D1 and its aspirin-triggered 17R epimer. Stereochemical assignments, anti-inflammatory properties, and enzymatic inactivation. *J Biol Chem* **282**, 9323-9334 (2007).
213. Bowers, R.C., Hevko, J., Henson, P.M. & Murphy, R.C. A novel glutathione containing eicosanoid (FOG7) chemotactic for human granulocytes. *J Biol Chem* **275**, 29931-29934 (2000).
214. Welch, J.S., Ricote, M., Akiyama, T.E., Gonzalez, F.J. & Glass, C.K. PPARgamma and PPARdelta negatively regulate specific subsets of lipopolysaccharide and IFN-gamma target genes in macrophages. *Proc Natl Acad Sci U S A* **100**, 6712-6717 (2003).
215. Zheng, Z., Kim, J.Y., Ma, H., Lee, J.E. & Yenari, M.A. Anti-inflammatory effects of the 70 kDa heat shock protein in experimental stroke. *J Cereb Blood Flow Metab* **28**, 53-63 (2008).
216. Serhan, C.N., Arita, M., Hong, S. & Gotlinger, K. Resolvins, docosatrienes, and neuroprotectins, novel omega-3-derived mediators, and their endogenous aspirin-triggered epimers. *Lipids* **39**, 1125-1132 (2004).
217. Bowers, R., *et al.* Oxidative stress in severe pulmonary hypertension. *Am J Respir Crit Care Med* **169**, 764-769 (2004).
218. Nadtochiy, S.M., Baker, P.R., Freeman, B.A. & Brookes, P.S. Mitochondrial nitroalkene formation and mild uncoupling in ischaemic preconditioning: implications for cardioprotection. *Cardiovasc Res* **82**, 333-340 (2009).
219. Kratz, F. Albumin as a drug carrier: design of prodrugs, drug conjugates and nanoparticles. *J Control Release* **132**, 171-183 (2008).

220. Fasano, M., *et al.* The extraordinary ligand binding properties of human serum albumin. *IUBMB Life* **57**, 787-796 (2005).
221. Hamilton, J.A., Era, S., Bhamidipati, S.P. & Reed, R.G. Locations of the three primary binding sites for long-chain fatty acids on bovine serum albumin. *Proc Natl Acad Sci U S A* **88**, 2051-2054 (1991).
222. Hamilton, J.A. Fatty acid interactions with proteins: what X-ray crystal and NMR solution structures tell us. *Prog Lipid Res* **43**, 177-199 (2004).
223. Makriyannis, A., Guo, J. & Tian, X. Albumin enhances the diffusion of lipophilic drugs into the membrane bilayer. *Life Sci* **77**, 1605-1611 (2005).
224. Narazaki, R., Hamada, M., Harada, K. & Otagiri, M. Covalent binding between bucillamine derivatives and human serum albumin. *Pharm Res* **13**, 1317-1321 (1996).
225. Aldini, G., *et al.* Albumin is the main nucleophilic target of human plasma: a protective role against pro-atherogenic electrophilic reactive carbonyl species? *Chem Res Toxicol* **21**, 824-835 (2008).
226. Tan, N.S., *et al.* Selective cooperation between fatty acid binding proteins and peroxisome proliferator-activated receptors in regulating transcription. *Mol Cell Biol* **22**, 5114-5127 (2002).
227. Verhoeckx, K.C., *et al.* A combination of proteomics, principal component analysis and transcriptomics is a powerful tool for the identification of biomarkers for macrophage maturation in the U937 cell line. *Proteomics* **4**, 1014-1028 (2004).
228. Buelt, M.K. & Bernlohr, D.A. Modification of the adipocyte lipid binding protein by sulfhydryl reagents and analysis of the fatty acid binding domain. *Biochemistry* **29**, 7408-7413 (1990).
229. Di Simplicio, P., Franconi, F., Frosali, S. & Di Giuseppe, D. Thiolation and nitrosation of cysteines in biological fluids and cells. *Amino Acids* **25**, 323-339 (2003).
230. Reich, E.E., *et al.* Formation of novel D-ring and E-ring isoprostane-like compounds (D4/E4-neuroprostanes) in vivo from docosahexaenoic acid. *Biochemistry* **39**, 2376-2383 (2000).
231. Avanti Polar Lipids, I. Di[3-deoxy-D-manno-octulosonyl]-Lipid A (ammonium salt). (ed. 699500s-1) (Alabaster, AL).
232. Fahy, E., *et al.* Update of the LIPID MAPS comprehensive classification system for lipids. *J Lipid Res* **50 Suppl**, S9-14 (2009).